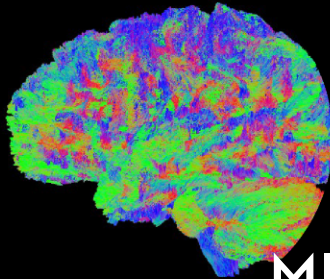
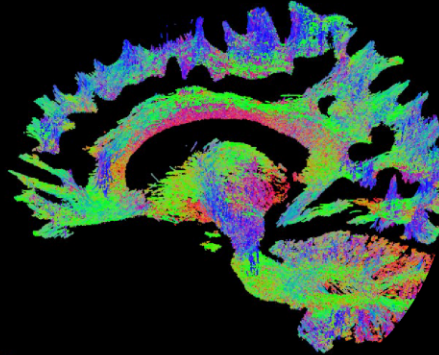
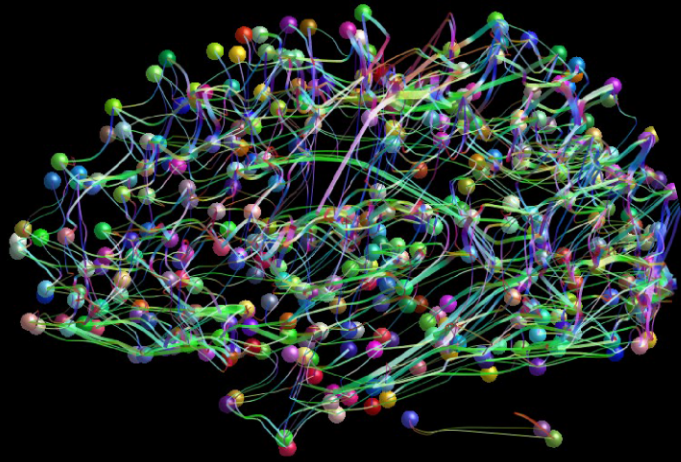




**TURUN
YLIOPISTO**
UNIVERSITY
OF TURKU



MICROSTRUCTURAL ANALYSIS OF DIFFUSE AXONAL INJURY AFTER TRAUMATIC BRAIN INJURY USING DIFFUSION-WEIGHTED MAGNETIC RESONANCE IMAGING

Mehrbod Mohammadian



TURUN
YLIOPISTO
UNIVERSITY
OF TURKU

MICROSTRUCTURAL ANALYSIS OF DIFFUSE AXONAL INJURY AFTER TRAUMATIC BRAIN INJURY USING DIFFUSION-WEIGHTED MAGNETIC RESONANCE IMAGING

Mehrbod Mohammadian

University of Turku

Faculty of Medicine
Department of Clinical Medicine
Clinical Neurosciences
Doctoral Programme in Clinical Research (DPCR)

Supervised by

Professor Olli Tenovuoto MD, Ph.D.
Department of Clinical Neurosciences, Faculty
of Medicine,
University of Turku,
Turku, Finland.

Adjunct Professor Timo Kurki MD, Ph.D.
Department of Radiology,
Faculty of Medicine
University of Turku,
Turku, Finland.

Dr. Timo Roine Ph.D.
Department of Neuroscience and
Biomedical Engineering,
Aalto University School of Science,
Espoo Finland.

Reviewed by

Professor Inga Koerte MD, Ph.D.
Department of Child and Adolescent Psychiatry,
Psychosomatic, and Psychotherapy,
Ludwig-Maximilians-Universität,
Munich, Germany.

Associate Professor Tim Dyrby Ph.D.
Department of Applied Mathematics and
Computer Science,
Technical University of Denmark,
Lyngby, Denmark.

Opponent

Professor, Asta Håberg MD, PhD.
Department of Neuromedicine,
Norwegian University of Science and Technology,
Trondheim, Norway.

The originality of this publication has been checked in accordance with the University of Turku quality assurance system using the Turnitin OriginalityCheck service.

Cover Image: Mehrbod Mohammadian

ISBN 978-951-29-8459-6 (PRINT)
ISBN 978-951-29-8460-2 (PDF)
ISSN 0355-9483 (Print)
ISSN 2343-3213 (Online)
Painosalama, Turku, Finland 2021

To my beloved parents and sister

UNIVERSITY OF TURKU

Faculty of Medicine

Department of Clinical Medicine

Clinical Neurosciences

MEHRBOD MOHAMAMDIAN: Microstructural analysis of diffuse axonal injury after traumatic brain injury using diffusion-weighted Magnetic resonance imaging

Doctoral Dissertation, 136 pp.

Doctoral Program in Clinical Research (DPCR)

April 2021

ABSTRACT

Diffuse axonal injury (DAI) has been considered to be one of the main mechanisms leading to permanent disability in patients with traumatic brain injury (TBI) leading to disturbance in axonal function and neuronal damage. Conventional neuroimaging techniques such as computed tomography and magnetic resonance imaging (MRI) are useful in detection of macroscopic lesions. However, due to their lack of sensitivity, they are not sensitive enough to detect DAI. Diffusion-weighted (DW) MRI is a non-invasive imaging method that can be sensitive to subtle white matter (WM) alterations and it is capable of providing information about structural brain connectivity in vivo. The aim of the present research was to study microstructural WM abnormalities following TBI using DW-MRI and advanced analysis techniques e.g. high angular resolution diffusion imaging (HARDI). Patients with mild TBI (mTBI) and orthopedically injured (OI) patients that served as control subjects underwent brain imaging and clinical assessments during the TBICare study. Whole brain global and local WM abnormalities associated with DAI were investigated using diffusion tensor imaging analysis methods and probabilistic tractography. In addition, brain structural connectivity was evaluated following mTBI. Furthermore, the associations of WM alterations and structural network properties with the outcome were assessed.

Patients with mTBI showed lower anisotropy and higher diffusivity measures at acute or sub-acute, and chronic stages of mTBI compared with controls. These WM alterations were susceptible to the average fiber orientation. Additionally, structural network connectivity was altered only locally and no differences were found between patients and controls in the global network properties. However, WM alterations and network metrics were significantly associated with the outcome. This study highlighted that novel advanced HARDI methods are promising tools to detect WM alterations already at the early stage after mTBI. Furthermore, we showed that disruptions in structural brain networks are associated with outcome, and suggest that network properties in the acute/subacute stage are promising imaging biomarkers for prognostic purposes.

KEYWORDS: Traumatic brain injury, diffuse axonal injury, diffusion-weighted magnetic resonance imaging, structural connectivity, outcome

TURUN YLIOPISTO

Lääketieteellinen tiedekunta

Kliiniset neurotieteet

Kliiniset neurotieteet

MEHRBOD MOHAMMADIAN: Tapaturmaiseen aivovammaan liittyvän diffuusin aksonivaurion hienorakenneanalyysi diffuusiopainotteisella magneettikuvauksella

Väitöskirja, 136 s.

Turun kliininen tohtorihjelma (TKT)

Huhtikuu 2021

TIIVISTELMÄ

Diffuusi aksonivaurio on suurin syy pysyvään työkyvyttömyyteen traumaattisen aivovamman jälkeen, ja johtaa häiriöihin aksonien toiminnassa sekä hermostovaurioihin. Tyypilliset aivokuvantamistekniikat kuten tietokonetomografia ja magneettikuvantaminen (MRI) ovat hyödyllisiä makroskooppisten vaurioiden havaitsemisessa, mutta ne eivät ole riittävän herkkiä diffuusin aksonivaurion havaitsemiseen. Diffuusiopainotettu MRI on kajoamaton kuvantamismenetelmä, joka voi olla sensitiivinen hienovaraisillekin valkean aineen muutoksille ja se pystyy antamaan tietoa hermoratojen muodostamista rakenteellisista yhteyksistä *in vivo*.

Tämän väitöstutkimuksen tavoite oli tutkia aivojen valkean aineen mikrorakenteellisia muutoksia traumaattisen aivovamman jälkeen käyttäen diffuusiopainotettua MRI:tä sekä edistyneitä analyysimenetelmiä. Potilaat, joilla oli todettu lievä aivovamma sekä verrokkeina toimineet ortopedisesti loukkaantuneet potilaat kuvattiin ja tutkittiin osana TBICare EU-hanketta. Paikallisia sekä koko aivojen valkean aineen mikrorakenteellisia ominaisuuksia tutkittiin käyttäen diffuusionensorimenetelmää (DTI) sekä probabilistista traktografiaa. Lisäksi aivojen rakenteellista konnektiivisuutta tutkittiin lievän aivovamman jälkeen. Myös valkean aineen muutosten ja rakenteellisten aivoverkoston ominaisuuksien suhdetta aivovamman jälkeiseen oirekuvaan tutkittiin.

Aivovammapotilailla oli alentunut anisotropia ja korkeampi diffusiviteetti sekä akuutissa/subakuutissa vaiheessa että kroonisessa vaiheessa verrattuna verrokkeihin. Nämä valkean aineen muutokset riippuivat myös hermoratojen suunnista. Aivojen rakenteellinen konnektiivisuus oli poikkeava vain lokaalisti eikä koko verkostoja kuvaavissa globaleissa mittareissa havaittu muutoksia. Valkean aineen muutokset ja sekä globaalit että paikalliset verkostomittarit liittyivät kuitenkin selvästi aivovamman jälkeisiin oireisiin.

Tämä tutkimus osoitti, että uudet diffuusiomagneettikuvien analyysimenetelmät ovat lupaavia työkaluja diffuusin aksonivaurion havaitsemiseen jo aikaisessa vaiheessa lievän traumaattisen aivovamman jälkeen. Lisäksi havaitsimme, että rakenteellisten aivoverkoston ominaisuudet liittyivät aivovamman jälkeisiin oireisiin vahvasti ja voivat auttaa jo aikaisessa vaiheessa myöhemmän oirekuvan ennustamisessa.

AVAINSANAT: traumaattinen aivovamma, diffuusi aksonivaurio, diffuusiopainotettu magneettikuvantaminen, rakenteellinen konnektiivisuus, oirekuva

Table of Contents

Abbreviations	8
List of Original Publications	9
1 Introduction	10
2 Review of the Literature	12
2.1 Traumatic brain injury	12
2.1.1 Pathology of traumatic brain injury	13
2.2 Neuroimaging in traumatic brain injury	14
2.2.1 Magnetic resonance imaging	16
2.2.2 Diffusion and diffusion-weighted magnetic resonance imaging	17
2.2.2.1 Diffusion tensor imaging (DTI)	19
2.2.2.1.1 Tract-based spatial statistics	21
2.2.2.2 Crossing fibers and constrained spherical deconvolution	22
2.2.2.3 Fiber tractography	23
2.2.2.4 Structural brain connectivity and graph theory	25
3 Aims	29
4 Materials and Methods	30
4.1 Study Subjects	30
4.1.1 Outcome	32
4.2 MRI acquisition	32
4.3 Image analysis	32
4.4 Statistical analyses	35
5 Results	37
5.1 White matter microstructural abnormalities in mTBI	37
5.1.1 Whole brain global approach (Publication I)	37
5.2 Structural brain network connectivity (Publication II)	40
5.3 Tract-bases spatial statistics and fiber orientation susceptibility (Publication III)	42
5.4 Correlation analyses	47
5.4.1 Correlation between global FA, age, Fazekas, time of scan post-injury, and outcome (Publication I)	47
5.4.2 Correlation between global and local network properties and outcome (Publication II)	48

5.4.3	Correlation between microstructural properties, average fiber orientation and outcome (Publication III)	49
6	Discussion	50
6.1	Global approach (Publication I)	50
6.2	Structural brain connectivity (Publication II).....	51
6.3	TBSS approach and the analysis of the principal fiber orientation (Publication III).....	52
6.4	Limitations.....	53
7	Summary/Conclusions	54
	Acknowledgements	55
	References	59
	Original Publications	75

Abbreviations

AD	Axial diffusivity
CSD	Constrained spherical deconvolution
CT	Computed tomography
DAI	Diffuse axonal injury
DTI	Diffusion tensor imaging
DW-MRI	Diffusion-weighted magnetic resonance imaging
FA	Fractional anisotropy
FDR	False discovery rate
fODF	Fiber orientation distribution function
FWE	Family-wise error
GCS	Glasgow coma scale
GLM	Generalized linear model
GM	Gray matter
GOSE	Extended Glasgow outcome scale
HARDI	High angular resolution diffusion-weighted imaging
ICC	Intraclass correlation coefficient
MD	Mean diffusivity
MRI	Magnetic resonance imaging
mTBI	Mild traumatic brain injury
OI	Orthopedically injured
PTA	Post-traumatic amnesia
RD	Radial diffusivity
RF	Radio frequency
rmANOVA	Repeated measures analysis of variance
ROI	Region of interest
SD	Spherical deconvolution
SWI	Susceptibility-weighted imaging
TBI	Traumatic brain injury
TBSS	Tract-based spatial statistics
TE	Echo time
TR	Repetition time
WM	White matter

List of Original Publications

This dissertation is based on the following original publications, which are referred to in the text by their Roman numerals:

- I Mehrbod Mohammadian, Timo Roine, Jussi Hirvonen, Timo Kurki, Henna Ala-Seppälä, Janek Frantzén, Ari Katila, Anna Kyllönen, Henna-Riikka Maanpää, Jussi Posti, Riikka Takala, Jussi Tallus, Olli Tenovuo. High angular resolution diffusion-weighted imaging in mild traumatic brain injury. *NeuroImage Clin.* 2017; 13: 174–180.
- II Timo Roine*, Mehrbod Mohammadian*, Jussi Hirvonen, Timo Kurki, Jussi P. Posti, Ari Katila, Riikka Takala, Jussi Tallus, Henna-Riikka Maanpää, Janek Frantzen, Virginia Newcombe, David Menon, Olli Tenovuo. Structural brain connectivity correlates with outcome in mild traumatic brain injury. (2021) (manuscript)
- III Mehrbod Mohammadian, Timo Roine, Jussi Hirvonen, Timo Kurki, Jussi P. Posti, Ari Katila, Riikka Takala, Jussi Tallus, Henna-Riikka Maanpää, Janek Frantzen, Peter J Hutchinson, Virginia Newcombe, David Menon, Olli Tenovuo. Alterations in microstructure and local fiber orientation of the white matter are associated with outcome following mild traumatic brain injury. *JNeurotrauma*, 2020 (<https://doi.org/10.1089/neu.2020.7081>).

* These authors contributed equally to this work

The original publications have been reproduced with the permission of the copyright holders. Original publications are referenced with corresponding Roman numerals as shown above throughout this doctoral thesis.

1 Introduction

Traumatic brain injury (TBI) is by definition any functional or pathological change to the brain that is caused by an external force (Menon et al., 2010) and with a rate of up to 40% deaths related to TBI either directly or indirectly, it is considered to be one of the foremost causes of death and disabilities across all ages (Hyder et al., 2007; Maas et al., 2017; Ng and Lee, 2019; Shenton et al., 2012). The majority of TBI patients have mild TBI (mTBI), ranging between 75% – 90% of all cases (Prince and Bruhns, 2017; Shenton et al., 2012). Patients with mTBI are often not diagnosed properly due to the lack of standard objective measures and are often not referred to the outpatient follow-up after being discharged from the emergency department of the hospitals (McCrea et al., 2017; Prince and Bruhns, 2017; Shenton et al., 2012). Nevertheless, patients with mTBI could be suffering from cognitive impairments and may show clinical symptoms days or months after the injury and in some cases with permanent disabilities (Nolin and Heroux, 2006; Prince and Bruhns, 2017; Ruff, 2005; Shenton et al., 2012; Vanderploeg et al., 2005). Studies have shown that a history of mTBI could result in Alzheimer’s or Parkinson’s later in the life of the patients even after complete recovery (Diaz-Arrastia and Vos, 2014; Perry et al., 2016).

One of the reasons that makes the diagnosis of mTBI challenging is that the conventional brain imaging methods such as computed tomography (CT) and magnetic resonance imaging (MRI) that are usually employed acutely to rule out severe pathologies such as intracranial bleedings or skull fractures, would indicate no abnormalities and are thus insensitive in detecting mTBI (Eierud et al., 2014; Mechtler et al., 2014; Shenton et al., 2012). Diffuse axonal injury (DAI) is suggested to be the main pathology behind mTBI (Browne et al., 2011). Several advanced brain imaging and analysis techniques are developed over the last two decades and are shown to be sensitive enough to detect subtle alterations that occur following mTBI (Kou et al., 2010; Shenton et al., 2012). In this doctoral research however, we focused on one particular MRI technique called diffusion-weighted MRI (DW-MRI). In the “*literature review*” chapter of this thesis, DW-MRI, its concept, acquisition, and analysis techniques are explained. Furthermore, diffusion tensor imaging (DTI) (Basser et al., 1994a) is a DW-MR technique that has opened new

windows into the field of neuroscience and neurology and is widely used to characterize white matter (WM) abnormalities in several brain disorders and injuries (Soares et al., 2013). Several studies have shown that DTI is capable of detecting subtle WM alterations associated with DAI at different time points post-injury in patients with mTBI (Inglese et al., 2005; Koerte et al., 2016; Shenton et al., 2012). DTI is a non-invasive method to investigate WM damage both quantitatively and qualitatively (Zakharova et al., 2014). Fiber tractography (Basser et al., 2000; Mori and van Zijl, 2002) is a method developed to visualize WM fiber tracts and to investigate the fiber bundles quantitatively *in vivo* (Budde et al., 2011; Shenton et al., 2012). Recently, TBI has been reported to affect brain connectivity both structurally and functionally and is said to be a “disorder of brain connectivity” (Fagerholm et al., 2015; Hayes et al., 2016; Imms et al., 2019). In this doctoral research we used advanced DW-MRI and image analysis methods to investigate WM microstructural properties and structural brain connectivity at acute or sub-acute and chronic stages of mTBI. Additionally, we investigated the associations between microstructural and structural brain network properties and patients’ outcome.

2 Review of the Literature

2.1 Traumatic brain injury

Any brain pathology or alterations in brain functionality caused by an external force is defined as TBI (Menon et al., 2010). TBI is a global health burden with an incidence of over two million cases annually in the European Union alone and it is estimated to be the prominent cause of neurodisability by 2030 (Maas et al., 2017). The annual incidence of TBI is increased by the rising number of concussions especially in youth sports and among war veterans who have been exposed to blast injuries (Laskowski et al., 2015) and also due to the aging population (Maas et al., 2017). Motor vehicle accidents and incident falls are the main causes of TBI (Galgano et al., 2017; Peeters et al., 2015). The severity of the injury is traditionally assessed based on the 13-point Glasgow coma scale (GCS) (Teasdale et al., 1978). The GCS is a clinical assessment of the patient's consciousness. TBI severity is classified into three groups, namely mild (GCS score ≥ 13), moderate (GCS score of 9–12), and severe (GCS score ≤ 8).

Despite the value of the GCS from a clinical standpoint in prognosis and management of TBI patients, the GCS score alone is not an ideal classification criterion as it is not specific for the type of pathophysiology of the TBI (Saatman et al., 2008). Criteria for ideal TBI classification are explained in more details in (Hawryluk and Manley, 2015), it is however beyond the scope of this doctoral thesis.

TBI is a heterogeneous injury and has complex pathophysiological mechanisms (Maas et al., 2017). Neuropathological classifications fall into two categories, namely diffuse vs. focal and primary vs. secondary injury.

Approximately 75%–90% of all TBI cases are classified as mTBI (Bazarian et al., 2005; Cassidy et al., 2004; Maas et al., 2017; Prince and Bruhns, 2017; Te Ao et al., 2014) and according to the definition of American Congress of Rehabilitation Medicine, TBI patients with at least one of the following manifestations are considered as patients with mTBI: I) Loss of consciousness of less than half an hour. II) Initial GCS score between 13 and 15. III) Post-traumatic amnesia of no more than 24 hours (American Congress of Rehabilitation Medicine Mild Traumatic Brain Injury Committee of the Head Injury Interdisciplinary Special Interest, 1993).

2.1.1 Pathology of traumatic brain injury

The cerebral cortex consists of neuron cell bodies. These neurons communicate with each other on both short distance via dendrites and long distance via axons. Brain regions are connected via axonal clusters called fiber tracts that consist of the WM pathway between segregated brain regions. WM tracts fan out in the cortex and are terminated at synaptic terminal(s) (Douglas et al., 2019).

Brain injury not only refers to a single event but rather refers to the series of progressive events or processes that occur after the initial injury and there are several types of neuropathologies that ensue brain injury (Gennarelli and Graham, 1998). Two main mechanisms have been defined for TBI: contact and acceleration/deceleration (Gennarelli, 1983). DAI and petechial WM hemorrhages are two categories of diffuse injury, which is a primary characteristics of TBI neuropathology. Different categories of brain injury pathology are demonstrated in Table 1.

Table 1. Different classifications of TBI pathology (modified and adapted from Povlishock and Katz, 2005).

	Focal injury	Diffuse Injury
Primary injury	Focal cortical contusion Deep cerebral hemorrhage Extracerebral hemorrhage	Diffuse axonal injury Petechial white matter hemorrhage
Secondary injury	Delayed neuronal injury Microvascular injury Focal hypoxic-ischemic injury Herniation Regional and diffuse hypometabolism	Delayed neuronal injury Microvascular injury Diffuse hypoxic-ischemic injury Diffuse hypometabolism Neuroinflammation Neurodegeneration

Focal injuries are features of moderate to severe TBI caused by the alterations in intra/extra axial neuronal compartments (McGinn and Povlishock, 2016). Compared to focal injuries, diffuse injuries that are commonly seen in patients with TBI of all severities, are more scattered throughout the brain hence damaged structures are widespread in the brain (McGinn and Povlishock, 2016). Milder head injuries (in most cases) are characterized by DAI. Furthermore, DAI is the main form of diffuse injury and it involves shearing and stretch of axons affecting axonal membrane stability and intracellular transport due to the acceleration/deceleration after TBI (Alexander, 1995; Katz et al., 2015). Diffuse neuronal damage and microstructural changes e.g. axonal disconnections are associated with DAI, which is shown to be a disease of axonal swelling and disconnection leading to disruption in excitatory and

inhibitory networks within the brain (McGinn and Povlishock, 2016). DAI can be a representation of axonal injury and could lead to axonal damage predominantly in deep white matter and sub-cortical structures of the brain persisting for a long term following TBI (Ng and Lee, 2019).

2.2 Neuroimaging in traumatic brain injury

Although imaging is not necessary for all patients with head injury (Glauser, 2004; Nagy et al., 1999), CT and MRI are the imaging modalities widely used at the acute phase of TBI to rule out the severe pathologies that require intervention and also to diagnose WM abnormalities associated with mTBI e.g. DAI. Early and as accurate as possible diagnosis of the injury could lead to a better rehabilitation/treatment plan (if needed) and would be helpful to improve the patient's outcome and would lead to better management or even prevention of the secondary injury (Fakhry et al., 2004; Lee and Newberg, 2005). Furthermore, knowing more about the severity of injury and distribution of DAI throughout the brain could be extremely informative to the clinician who can associate localization with symptoms and also with more targeted treatment. A conventional CT scan is the modality of choice at the acute phase of TBI because of its availability and speed. Being cost-effective and having a short scanning time with a high sensitivity to evaluate bony structures e.g. skull fractures makes CT still the main modality after TBI especially in more severe cases as well as mTBI patients older than 60 (Kelly et al., 1988; Le and Gean, 2009; Lee and Newberg, 2005; Yealy and Hogan, 1991). MRI is usually performed after an initial CT scan (Yealy and Hogan, 1991) and it is superior to CT in detecting hematomas and other types of early bleeds (Lee and Newberg, 2005). Furthermore, CT scans and MRI can only show abnormalities in 10% and 30% percent of patients with mTBI respectively (Borg et al., 2004; Koerte et al., 2016; Mittl et al., 1994). Although conventional MRI is superior to CT in detecting abnormalities associated with mTBI, it still is not sensitive enough to detect the majority of abnormalities associated with mTBI e.g. DAI. The aforementioned conventional modalities are shown to suffer from poor sensitivity to more subtle changes following TBI, for instance, DAI (Koerte et al., 2016; Shenton et al., 2012). DAI is the main cause of cognitive impairments after TBI (Le and Gean, 2009) and CT lacks the sensitivity to detect it (Provenzale, 2010; Su and Bell, 2016). MRI is superior to CT in detecting DAI (Jones et al., 1998; Lee et al., 2008; Niogi and Mukherjee, 2010) as shown in Figure 1 (Bigler, 2005). Acute DAI lesions are often seen as multiple foci of increased (hyperintense) and decreased (hypointense) signals on T2 and T1-weighted MR images. Recently, the term traumatic axonal injury is used more often in the field due to the fact that these lesions are multifocal rather than diffuse. At the chronic phase of TBI, DAI lesions often consist of hemosiderin staining, gliosis, and

non-specific atrophies (Le and Gean, 2009). Furthermore, these lesions can be visible on T2*-weighted MRI as signal hypointensities (Douglas et al., 2018; Le and Gean, 2009; Levi et al., 1990). These lesions are often seen in the gray-white matter junction and within the WM in patients with mTBI (Koerte et al., 2016). There are great computer models out there that have tested and proven the vulnerability of the gray matter / white matter interjunction to shear injury and particularly the sulcal regions (Ghajari et al., 2017).

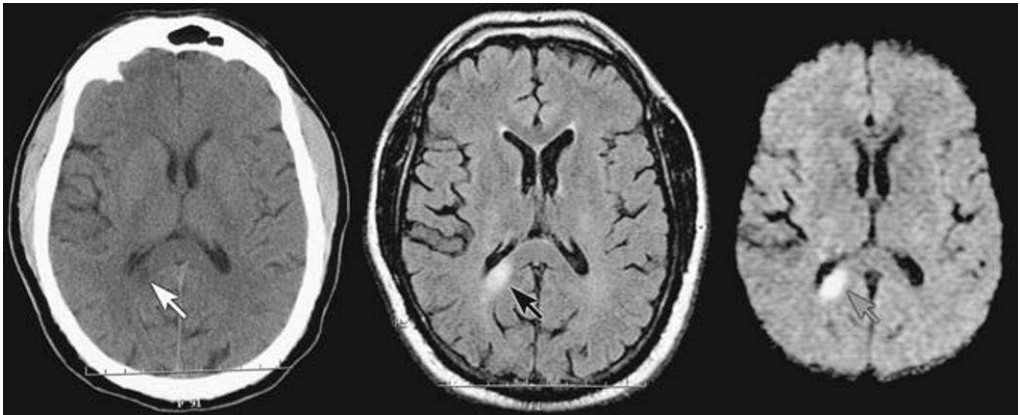


Figure 1. Magnetic resonance imaging (MRI) is better in detecting subtle abnormalities. Computed tomography (CT) scan (A); Fluid-attenuated inversion recovery (FLAIR) (B); Diffusion-weighted MRI (DW-MRI) (C) (adapted from (Bigler, 2005)).

In conjunction with the conventional CT and MR images, more sensitive imaging modalities are often performed to shed more light on mTBI and the mechanisms behind the abnormalities associated with mTBI. Several advanced neuroimaging methods have been developed for better diagnostic and prognostic purposes. High-resolution MR images (to evaluate brain structure), DW-MRI (to study microstructural architecture), dynamic susceptibility contrast MRI, single-photon emission tomography, and arterial spin labeling (to understand blood flow), susceptibility-weighted imaging (SWI) (to assess microhemorrhages) (Barnes and Haacke, 2009), positron emission tomography, and functional MRI (fMRI) (to evaluate brain metabolism and function) are the modalities that could facilitate our understanding of mTBI and have shown to be promising neuroimaging techniques. A summary of the modalities widely used in mTBI, their functions, and advantages are explained by Shenton et al.

2.2.1 Magnetic resonance imaging

The principle of MRI relies in the magnetization properties of the hydrogen [^1H] nucleus, which is found abundantly in the human body as free water to tissue-bound hydrogen hence making it a suitable candidate for clinical applications. In the absence of an external strong static magnetic field (B_0), hydrogen nuclei have random orientations without any net magnetization. However, when B_0 magnetic field is applied, these protons are aligned non-randomly parallel or anti-parallel to the direction of the B_0 field, which would result in a net magnetic moment (Bushberg et al., 2012; Grover et al., 2015) as shown in Figure 2. The nucleus's angular momentum causes the nucleus to precess around the B_0 axis (Figure 3). This precession occurs at a specific angular frequency called the Larmor frequency proportional to the strength of the external magnetic field. Larmor frequency is described by the Larmor equation (2.1):

$$\omega = \gamma B_0 \quad (2.1)$$

where ω is the Larmor frequency, γ is the gyromagnetic ratio, which is 42.58 (MHz/T) for [^1H] in a 1 Tesla magnetic field, and B_0 is the strength of the external magnetic field.

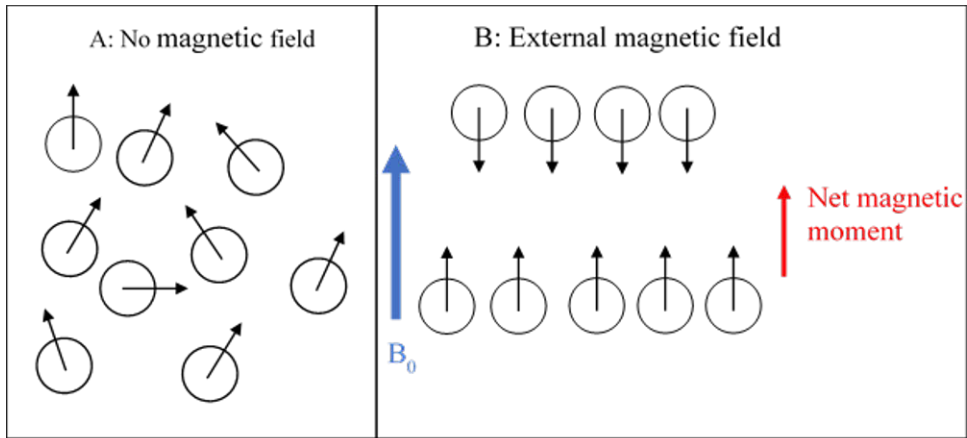


Figure 2. Distribution of hydrogen protons in both without and with the presence of an external magnetic field. **A.** Random orientations of the protons in the absence of an external magnetic field. **B.** Protons are aligned in the direction of the applied external magnetic field.

When a radio frequency (RF) pulse is applied at the Larmor frequency, the net magnetization is flipped from its original direction at equilibrium (the direction of B_0) and protons will be excited by absorbing energy. RF pulses are usually short. Excited protons will be dephased in order to return to the equilibrium and would

induce a signal called “free induction decay” (FID), after the RF pulse is applied. Applying several RF pulses would result in a number of FID signals, which then can be averaged to improve the signal to noise ratio. The averaged FID can then be transformed into an image using mathematical procedures. Flip angles of 90 and 180 degree are the most common flip angles in MR imaging. Spin-echo pulse sequence is one of the most common sequences used to acquire MR images (Jung and Weigel, 2013).

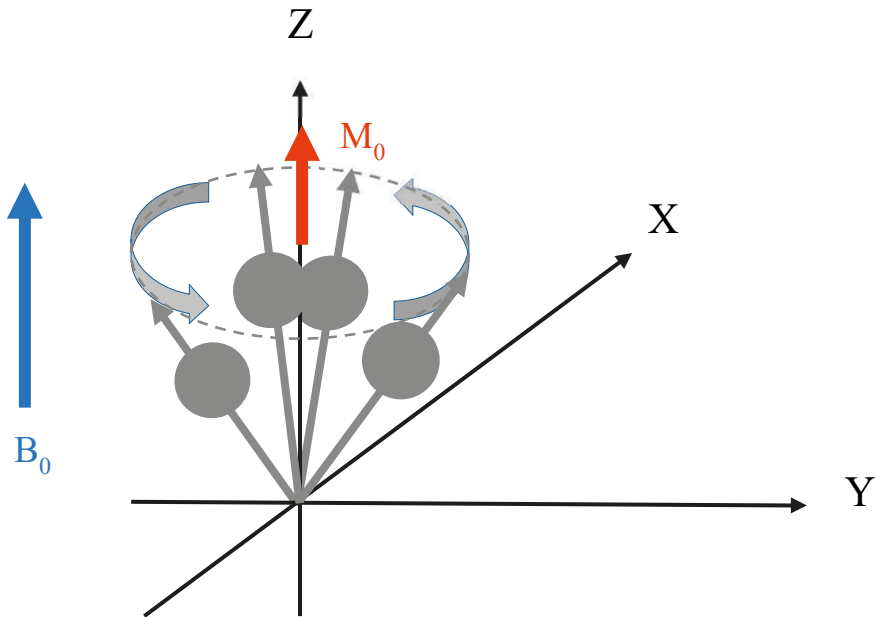


Figure 3. Nuclei precess around the axis of the external field (B_0). M_0 is the direction of the net magnetization.

2.2.2 Diffusion and diffusion-weighted magnetic resonance imaging

Molecules are displaced freely in a liquid or a gas due to thermal energy when there are no obstacles in their way. This flux resulted by the random Brownian motion of particles can be characterized by a diffusion coefficient (D). Einstein’s equation defines that the distribution of the particles’ displacement follows a Gaussian function (Einstein, 1905) of time as shown in (equation 2.2). Where $\langle r^2 \rangle$ is the particles’ mean squared displacement, D is the diffusion coefficient, and Δt is the duration of diffusion.

$$\langle r^2 \rangle = 2D\Delta t \quad (2.2)$$

The human body has different types of tissues and all of them have both intracellular and extracellular compartments. Approximately 60% of the human body consists of water, two-thirds of which is considered to be intracellular (Bianchetti et al., 2009; Hill, 1990). DW-MRI (Le Bihan and Breton, 1985; Wesbey et al., 1984) is based on the Brownian motion of water molecules in the presence of a strong magnetic field (Le Bihan, 2010, 1991).

Water molecules diffuse more freely in the extracellular environment as opposed to the more restricted diffusion in the intracellular environment e.g. in brain WM. Because of the various cellular characteristics of different tissues in the body, diffusion properties vary in different tissues, and different pathologies could affect these diffusion characteristics (Baliyan et al., 2016). Douek and coworkers suggested that the hindrance of diffusion of water molecules in brain WM is due to the presence of fiber tracts and it is anisotropic i.e. diffusion is faster along the direction of the fiber tracts and slower perpendicular to the tracts (Douek et al., 1991).

DW images alone can only give qualitative information. However, by acquiring more than one DW image, one will be able to estimate the diffusivity quantitatively (Jones, 2004). DW-MR images have shown superiority over conventional MR images in detecting DAI quantitatively (Zheng et al., 2006). Signal intensity in the DW-MRI is described by equation (2.3). Where I_0 the signal intensity without any diffusion weighting, TE is the time of echo, T2 is the transverse relaxation time (spin-spin), D is the diffusion coefficient, and b is the parameter known as the “b-value” and denotes the amount of the diffusion-weighting (Jones, 2004).

$$I = I_0 e^{-TE/T2} e^{-bD} \quad (2.3)$$

Diffusion signal can be measured by MRI using a conventional spin-echo sequence. The diffusion-weighting is achieved by using two gradients before and after the 180 degree RF pulse as shown in Figure 4 (Stejskal and Tanner, 1965). The first gradient is applied to dephase the spins of water molecules, and the latter gradient applied after the 180-degree pulse, will rephase the spins. If water molecules have displaced during the time between the two gradients, a signal loss related to diffusivity will be observed. Stejskal and Tanner showed that this signal loss can be defined according to equation (2.4) by assuming that the water molecules displacement follows a Gaussian distribution. In equation (2.4), S_0 is the signal without any diffusion-weighting (also known as b_0), D denotes the diffusion coefficient, and b is the b-value. A b-value of 800 – 3000 s/mm² is commonly used in obtaining DW-MR images.

$$S = S_0 e^{-bD} \quad (2.4)$$

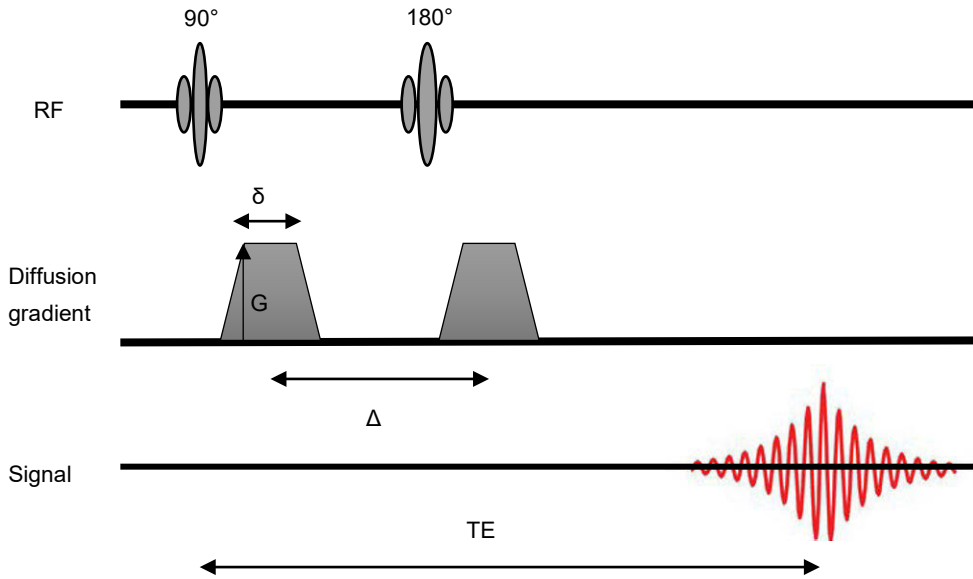


Figure 4. Schematic of Spin-Echo sequence. The first gradient with the magnitude of G and duration of δ would dephase the spins and the second gradient will be applied after the interval of Δ to rephase the phase that was introduced by the first gradient completely. The diffusion-weighted spin-echo signal is acquired after the rephasing of the spins introduced by the second gradient. TE: echo time, RF: radio frequency

2.2.2.1 Diffusion tensor imaging (DTI)

DTI is one of the commonly used methods for visualization and analyzing diffusion (Basser et al., 1994b, 1994a). In order to calculate the diffusion tensor, images in at least six different diffusion directions need to be acquired. The diffusion tensor, D , is a 3 by 3 symmetric matrix:

$$D = \begin{bmatrix} D_{xx} & D_{xy} & D_{xz} \\ D_{xy} & D_{yy} & D_{yz} \\ D_{xz} & D_{yz} & D_{zz} \end{bmatrix} \quad (2.5)$$

The diffusion tensor can be visualized as an ellipsoid and the diagonal elements are the diffusion eigenvalues along the three principal axes (Figure 5). Diffusion properties can be defined using these eigenvalues and their corresponding eigenvectors. The principal orientation of the diffusion is along the eigenvector of the largest eigenvalue (λ_1) (Figure 5). Scalar matrix derived from the diffusion tensor, that describe anisotropy and diffusivity, are used to describe the microstructural properties underlying brain WM. Fractional anisotropy (FA) and mean diffusivity (MD) (Basser and Pierpaoli, 1996) are widely used metrics to describe diffusion quantitatively. FA value varies from 0 to 1 and it is a measure of

the directional coherence of the diffusion of water molecules. In isotropic diffusion, all eigenvalues are equal, and therefore, FA=0. Larger FA is associated with more anisotropic diffusion. FA of 1 happens when only one eigenvalue is non-zero. MD is an average of diffusion in all directions, i.e. average of all eigenvalues, and it is an indication of the overall diffusion. Furthermore, axial diffusivity (AD) and radial diffusivity (RD) are other measures of interest in DTI studies as they describe diffusion in a more direction-specific manner. AD describes the diffusion parallel to and RD diffusion perpendicular to the principal fiber orientation (denoted by the first eigenvector). All these measures are shown in Figure 5.

$$FA = \frac{\sqrt{(\lambda_1 - \lambda_2)^2 + (\lambda_1 - \lambda_3)^2 + (\lambda_2 - \lambda_3)^2}}{2\sqrt{\lambda_1^2 + \lambda_2^2 + \lambda_3^2}} \quad (2.6)$$

$$MD = \frac{\lambda_1 + \lambda_2 + \lambda_3}{3} = \frac{D_{xx} + D_{yy} + D_{zz}}{3} \quad (2.7)$$

$$AD = \lambda_1 \quad (2.8)$$

$$RD = \frac{\lambda_2 + \lambda_3}{2} \quad (2.9)$$

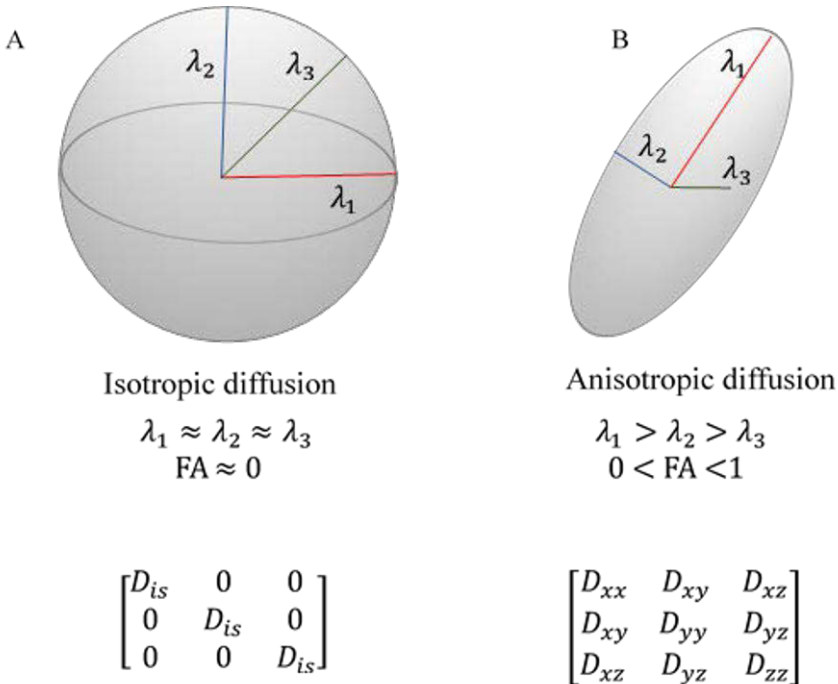


Figure 5. Diffusion ellipsoids and eigenvalues. Diffusion is equal in all direction in an isotropic diffusion D_{is} and FA is almost zero (A), Diffusion is anisotropic and is more than zero. Diffusion is along the direction of the longest eigenvalue (B).

Several more complex metrics, for instance, the Westin coefficients (Westin et al., 2002), have been developed to characterize quantitatively the properties of the diffusion tensor.

DTI was first used in mTBI by Arfanakis et al, (Arfanakis et al., 2002) and it has been shown to be helpful in understanding TBI (Bigler, 2011). Furthermore, computational models suggest that the orientation of WM fibers could predict the degree of injury in DAI (Wright and Ramesh, 2012).

2.2.2.1.1 Tract-based spatial statistics

Tract-based spatial statistics (TBSS) is a method to investigate the WM of the brain voxel-wise. It is a method that does not require a priori hypotheses regarding the localization of differences in WM microstructure.. TBSS is a DTI-based method and a part of the FMRIB Software Library (FSL) (Jenkinson et al., 2012; Smith et al., 2004), suited for structural brain MR image analysis. TBSS creates a WM skeleton from the mean FA image of the whole sample. This WM skeleton consists of the centers of the fiber tracts present in all subjects of the whole cohort. In order to map each subject's skeleton to the mean FA skeleton, TBSS first registers all subjects FA images non-linearly (Jesper L R Andersson et al., 2007; Jesper L.R. Andersson et al., 2007; Jenkinson and Smith, 2001) to a known target that is either derived from the study (study-specific) or is a pre-defined FA map present in the FSL library. Once all FA images are aligned to the target, a mean FA image of the sample is created depicting WM pathways that are on average common among all subjects. Skeletonization is then achieved by searching for the local voxel with the highest FA value in the perpendicular direction to the center of the tract for each subject. A threshold of FA value of 0.2 to 0.3 is usually applied to the voxels in the skeleton to exclude voxels from the gray matter (GM) or cerebrospinal fluid. Figure 6 shows a thresholded mean FA skeleton from our study. Each subject's FA image is then projected to the thresholded mean FA skeleton. At the final stage of analysis, voxel-wise analysis is performed using non-parametric general linear model (GLM).

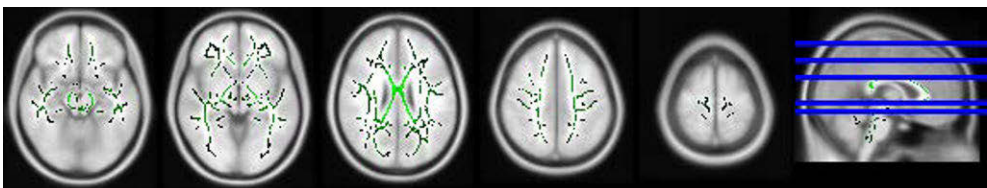


Figure 6. Mean fractional anisotropy (FA) skeleton created from our cohort using tract-based spatial statistics. Threshold for FA value was set at 0.3.

TBSS has been widely used in Alzheimer’s (Liu et al., 2011; Patrick et al., 2020), stroke (Zuo et al., 2018), bipolar disorder (Linke et al., 2020), and TBI (Hashim et al., 2017; Ilvesmäki et al., 2014; Narayana et al., 2014; Wu et al., 2018; Yamagata et al., 2020)

2.2.2.2 Crossing fibers and constrained spherical deconvolution

Although DTI gives valuable information about the microstructural properties of the WM, it suffers from inherent limitations. In DTI, it is assumed that water diffusion follows a Gaussian distribution in each voxel (Alexander et al., 2000) hence it is not optimal especially for tractography purposes. Moreover, DTI is incapable of detecting complex fiber orientations (crossing fibers) in a voxel, which is a major shortcoming and present in the majority of WM voxels (Jeurissen et al., 2013). As presented in Figure 7, the tensor model estimates a highly isotropic diffusion, when multiple fiber orientations are present in a voxel. Novel high angular resolution diffusion-weighted imaging (HARDI) (Tuch et al., 2002) methods have been developed to address the crossing fiber issue and are shown to be more reliable than conventional DTI methods (Mori and van Zijl, 2002). There are different HARDI approaches that can be used to estimate the fiber orientations (Tuch, 2004; Tournier et al., 2004; Alexander, 2005; Wedeen et al., 2005; Dell’Acqua et al., 2007; Descoteaux et al., 2009). A widely used approach is to estimate the diffusion orientation distribution, where a larger density function is observed along the fiber orientations. Diffusion spectrum imaging (Wedeen et al., 2005) and Q-ball imaging (Tuch, 2004) are methods that estimate the diffusion orientation density function. Another approach is the direct estimation of the fiber orientation distribution function (fODF) via spherical deconvolution (SD) (Tournier et al., 2004). In SD, diffusion signal is modeled with a convolution of the fODF and the response function, which is the

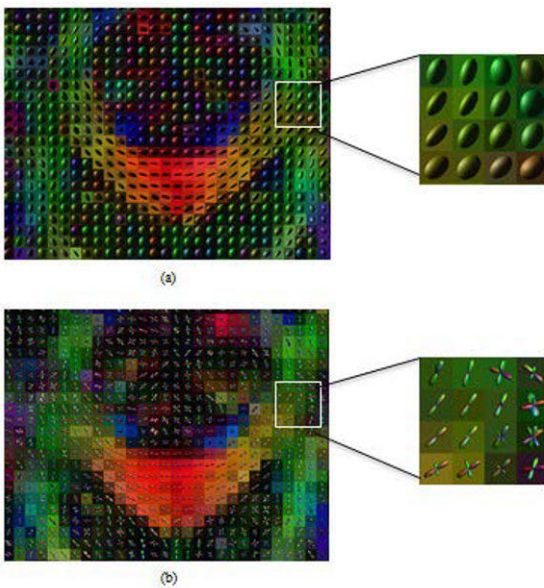


Figure 7. Diffusion ellipsoids in voxels with multiple fibers (a) multiple fiber orientations estimated using constrained spherical deconvolution (b)

estimated response from a single coherently oriented fiber population (Tournier et al., 2004) as illustrated in Figure 8 (Dell'Acqua and Tournier, 2019). It is shown that eliminating negative values of the fODF by using constraints in the deconvolution, could suppress the noise, therefore, improving the results (Tournier et al., 2007). This method is called constrained spherical deconvolution (CSD). The mathematics behind CSD is beyond the scope of this thesis.

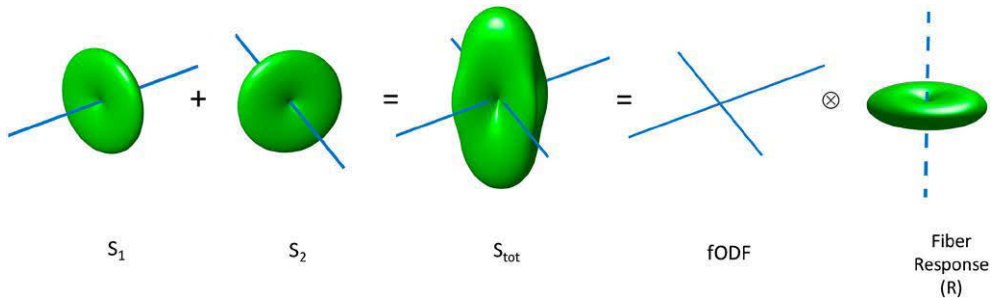


Figure 8. An illustration of the spherical convolution approach: multiple fiber populations within a voxel contribute with additive signals (S_1 , S_2) to the total DW signal (S_{tot}). Under the assumption of a common fiber signal profile, this is equivalent to the convolution over the sphere of an fODF with a chosen fiber response function (R) (adapted from Dell'Acqua and Tournier, 2019).

2.2.2.3 Fiber tractography

Fiber tractography is a widely used method to reconstruct and visualize WM pathways *in vivo* (Basser et al., 2000; Mori et al., 1999) and has been considered one of the main applications of DW-MRI. Various DTI-based (Basser et al., 2000; Conturo et al., 1999; Mori et al., 1999) and HARDI or DSI-based (Behrens et al., 2007; Jeurissen et al., 2011; Tournier et al., 2012; Wedeen et al., 2008) reconstruction methods have been developed to track WM pathways *in vivo*. HARDI-based tractography approaches have been shown to be superior to DTI-based methods (e.g. Farquharson et al. 2013) especially when the aim is to investigate structural brain network (Gigandet et al., 2013). Using higher order models would result in more accurate and reliable WM fiber tracts compared to DTI-based tractography algorithms (Farquharson et al., 2013).

Streamline or fiber tractography is the integration of fiber orientations into connected pathways between brain regions (Behrens and Jbabdi, 2009). A streamline can be represented as a space-curve in three dimensions as shown in Figure 9 (Basser et al., 2000) where vector r denotes the streamline location as a function of length along the streamline s . Moreover, the tangent to streamline $t(s)$ is the estimate of the local fiber orientation, which is the orientation of the principal eigenvector of the tensor in tensor models. Fiber trajectories can be reconstructed by starting at a seed

point step-by-step following the local vector information (Behrens and Jbabdi, 2009). Streamline tractography is performed with prior anatomical knowledge meaning that streamlines can be seeded from every voxel in the brain but they are only retained if the anatomical criteria are met. These streamlines usually pass through white matter regions for example from region A to an end at the final region B as depicted in Figure 10. In probabilistic tractography approaches e.g. CSD-based tractography, tracking algorithm is able to track through regions based on the percentage of confidence that diffusion from seed point A passes through region B.

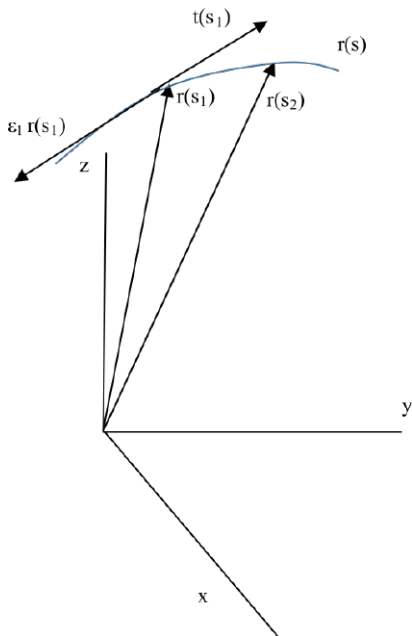


Figure 9. Representation of a white matter fiber trajectory as a space curve, $r(s)$. The local tangent vector, $t(s_1)$, is identified with the eigenvector, $\epsilon_1(r(s_1))$, associated with the largest eigenvalue of the diffusion tensor, D at position $r(s_1)$. Adapted from (Basser et al., 2000)

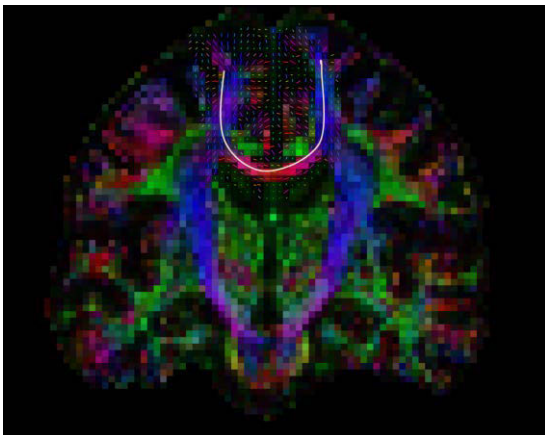


Figure 10. Example of DTI streamlines on coronal slices of the human brain. The white streamline corresponds to the corpus callosum.

Tractography methods can be categorized based on the number of fiber orientations (single or multiple fiber orientations), global or local estimation of the fiber tracts, or deterministic or probabilistic tractography (Bastiani et al., 2012). Choosing the right tractography algorithm and tuning its parameters could largely affect the results of tractography (Bastiani et al., 2012). Probabilistic whole brain CSD-based tractography is conducted in this doctoral research as illustrated in Figure 11.

CSD-based tractography is extensively used in neuroscience and clinical research for example in Alzheimer’s disease (Mito et al., 2018; Reijmer et al., 2012), autism spectrum disorder (Dimond et al., 2019; U. Roine et al., 2015), multiple sclerosis (Lipp et al., 2020), Parkinson’s disease (Petersen et al., 2017), Huntington disease (McColgan et al., 2017), TBI (van der Horn et al., 2017), and stroke (Snow et al., 2016).

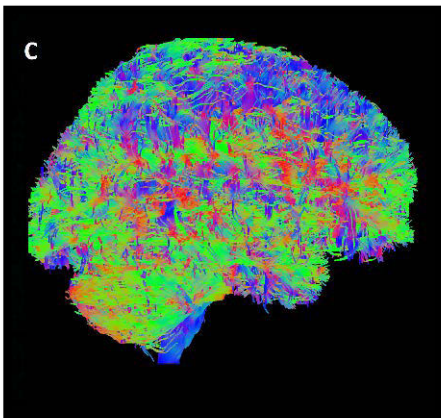


Figure 11. Whole brain tractogram using constrained-spherical deconvolution-based tractography

2.2.2.4 Structural brain connectivity and graph theory

Recently, researchers have been capable of investigating brain structural connectivity due to the development of novel DW-MRI techniques and novel tractography algorithms. Structural brain connectivity networks, also referred to as “*connectome*” or “*connectomics*”, can be presented as a connectivity matrix and can be investigated by using graph theoretical network analysis methods (E. Bullmore and Sporns, 2009; Hagmann et al., 2008, 2007; Iturria-Medina et al., 2007; Mears and Pollard, 2016; Sporns et al., 2005; Tournier, 2019). Structural “*connectome*” analysis is a robust method (Bonilha et al., 2015; Roine et al., 2019) and has been applied in different brain diseases and disorders such as Alzheimer’s disease (La Rocca et al., 2018; Tucholka et al., 2018), healthy aging (Hirsiger et al., 2016), Parkinson’s disease (Tessitore et al., 2016), and TBI (Chung et al., 2019; Spielberg et al., 2015; van der Horn et al., 2017; Wang et al., 2019; Xiao et al., 2015; Zhou,

2017). Structural connectome not only could provide useful information as to how these brain disorders could affect the connectivity between different brain regions, but also would facilitate the early diagnosis of these disorders (Liu et al., 2017).

Choosing the seeding locations is known to have an effect in reconstructing brain network (Buchanan et al., 2014; Li et al., 2012; Zalesky et al., 2010). A connectivity matrix consists of nodes and edges, where parcellated cortical and subcortical GM regions are considered as nodes, and streamlines from the whole brain tractography are the edges of the graph (E. Bullmore and Sporns, 2009; Mears and Pollard, 2016). GM parcellation is usually performed on T1-weighted MR images. Numerous methods have been employed to parcellate the brain (Tournier, 2019) (Huo et al., 2018; O’Muircheartaigh and Jbabdi, 2018; Tzourio-Mazoyer et al., 2002). FreeSurfer’s surface based parcellation (Desikan et al., 2006; Fischl, 2012; Fischl et al., 2002) has been shown to be robust (Desikan et al., 2006) and is commonly used to anatomically parcellate and label brain images (Li et al., 2013). A FreeSurfer parcellated T1-weighted MR image of a control subject is illustrated in Figure 13.

The brain is considered to be a complex network of neurons that are interconnected, and the behavior of such a network can be studied using graph theoretical analysis methods (Sporns, 2012). Once nodes and edges are defined, a graph can be formed. The existence of edges between two (or more) nodes indicates that they are connected. The connections between nodes can be directed/undirected and weighted/unweighted as shown in Figure 12 (Bullmore and Bassett, 2011; Hart et al., 2016; Rubinov and Sporns, 2010). The weighted undirected graph model (Figure 12. C), is used to investigate brain structural connectivity. In a structural brain network, for example, the number of streamlines between two connected brain regions could be assigned to edges as weights (Hagmann et al., 2008). Characteristics of a brain network can be investigated both globally and locally using mathematical and topological analysis approaches (Hart et al., 2016; Rubinov and Sporns, 2010).

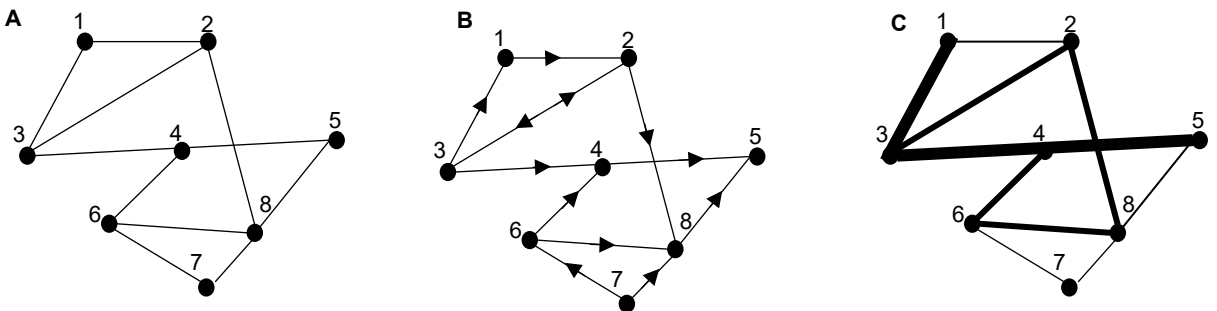


Figure 12. Examples of an undirected and unweighted graph (A), A directed but not weighted graph (B), and a weighted undirected graph (C).

Numerous network properties have been defined to describe the structural connectivity. The metrics that are used in this study are explained in more details below.

Degree: The degree of a node is simply the number of connections that the node has with other nodes and the degree distribution of all nodes could be a representation of the network density (Rubinov and Sporns, 2010).

Global strength: The strength of a complex network can be characterized by averaging the degree of all nodes in the network (Liu et al., 2017).

Local strength: Local strength of a node is the sum of the weights linking that node to other nodes in the network (Onnela et al., 2005).

Clustering coefficient: The clustering coefficient of a node is defined as a fraction of the connected edges between a node and its neighbors to the all possible links between the node and its neighbors, and can be a measure to investigate the segregation of the network when averaged across all nodes i.e. global network clustering coefficient (Rubinov and Sporns, 2010; Watts and Strogatz, 1998).

Characteristic path length: Mean of the shortest path length for any chosen pair of nodes in the network is defined as characteristics path length and could be an indication of the network integrity (Rubinov and Sporns, 2010; Watts and Strogatz, 1998). Characteristic path length will be larger if there is a disruption in the connection between the nodes. For example, if the direct connection between two nodes is disrupted, then the connection (if any) between the nodes will be via another node hence a longer path.

Betweenness centrality: Betweenness centrality is defined as a fraction of shortest path lengths passing through a node, and shows how often a node is included in the shortest path between any pair of nodes, meaning that a node is effective in the flow of the information within the network (Brandes, 2001; Freeman, 1978; Liu et al., 2017; Rubinov and Sporns, 2010).

Global efficiency: Global efficiency is a network measure indicating the integrity of the network that could characterize the capability of information exchange in the network. It is defined as the mean inverse of the shortest path length (Achard and Bullmore, 2007; Latora and Marchiori, 2001; Liu et al., 2017; Rubinov and Sporns, 2010).

Local efficiency: Local efficiency of a node is defined as the global efficiency of a selected sub-network that includes the node itself and its neighbors. The local efficiency of the whole graph is the average of local efficiency calculated from all nodes (Latora and Marchiori, 2001; Liu et al., 2017; Rubinov and Sporns, 2010).

Small-worldness: A small-world network is a network that is both highly integrated i.e. short characteristic path length and segregated i.e. high clustering coefficient. A network is considered to be small-world if the ratio of the characteristic path length divided by the clustering coefficient is more than 1 (Achard

and Bullmore, 2007; Bullmore and Bassett, 2011; Hagmann et al., 2007; Latora and Marchiori, 2001; Rubinov and Sporns, 2010; Sporns and Zwi, 2004; Watts and Strogatz, 1998). Brain structural network is considered to be a small-world network (E. T. Bullmore and Sporns, 2009; Hilgetag and Goulas, 2016).

Graph theoretical network analyses have been used in different brain disorders and brain injuries to investigate the structural brain network connectivity e.g. in stroke (Lee et al., 2019; Sotelo et al., 2020; Yang et al., 2019; Zhang et al., 2017), Parkinson's disease (Barbagallo et al., 2017; Horn et al., 2017; Mishra et al., 2020; Mosley et al., 2019; Zhou et al., 2020), Alzheimer's (Feng et al., 2019; Matthews et al., 2013; Shigemoto et al., 2018), Schizophrenia (Yeo et al., 2016), and TBI (Caeyenberghs et al., 2014; Fagerholm et al., 2015; Imms et al., 2019; Jolly et al., 2020; van der Horn et al., 2016).

3 Aims

The aim of this research was to look for imaging markers for DAI in patients with mTBI. We aimed to identify imaging biomarkers both for diagnostic and prognostic purposes. To this end, we studied microstructural properties of WM following mTBI and investigated the difference in these properties between patients with mTBI and orthopedically injured (OI) controls using CSD-based probabilistic tractography, graph theoretical network analysis, and TBSS. General and specific aims of each part of this study are as follows:

- To identify a sensitive analysis approach to be used as a diagnostic tool to detect WM abnormalities associated with DAI in patients with mTBI. To this end, we studied the whole brain global differences in WM microstructure using brain's skeletonized FA, whole brain tractography, and a fiber-orientation invariant approach in patients with mTBI at the acute/sub-acute phase compared with OI controls. (I)
- To assess the diagnostic and prognostic ability of structural brain network metrics in patients with mTBI. To this end, we investigated the structural network connectivity of the brain in acute/sub-acute and chronic phase in patients with mTBI compared with OI controls and the association of the network properties with the patients' outcome (II).
- To assess the ability of TBSS, as a commonly used DTI-based approach, to detect WM abnormalities associated with DAI in the chronic stage in patients with mTBI and also to evaluate the directional susceptibility of WM abnormalities following mTBI. To this end, we studied the local voxel-wise differences in WM microstructure using TBSS, and investigated directional susceptibility of the differences in patients with mTBI compared with OI controls (III).

4 Materials and Methods

4.1 Study Subjects

This study was a clinical study including approximately 200 patients with TBI that were recruited during the years 2011-2014 as part of the TBICare project in Turku University Hospital, Turku, Finland. In this study, patients were chosen according to the following inclusion and exclusion criteria that are explained in detail in Takala et al., 2015 (Takala et al., 2015).

Patients who were older than 16 years old and diagnosed clinically as patients with TBI were included in this study. Patients with the following criteria were excluded from the study: “chronic subdural hematoma, inability to live independently because of preexisting brain disease, TBI or suspected TBI not needing head CT scan based on the NICE criteria, >2 weeks from the injury, not living in the district and thus preventing follow-up visits (Turku), not speaking the native language, and no consent received” (Takala et al., 2015).

Patients were divided into four categories of OI trauma controls (who had extracranial injuries but no signs or history of any CNS damage), patients with mTBI who had not recovered completely and who did not have any visible traumatic abnormalities on both CT and MRI scans (symptomatic DAI), patients with mTBI who had completely recovered and had no visible abnormalities in their MR scans (recovered DAI), and patients with mTBI who had visible macroscopic lesions of less than 1 mm³ in their conventional MR images (complicated DAI). The reason behind choosing OI trauma controls over healthy controls was that using OI trauma controls could yield results closer to the reality. Also, imaging was only one part of this large study (TBICare), and one of the main aims was to assess TBI biomarkers, that is why we needed extracranial injuries as controls in order to find out what biomarkers are related to TBI and what to trauma in general. Furthermore, all patients were then pooled into one cohort of patients with mTBI. Patients with mTBI were further divided into two groups based on the duration of their PTA (**I**). Demographics of the subjects included in this study are presented in Tables 2 and 3.

Table 2. Characteristics of the study subjects and injury to MR imaging intervals (*Publication I*).

Study group	Number of subjects	Age (years) (mean±std) (min-max)	Gender	Imaging time (days) (mean±std) (min-max)
mTBI patients (GCS>=13)	102	47±20 18-84	70 M 32 F	21±15 1-52
mTBI patients (GCS>=13 & PTA<24 hours)	78	45±20 18-84	52 M 26 F	21±15 2-51
mTBI patients (GCS>=13 & PTA>24 hours)	24	55±16 20-78	18 M 6 F	21±16 1-52
Orthopedically-injured Controls	30	50±20 22-90	14 M 16 F	

Table 3: Demographic and characteristics of mild traumatic brain injury and orthopedic control subjects (*Publications II, III*).

Characteristic	mTBI (n=85)	Orthopedic controls (n=30)	P-value
Age (mean [SD] years)	47 (20)	50 (20)	0.472*
Sex (number [%])			0.026**
Male	59 (69)	14 (46.7)	
Female	26 (31)	16 (53.3)	
Glasgow Coma Scale (number [%])			
GCS = 13	3 (3.5)	-	
GCS = 14	21 (24.7)	-	
GCS = 15	61 (71.8)	-	
Cause of injury (number [%])			
Road Traffic accident	27 (31.8)	-	
Incident fall	43 (50.6)	-	
Other non-intentional injury	5 (5.9)	-	
Violence/assault	8 (9.4)	-	
Other	2 (2.4)	-	
extended Glasgow Outcome Scale (GOSE) (number [%])			
GOSE = 8	31 (36.5)	-	
GOSE = 7	29 (34.1)	-	
GOSE = 6	11 (12.9)	-	
GOSE = 5	3 (3.5)	-	
GOSE = 4	5 (5.9)	-	
GOSE = 3	5 (5.9)	-	
Missing	1 (1.2)	-	
WM hyperintensity Fazekas score (number [%])			
Absent	49 (57.6)	21 (70)	0.50**
Punctate foci	17 (20)	6 (20)	
Beginning confluence	14 (16.5)	2 (6.7)	
Large confluent areas	5 (5.9)	(3.3)	

*student t-test significance; ** Chi-square significance.

4.1.1 Outcome

Patient's outcome was assessed using Glasgow Outcome Scale Extended (GOSE) (Wilson et al., 1998) at the time of the second scan approximately eight months post-injury. GOSE scale classifies patients into eight groups ranging from death (GOSE=1) to complete recovery (GOSE=8).

In this thesis, when the outcome is mentioned, it refers to GOSE.

A dichotomized outcome was defined to classify patients into patients with mTBI that have completely recovered and those with incomplete recovery after injury (**II**).

4.2 MRI acquisition

One-hundred and two patients with mTBI underwent MR imaging within the first two months (2.12 ± 14.9 days) (**I**) and eighty-five of these patients have been scanned again on average eight months after the injury (**II**, **III**). Additionally, 30 OI controls were scanned (**II**, **III**), 21 of whom were scanned a second time approximately 6 months after the initial MR imaging (**I**). It should be noted that patients with TBI who required acute CT scans were included in this study and the MRI was performed additionally as part of the research protocol.

MR acquisition was performed utilizing a Siemens 3T scanner (Magnetom Verio 3T, Siemens Healthcare, Erlangen, Germany). Structural T1-weighted images were obtained using MPRAGE sequence in 176 axial slices with a voxel size of $1 \times 1 \times 1$ mm. Other parameters for 3-D T1-weighted images were TE = 2.98 ms, TR = 2.3 s, flip angle = 9° . DW-MR images were obtained using spin-echo echo-planar imaging in 77 axial slices with a voxel size of $2 \times 2 \times 2$ mm. TE and TR were 106 ms and 11.7s, respectively. Diffusion gradient with a b-value of 1000 s/mm^2 was applied in 64 directions.

Additional sequences were acquired from all subjects including SWI, PD-T2-weighted, axial FLAIR, and gradient-echo images. Furthermore, WM hyperintense lesions were graded using Fazekas score (Fazekas et al., 1987) to account for the WM abnormalities due to chronic small vessel disease.

4.3 Image analysis

DW-MR images were analyzed using ExploreDTI (Leemans et al., 2009) (**I-III**), MATLAB (Mathworks, Natick, MA, USA) (**I-II-III**), FSL (Jenkinson et al., 2012) (**III**), MRtrix 3 (Tournier et al., 2012) (**II**), and FreeSurfer (Fischl, 2012; Fischl et al., 2004) (**II**). DW-MR data were denoised, corrected for bias field, subject motion, and eddy current distortions prior to analysis in all publications included in this doctoral research (all references). FA skeleton was reconstructed based on the TBSS

approach (**I, III**). fODFs were estimated with CSD using up to 6th order spherical harmonics ($l_{\max} = 6$) (Tournier *et al.*, 2004, 2007) (**I, II**) and with the recursive calibration of the single-fiber response function (Tax *et al.*, 2014) (**I**). Analysis methods will be explained in more detail separately for each of the publications in the following paragraphs.

Fiber crossing invariant global approach (I)

In this study, a whole brain fiber tractography was performed using CSD-based probabilistic tractography with an angular threshold of 45 degrees, fODF of more than 0.1, and a step size of 1mm (**I**). Anatomically constrained CSD-based probabilistic tractography was utilized to generate 10 million streamlines for investigating brain structural connectivity (**II**).

Because diffusion metrics are affected by the complex fiber configurations as an inherent shortcoming of DTI, we decided to look only into voxels that have only one fiber orientation within the WM skeleton i.e. a fiber-orientation invariant approach (**I**). Additionally, whole brain CSD-based probabilistic tractography was performed and generated on average 360,000 and 380,000 streamlines in patients with mTBI and OI controls respectively (**I**). Average microstructural properties of the tractograms were calculated by calculating the weighted average sum of voxel-wise multiplication of a track density image and microstructural values in the native space. Global microstructural properties were calculated using the aforementioned approaches in the whole cohort, compared to OI controls. In addition, microstructural properties were compared with patients with mTBI with PTA of more than 24h and less than 24h as well as patients. Global FA values were calculated from the whole skeletonized WM, WM skeletons with a single-fiber, and from the whole brain tractogram. The diffusivity measures were calculated only from the single-fiber WM skeleton.

Structural brain network connectivity (II)

Parcellated T1-weighted images and CSD-based probabilistic tractography were used to construct a brain structural network. T1-weighted images were parcellated utilizing FreeSurfer (Fischl *et al.*, 2004; Fischl, 2012). Desikan-Killiany atlas (Desikan *et al.*, 2006) was then used to define a total of 84 GM brain regions that constituted the nodes of the structural network. A connectivity matrix of 84×84 was then constructed for each subject by assigning tracts to the 84 GM areas (Figure 13).

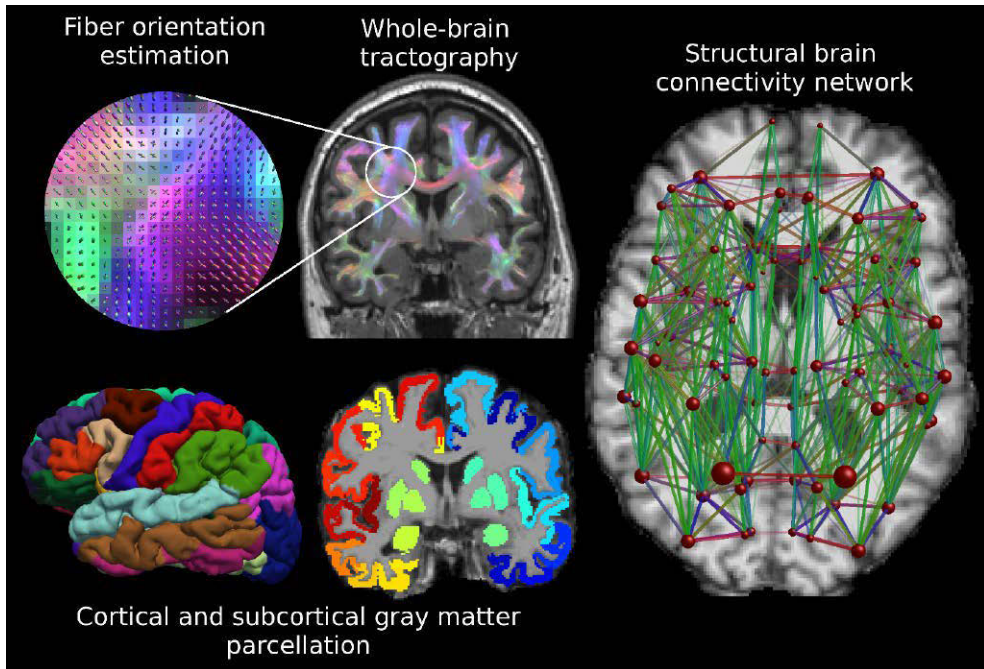


Figure 13. Brain cortical and subcortical gray matter parcellation, whole brain tractography using constrained-spherical deconvolution and the reconstructed structural brain network (Roine et al. 2021)

Graph theoretical analysis (II)

The structural brain connectivity networks were investigated by using graph theoretical analysis with the Brain Connectivity Toolbox (Rubinov and Sporns, 2010). We investigated seven global network properties: betweenness centrality (Freeman, 1978; Brandes, 2001), normalized clustering coefficient (Watts and Strogatz, 1998; Onnela *et al.*, 2005; Saramäki *et al.*, 2007), normalized global efficiency (Latora and Marchiori, 2001), normalized characteristic path length (Watts and Strogatz, 1998), small-worldness (Watts and Strogatz, 1998), degree and strength (Bullmore and Sporns, 2009); and three local network properties: betweenness centrality, local efficiency, and strength. The network properties are explained in the literature review chapter of this thesis. Normalization of the networks was performed by comparing them to 100 randomized networks with equal weight, degree, and strength distributions (Rubinov and Sporns, 2011).

Tract-based spatial statistics following mTBI (III)

TBSS approach (explained in chapter 2 of the current thesis) was used to investigate WM abnormalities following mTBI at the voxel level. Microstructural properties

(FA, MD, RD, and AD) were calculated along the skeletonized WM. FSL's *randomize* tool was then used to perform voxel-wise statistics with 5000 permutations and a cluster free threshold enhancement technique (Smith and Nichols, 2009). In order to rule out the possibility of WM hyperintensities driving the results, we repeated the analyses in the same manner, restricted to patients and controls who had no WM hyperintensities i.e. a Fazekas score of zero. This reduced the number of subjects to 49 patients with mTBI and 21 OI controls. We used a cluster-based analysis, and clusters with more than 10 voxels were investigated further. JHU ICBM DTI WM atlas (Mori et al., 2008) consisting of 48 WM regions was then used to define the regions within each cluster.

Orientation susceptibility analysis (III)

We hypothesized that fibers with the same average orientation might be affected in a similar way. To this end, we analyzed the principal eigenvector of the diffusion tensor in the WM areas that showed abnormalities in the TBSS analysis. Similar to microstructural properties, principal eigenvectors were projected into the WM skeleton and they were rotated to balance for the difference in image orientation between all subjects before calculating the average orientation of the tensors within voxels. We mapped the frequency of the significant voxels on a unit sphere, based on the average orientation to visualize the susceptibility of these WM abnormalities to certain fiber orientations. We used K-means clustering to define clusters based on the specific directionality of the voxels. The optimal number for the number of clusters was calculated as $k=4$ using the Silhouettes method (Rousseeuw, 1987). Then, the average of all microstructural properties with statistically significant results was calculated within each directionally-dependent cluster in patients and the association between average microstructural values and patients' outcome was then assessed.

4.4 Statistical analyses

Normality of all the data used in this doctoral research were assessed using the Kolmogorov-Smirnov test as well as Levine's test to assess the equality of variance. Consequently, appropriate statistical tests were chosen accordingly.

In publication (I), GLM and repeated measures analysis of variance (rmANOVA) were used to evaluate the WM microstructural properties using the whole brain global approach. Group and analysis approach were used as between and within subject factors in rmANOVA analyses. Age and Fazekas were used as covariates in all the statistical models. Results of rmANOVA were corrected for multiple comparisons using Bonferroni correction. Furthermore, the association

between microstructural properties and outcome, scanning time from injury, and age were assessed using parametric Pearson's correlation. A non-parametric Spearman's rank correlation was used to investigate the association of microstructural properties and Fazekas score. Additionally, intraclass correlation coefficient (ICC) analysis (Owen et al., 2013; Shrout, 1998; Shrout and Fleiss, 1979) was performed to assess the reproducibility of the three analysis approaches in 21 controls with repeated scans.

In publication (II), GLM with age and gender as covariates was used to investigate the differences in network properties between patients with mTBI and OI controls. Partial correlations accounting for age and gender were used to evaluate the correlation between network properties and patients' outcome. Results were corrected for multiple comparisons using Bonferroni correction and false discovery rate (FDR) correction.

In publication (III), GLM was used to assess the microstructural properties voxel-wise. Age, gender, and Fazekas score were accounted for in the analyses. TBSS results were corrected for multiple comparisons using family-wise error (FWE) rate. Partial Spearman's correlation was used to assess the correlation between microstructural properties and outcome accounting for age, gender, and Fazekas score. Results were corrected for multiple comparisons using Bonferroni's correction for the number of clusters.

Statistical analyses were performed in SPSS (versions 23, 24, 25, SPSS, IBM, New York, NY), and a 95% confidence interval was used to assess the significance of the results (I, II, III). MATLAB (versions R2017a, and 2018b, MathWorks, MA, USA) (I, II, III) and Python 3.6 (III) were used for visualization of the results and creating the plots.

5 Results

5.1 White matter microstructural abnormalities in mTBI

5.1.1 Whole brain global approach (Publication I)

Lower FA and higher RD were observed in patients with mTBI compared to controls. Patients with mTBI had lower FA ($P=0.002$) and higher RD ($p=0.011$) compared with control subjects. A similar trend was found when patients were divided into two groups with a PTA of less than a day and more than a day. Lower FA was found in patients with mTBI with a PTA of less than a day ($P=0.006$) and in patients with a PTA of more than a day ($P=0.003$) compared with controls. RD was higher in patients with mTBI with a PTA of less than a day ($P=0.033$) and in patients with mTBI with a PTA of more than a day ($P=0.006$) compared with controls.

Furthermore, voxels with lower FA were more dominant in patients with mTBI, while controls had more voxels with high FA values in FA histograms (Figure 14). No differences were found in MD or AD between patients with mTBI and controls. Microstructural properties in patients with mTBI and controls are shown in Tables 4 and 5. Additionally, we showed that when the analysis is restricted to voxels with a single fiber in the WM skeleton, more significant results are yielded compared to the whole skeleton and whole brain tractography approaches (Table 4). Histograms of FA values calculated, using each of the three methods, showed that higher mean FA values are found using the single-fiber approach compared to the other two approaches (Figure 15).

ICC showed that FA and RD of the single-fiber approach were the most robust and reproducible microstructural properties with an ICC of 0.970 and 0.979 respectively. ICC results are shown in Table 6.

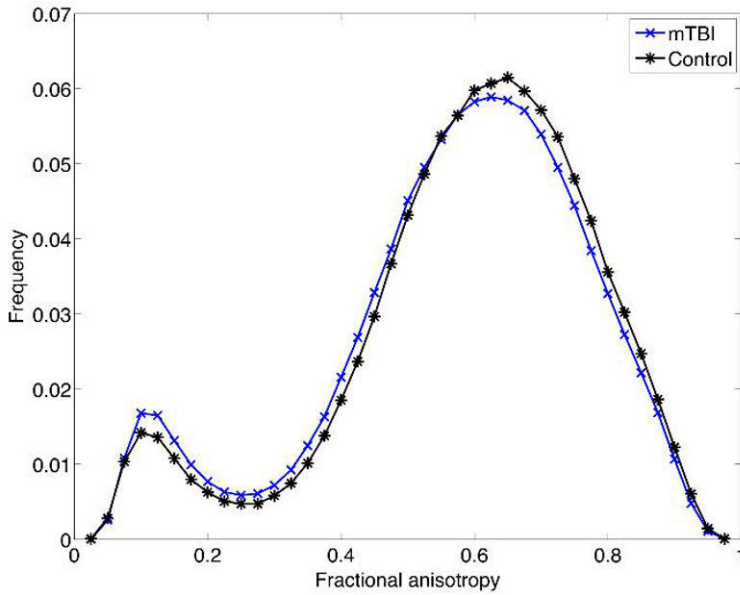


Figure 14. Histograms of FA values in patients with mild traumatic brain injury and control subjects

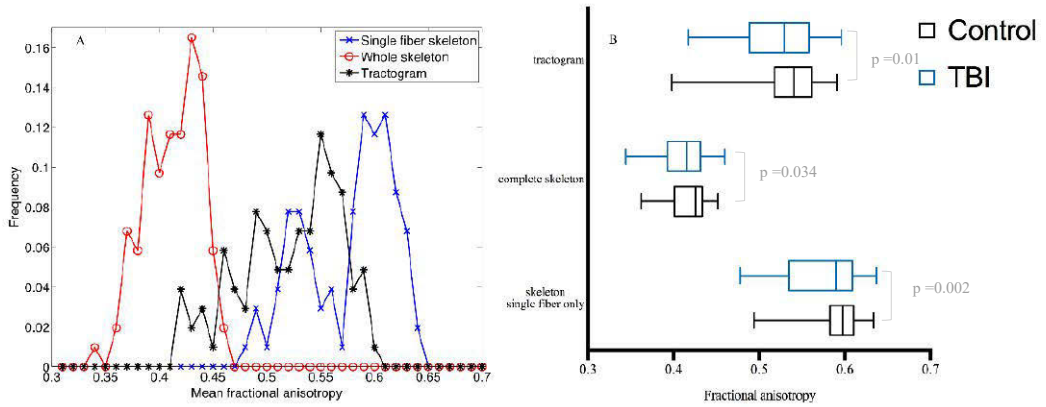


Figure 15. Histogram of FA values calculated from single-fiber skeleton, whole skeleton, and tractogram (A) and comparison of these FA values with any of the approaches between patients with mild traumatic brain injury and controls (B).

Table 4. Global fractional anisotropy (FA) values measured with the three different methods in acute or sub-acute mild traumatic brain injury (mTBI defined as GCS \geq 13, GCS \geq 13 and post traumatic amnesia (PTA) less than 24 hours, GCS \geq 13 and PTA more than 24 hours) vs controls. Age and white matter hyperintensities (measured by Fazekas scale) were used as covariates.

Study group	FA skeleton, single-fiber only		FA skeleton		FA tractogram	
	mean \pm SD	F-value (P-value)	mean \pm SD	F-value (P-value)	mean \pm SD	F-value (P-value)
All mTBI (GCS \geq 13)	0.576 \pm 0.042	9.917 0.002	0.412 \pm 0.025	4.606 0.034	0.521 \pm 0.047	6.764 0.010
Controls	0.591 \pm 0.034		0.419 \pm 0.021		0.534 \pm 0.043	
mTBI (GCS \geq 13 & PTA<24 h)	0.582 \pm 0.040	7.808 0.006	0.416 \pm 0.022	3.195 0.077	0.527 \pm 0.048	4.806 0.031
Controls	0.591 \pm 0.034		0.419 \pm 0.021		0.534 \pm 0.043	
mTBI (GCS \geq 13 & PTA>24 h)	0.556 \pm 0.042	9.497 0.003	0.399 \pm 0.030	5.954 0.018	0.501 \pm 0.040	6.565 0.013
Controls	0.591 \pm 0.034		0.419 \pm 0.021		0.534 \pm 0.043	

Table 5. Global mean (MD), axial (AD) and radial (RD) diffusivity values measured with the single-fiber skeleton approach in acute or sub-acute mild traumatic brain injury (mTBI defined as GCS \geq 13, GCS \geq 13 and post traumatic amnesia (PTA) less than 24 hours, GCS \geq 13 and PTA more than 24 hours) vs controls. Age and white matter hyperintensities (measured by Fazekas scale) were used as covariates.

Study group	MD ($\times 10^{-3}$ mm 2 /s)		AD ($\times 10^{-3}$ mm 2 /s)		RD ($\times 10^{-3}$ mm 2 /s)	
	mean \pm SD	F-value (P-value)	mean \pm SD	F-value (P-value)	mean \pm SD	F-value (P-value)
All mTBI (GCS \geq 13)	0.783 \pm 0.073	2.801 0.097	1.389 \pm 0.081	1.528 0.219	0.560 \pm 0.105	6.672 0.011
Controls	0.765 \pm 0.058		1.368 \pm 0.073		0.525 \pm 0.085	
mTBI (GCS \geq 13 & PTA<24 h)	0.775 \pm 0.073	1.677 0.198	1.383 \pm 0.083	0.808 0.371	0.546 \pm 0.103	4.671 0.033
Controls	0.765 \pm 0.058		1.368 \pm 0.073		0.525 \pm 0.085	
mTBI (GCS \geq 13 & PTA>24 h)	0.809 \pm 0.066	3.99 0.051	1.411 \pm 0.074	2.403 0.127	0.604 \pm 0.103	8.087 0.006
Controls	0.765 \pm 0.058		1.368 \pm 0.073		0.525 \pm 0.085	

Table 6. Reproducibility measured with intraclass correlation coefficient (ICC) of the global microstructural properties (In 21 control subjects with repeated scans).

Microstructural property	ICC
FA, single-fiber skeleton	0.970
FA, whole skeleton	0.920
FA, tractogram	0.958
MD, single-fiber skeleton	0.939
RD, single-fiber skeleton	0.979
AD, single-fiber skeleton	0.863

FA: fractional anisotropy; MD: mean diffusivity; RD: radial diffusivity; AD: axial diffusivity

5.2 Structural brain network connectivity (Publication II)

No significant differences were found in global network properties between patients with mTBI ($n = 85$) at either of the acute/sub-acute or the chronic stage compared to controls ($n = 30$) (Figures 16 and 17). However, there were differences between patients with mTBI in both acute/sub-acute and chronic stages compared to controls in all three local network properties investigated in this study (Figure 18). These differences were found in several brain areas, although only an increased betweenness centrality in patients with mTBI at the chronic stage in the right pars opercularis was statistically significant after correcting for multiple comparisons.

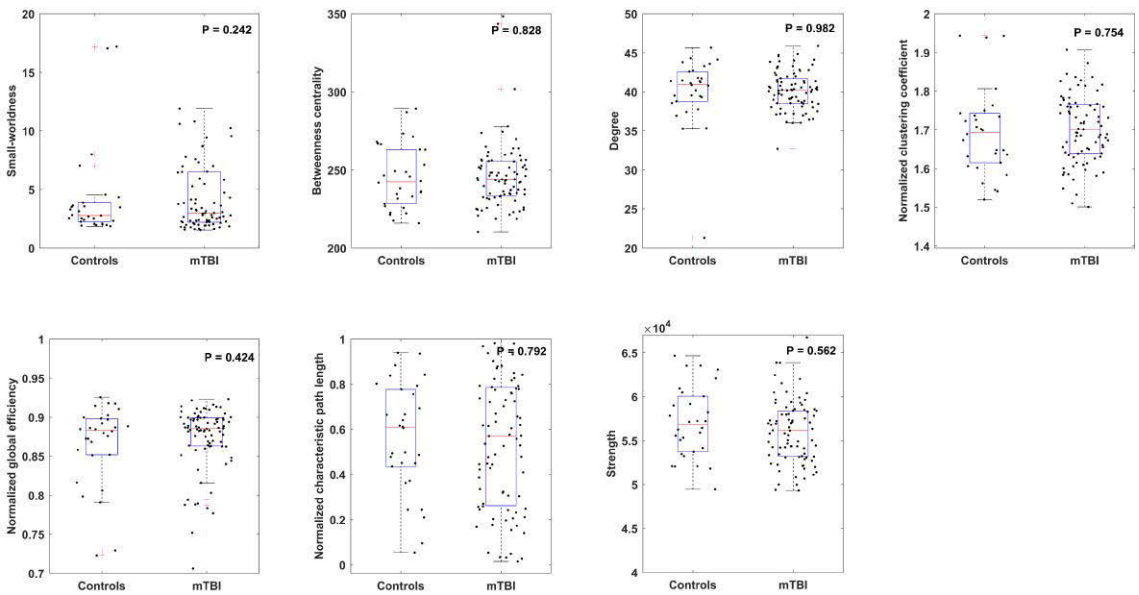


Figure 16. Boxplots of global network measures in patients with mild traumatic brain injury at the acute/sub-acute stage compared to controls.

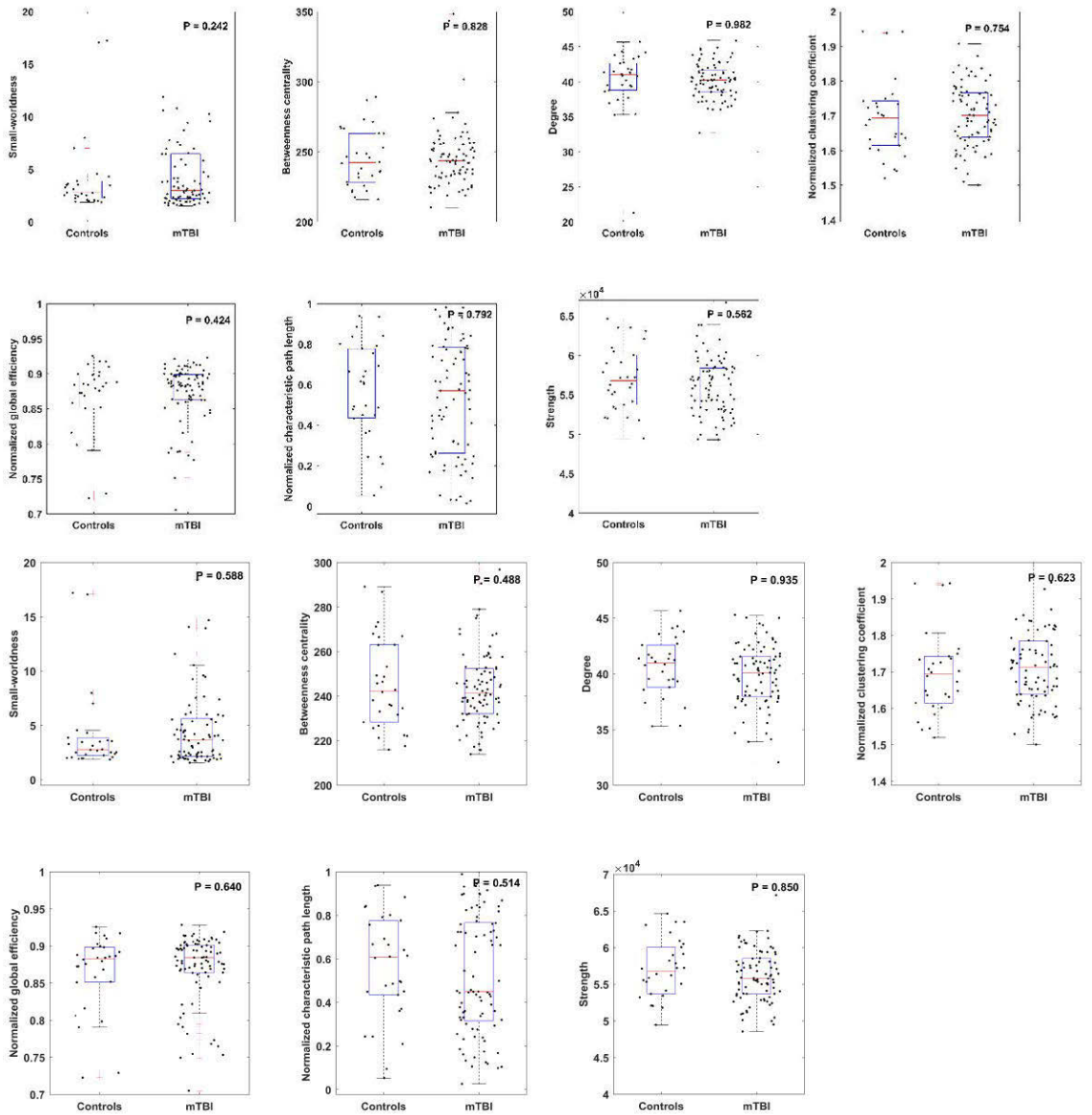


Figure 17. Boxplots of global network measures in patients with mild traumatic brain injury at the chronic stage compared to controls.

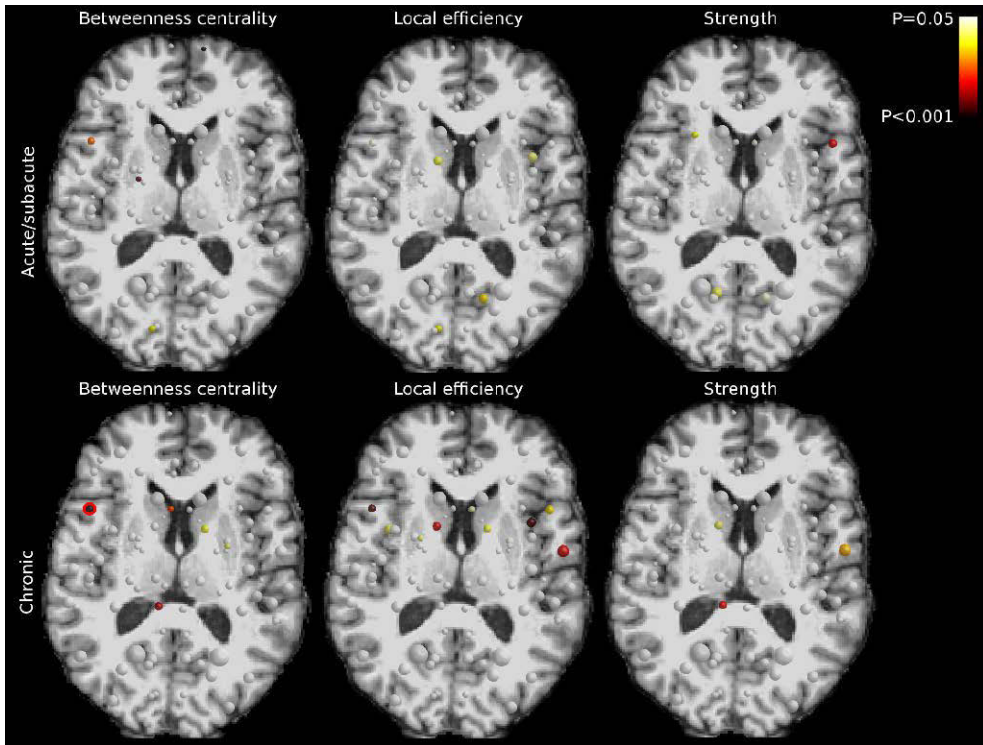


Figure 18. Local differences in the structural brain connectivity networks between patients with mild traumatic brain injury and control subjects. The size of the nodes corresponds to the volume of the gray matter area and the color describes the statistical significance (P-value) of the differences. Age and gender were used as covariates. Significant differences after Bonferroni correction for multiple comparisons are emphasized with red circles.

5.3 Tract-bases spatial statistics and fiber orientation susceptibility (Publication III)

Patients ($n = 85$) had significantly lower FA and higher MD and RD compared to controls ($n = 30$) in various WM regions, as shown in Figure 19. No significant differences were found in AD between patients with mTBI and controls. Significant clusters and their belonging brain areas are demonstrated in Tables 7, 8, and 9 in more detail. When only subjects with a Fazekas score of zero were only considered, differences were found between patients and controls in MD and RD (Figure 20).

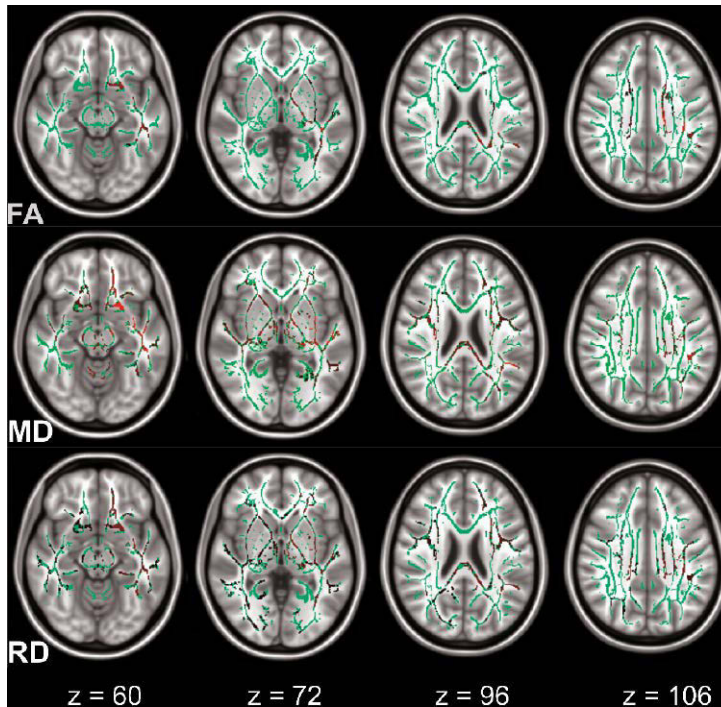


Figure 19. Voxel-wise analysis of diffusion-weighted images shows significantly decreased fractional anisotropy (FA) and increased mean (MD) and radial diffusivity (RD) in patients with mild traumatic brain injury in the chronic stage compared with orthopedically injured controls. Significant voxels are overlaid on T1-weighted MR image.

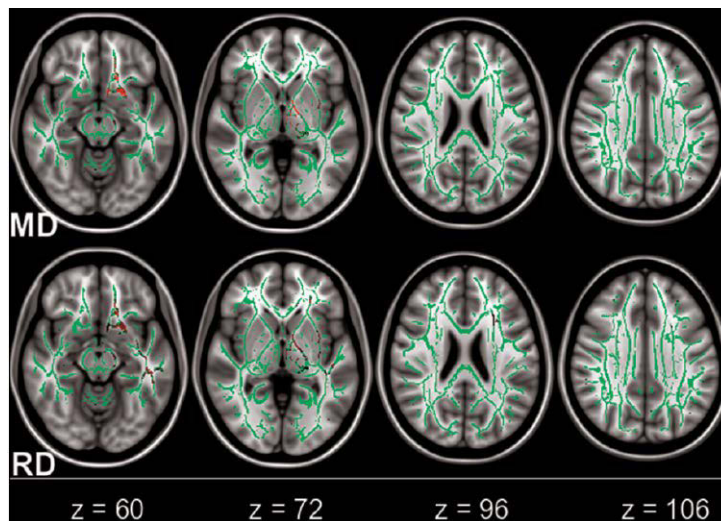


Figure 20. Voxel-wise analysis of diffusion-weighted images shows significantly increased mean (MD) and radial diffusivity (RD) in patients with mild traumatic brain injury without any white matter hyperintensities in the chronic stage compared with orthopedically injured controls. Significant voxels are overlaid on the T1-weighted MR image.

Table 7. The brain regions in the clusters with significant differences in fractional anisotropy ($P < 0.05$, corrected for family-wise error rate) between patients with mild traumatic brain injury in the chronic stage and orthopedic control subject in tract-based spatial statistics analysis. The regions according to JHU white matter atlas with at least 5 % cluster volume or peak significance are included in the table.

Cluster size (#voxels)	Regions in the cluster (% of the cluster)	mTBI	Control	P-value
2654	Superior corona radiata L* (12.96) Body of corpus callosum (33.04) Splenium of corpus callosum (26.04) Superior corona radiata R (14.62) Posterior corona radiata R(6.29)	0.521 ± 0.082	0.60 ± 0.08	0.031
1937	Retrolenticular part of internal capsule L* (11.15) Anterior limb of internal capsule L (12.91) Posterior limb of internal capsule L (21.22) Superior corona radiata L (11.20) External capsule L (29.32)	0.60 ± 0.07	0.64 ± 0.07	0.034
469	Sagittal stratum (include inferior longitudinal fasciculus and inferior fronto-occipital fasciculus) L* (57.99) Posterior thalamic radiation (include optic radiation) L (39.87)	0.63 ± 0.08	0.68 ± 0.07	0.037
310	Superior longitudinal fasciculus L* (100)	0.48 ± 0.09	0.52 ± 0.08	0.033
204	Retrolenticular part of internal capsule L* (38.72) Posterior corona radiata L (27.45) Posterior thalamic radiation (include optic radiation) L (33.82)	0.64 ± 0.05	0.67 ± 0.06	0.034
168	Superior longitudinal fasciculus L*(100)	0.62 ± 0.09	0.68 ± 0.06	0.032
120	External capsule L* (90.83) Retrolenticular part of internal capsule L (9.17)	0.56 ± 0.08	0.59 ± 0.07	0.04
74	Cerebral peduncle L* (100)	0.74 ± 0.06	0.77 ± 0.04	0.038
34	Anterior limb of internal capsule L* (100)	0.35 ± 0.07	0.39 ± 0.09	0.039
24	Splenium of corpus callosum* (100)	0.68 ± 0.06	0.72 ± 0.06	0.037

* Region with the maximum significance in the cluster.

Table 8: The brain regions in the clusters with significant differences in mean diffusivity ($P < 0.05$, corrected for family-wise error rate) between patients with mild traumatic brain injury in the chronic stage and orthopedic control subject in tract-based spatial statistics analysis. The regions according to JHU white matter atlas with at least 5 % cluster volume or peak significance are included in the table.

Cluster size (#voxels)	Regions in the cluster (% of the cluster)	mTBI ($\times 10^{-3} \text{mm}^2/\text{s}$)	Control ($\times 10^{-3} \text{mm}^2/\text{s}$)	P-value
5933	Uncinate fasciculus L* (0.89) Body of corpus callosum (12.54) Splenum of corpus callosum (18.62) Anterior limb of internal capsule L (7.26) Posterior limb of internal capsule L (7.74) Retrolenticular part of internal capsule L (6.69) Anterior corona radiata L (9.00) Superior corona radiata L (8.19) Posterior thalamic radiation (include optic radiation) L (0.62) External capsule L (12.74)	0.76 ± 0.11	0.69 ± 0.15	0.019
3379	Cerebral peduncle R* (6.51) Anterior limb of internal capsule R (8.35) Posterior limb of internal capsule R (11.63) Retrolenticular part of internal capsule R (9.06) Anterior corona radiata R (14.80) Superior corona radiata R (13.76) External capsule R (16.54)	0.85 ± 0.12	0.79 ± 0.11	0.027
740	Inferior cerebellar peduncle R* (18.65) Middle cerebellar peduncle (53.92) Medial lemniscus R (4.60) Superior cerebellar peduncle R (22.84)	0.73 ± 0.10	0.65 ± 0.10	0.024
655	Middle cerebellar peduncle* (74.81) Inferior cerebellar peduncle L (20.46) Superior cerebellar peduncle L (4.73)	0.61 ± 0.06	0.54 ± 0.06	0.033
217	Sagittal stratum (include inferior longitudinal fasciculus and inferior fronto-occipital fasciculus) L* (95.85)	0.77 ± 0.11	0.71 ± 0.10	0.020
162	Superior longitudinal fasciculus L* (100)	0.73 ± 0.10	0.70 ± 0.09	0.026
157	Superior longitudinal fasciculus L* (96.18)	0.71 ± 0.12	0.67 ± 0.12	0.035
113	Sagittal stratum (include inferior longitudinal fasciculus and inferior fronto-occipital fasciculus) L* (1.77) Posterior thalamic radiation (include optic radiation) L (98.23)	0.77 ± 0.11	0.73 ± 0.11	0.034
86	Superior cerebellar peduncle L* (86.05) Medial lemniscus L (13.95)	0.76 ± 0.08	0.71 ± 0.06	0.038
77	Posterior thalamic radiation (include optic radiation) L* (100)	0.81 ± 0.14	0.77 ± 0.08	0.034
66	Superior longitudinal fasciculus L* (100)	0.70 ± 0.11	0.66 ± 0.10	0.037
53	Middle cerebellar peduncle* (81.13) Pontine crossing tract (a part of MCP) (18.88)	0.69 ± 0.09	0.65 ± 0.08	0.039
48	Superior longitudinal fasciculus L* (100)	0.70 ± 0.10	0.66 ± 0.09	0.037
45	Anterior corona radiata R* (88.89) Genu of corpus callosum (11.11)	0.78 ± 0.11	0.73 ± 0.10	0.038
41	Medial lemniscus R* (100)	0.73 ± 0.14	0.68 ± 0.14	0.039
20	Anterior corona radiata L* (100)	0.74 ± 0.09	0.70 ± 0.09	0.037
18	Superior longitudinal fasciculus L* (100)	0.71 ± 0.09	0.69 ± 0.09	0.038
17	Superior longitudinal fasciculus R* (100)	0.73 ± 0.08	0.67 ± 0.09	0.034
17	Anterior corona radiata R* (100)	0.73 ± 0.10	0.70 ± 0.10	0.035
17	Anterior limb of internal capsule L* (100)	0.77 ± 0.13	0.72 ± 0.13	0.031
16	Superior longitudinal fasciculus L* (100)	0.70 ± 0.12	0.66 ± 0.15	0.038
16	Posterior limb of internal capsule R* (100)	0.68 ± 0.08	0.63 ± 0.08	0.031
15	Superior longitudinal fasciculus L* (100)	0.71 ± 0.09	0.65 ± 0.08	0.037
14	Splenum of corpus callosum* (78.57) Posterior thalamic radiation (include optic radiation) L (21.43)	0.82 ± 0.10	0.77 ± 0.11	0.034
13	Posterior corona radiata R* (100)	0.79 ± 0.11	0.75 ± 0.08	0.038
13	Cerebral peduncle R* (30.77) Posterior limb of internal capsule R (69.23)	0.72 ± 0.07	0.70 ± 0.05	0.036
12	Anterior corona radiata L* (100)	0.73 ± 0.11	0.68 ± 0.10	0.042
10	Superior longitudinal fasciculus L* (100)	0.73 ± 0.11	0.69 ± 0.09	0.026

* Region with the maximum significance in the cluster.

Table 9: The brain regions in the clusters with significant differences in radial diffusivity ($P < 0.05$, corrected for family-wise error rate) between patients with mild traumatic brain injury in the chronic stage and orthopedic control subject in tract-based spatial statistics analysis. The regions according to JHU white matter atlas with at least 5 % cluster volume or peak significance are included in the table.

Cluster size (#voxels)	Regions in the cluster (% of the cluster)	mTBI ($\times 10^{-3} \text{mm}^2/\text{s}$)	Control ($\times 10^{-3} \text{mm}^2/\text{s}$)	P-value
8592	Uncinate fasciculus L* (0.65) Body of corpus callosum (9.23) Splenium of corpus callosum (13.90) Posterior limb of internal capsule L (5.96) Anterior corona radiata L (7.68) Superior corona radiata R (5.24) Superior corona radiata L (7.29) External capsule L (9.85)	0.55 ± 0.11	0.49 ± 0.13	0.017
1225	Posterior limb of internal capsule R* (4.49) Anterior limb of internal capsule R (18.53) Anterior corona radiata R (28.98) Superior corona radiata R (17.47) External capsule R (28.57) Superior fronto-occipital fasciculus (could be a part of anterior internal capsule) R (1.88) Uncinate fasciculus R (0.08)	0.39 ± 0.07	0.35 ± 0.09	0.033
310	Superior longitudinal fasciculus L* (98.39)	0.53 ± 0.10	0.49 ± 0.06	0.019
216	Superior longitudinal fasciculus L* (99.54)	0.44 ± 0.12	0.37 ± 0.07	0.019
204	Posterior thalamic radiation (include optic radiation) R* (78.92) Sagittal stratum (include inferior longitudinal fasciculus and inferior fronto-occipital fasciculus) R (21.08)	0.49 ± 0.08	0.43 ± 0.08	0.042
178	Cingulum (hippocampus) R* (100)	0.49 ± 0.10	0.43 ± 0.05	0.042
164	Superior cerebellar peduncle R* (17.68) Middle cerebellar peduncle (26.83) Medial lemniscus R (6.71) Inferior cerebellar peduncle R (48.78)	0.58 ± 0.13	0.50 ± 0.11	0.047
147	Middle cerebellar peduncle* (100)	0.51 ± 0.09	0.46 ± 0.08	0.047
90	Superior longitudinal fasciculus R* (91.11) Superior corona radiata R (8.89)	0.62 ± 0.17	0.56 ± 0.14	0.033
76	Fornix (cres) / Stria terminalis (cannot be resolved with current resolution) L* (100)	0.58 ± 0.11	0.54 ± 0.12	0.024
72	Superior longitudinal fasciculus L* (100)	0.52 ± 0.10	0.46 ± 0.09	0.026
68	Posterior thalamic radiation (include optic radiation) L* (100)	0.54 ± 0.17	0.45 ± 0.08	0.034
57	Superior longitudinal fasciculus R* (100)	0.50 ± 0.11	0.46 ± 0.09	0.045
53	Cingulum (cingulate gyrus) L* (54.72) Splenium of corpus callosum (45.28)	0.46 ± 0.07	0.41 ± 0.07	0.027
50	Splenium of corpus callosum* (80) Posterior corona radiata R (20)	0.40 ± 0.09	0.36 ± 0.10	0.045
49	Cingulum (cingulate gyrus) R* (81.63) Splenium of corpus callosum (18.37)	0.46 ± 0.09	0.41 ± 0.07	0.043
46	Posterior thalamic radiation (include optic radiation) R* (100)	0.53 ± 0.14	0.49 ± 0.10	0.038
40	Superior longitudinal fasciculus L* (100)	0.51 ± 0.10	0.48 ± 0.09	0.027
32	Superior longitudinal fasciculus R* (100)	0.45 ± 0.10	0.42 ± 0.09	0.040
32	Middle cerebellar peduncle* (100)	0.32 ± 0.06	0.27 ± 0.05	0.050
27	Cingulum (hippocampus) R* (100)	0.47 ± 0.07	0.45 ± 0.08	0.045
25	Anterior limb of internal capsule L* (100)	0.64 ± 0.15	0.58 ± 0.14	0.030
23	Cingulum (hippocampus) L* (100)	0.46 ± 0.09	0.42 ± 0.07	0.022
17	Cingulum (cingulate gyrus) L* (100)	0.44 ± 0.09	0.39 ± 0.07	0.027
16	Superior longitudinal fasciculus L* (100)	0.45 ± 0.10	0.42 ± 0.09	0.046
16	Anterior corona radiata R* (100)	0.54 ± 0.11	0.51 ± 0.09	0.033
16	Posterior limb of internal capsule R* (100)	0.52 ± 0.09	0.46 ± 0.08	0.033
15	Cingulum (cingulate gyrus) L* (100)	0.39 ± 0.08	0.37 ± 0.07	0.031
15	Superior longitudinal fasciculus L* (100)	0.45 ± 0.09	0.39 ± 0.08	0.031
13	Superior longitudinal fasciculus L* (100)	0.56 ± 0.12	0.53 ± 0.13	0.035
13	Posterior corona radiata R* (100)	0.56 ± 0.14	0.52 ± 0.13	0.022
12	Cerebral peduncle R* (100)	0.40 ± 0.09	0.37 ± 0.07	0.033
11	Superior longitudinal fasciculus R* (100)	0.48 ± 0.08	0.45 ± 0.09	0.043
11	Cingulum (cingulate gyrus) R* (100)	0.45 ± 0.08	0.41 ± 0.08	0.043
11	Sagittal stratum (include inferior longitudinal fasciculus and inferior fronto-occipital fasciculus) L* (100)	0.62 ± 0.28	0.58 ± 0.12	0.024

*Region with the maximum significance in the cluster.

Analysis of the principal fiber orientation resulted in 4 clusters in voxels with similar average fiber orientations. Similar clusters were found for all the microstructural properties that showed significant differences between patients with mTBI and controls. The frequency of the voxels with similar average orientations, as well as the four orientation-dependent clusters, are shown for each measure in Figure 21.

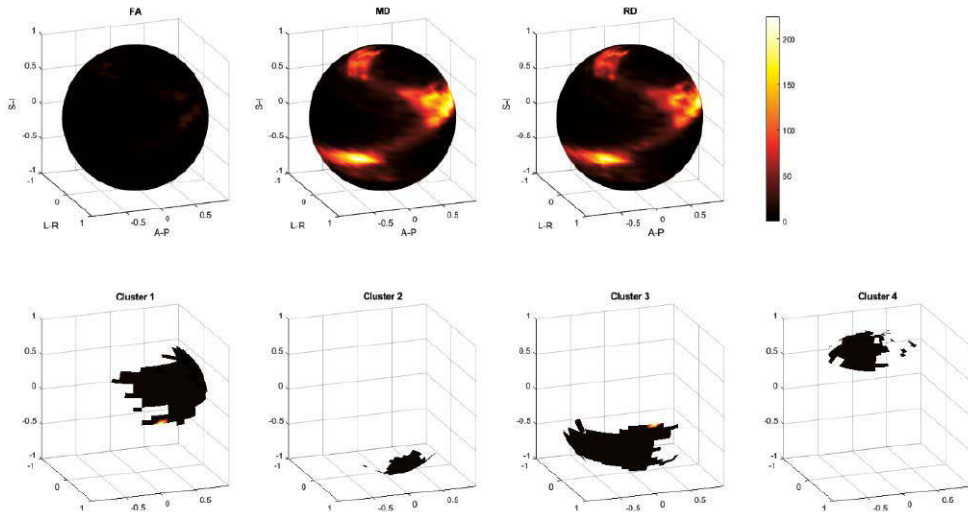


Figure 21. Directional analysis of the significant microstructural differences in the chronic stage of TBI compared to control subjects. The number of voxels with significant differences is mapped onto the unit sphere according to the principal fiber orientation in the corresponding voxel. Four clusters of significant changes in fractional anisotropy (FA), mean diffusivity (MD), and radial diffusivity (RD) are found in certain orientations. Anterior-Posterior (A-P); Left-Right (L-R); Superior-Inferior (S-I).

5.4 Correlation analyses

5.4.1 Correlation between global FA, age, Fazekas, time of scan post-injury, and outcome (Publication I)

In the whole cohort, FA was positively correlated with the outcome ($r=0.363$, $p<0.001$), and it was negatively correlated with Fazekas ($r=-0.619$, $p<0.001$) and age ($r=-0.787$, $p<0.001$). FA was significantly correlated with the outcome ($r=0.341$, $p=0.004$), Fazekas ($r=-0.646$, $p<0.001$), and age ($r=-0.814$, $p<0.001$) in patients with mTBI and $PTA \leq 24$ h. In patients with PTA of more than a day, FA was only correlated with age ($r=-0.639$, $p<0.001$). No significant correlations were found between FA and the time of scan post-injury, neither in the whole cohort nor in any of the dichotomized patient groups based on PTA.

5.4.2 Correlation between global and local network properties and outcome (Publication II)

Local efficiency and strength in the left putamen were significantly associated with outcome in both acute/sub-acute and chronic stages in patients with mTBI. Higher local efficiency and strength were associated with better outcome in the left putamen in acute/subacute stage of mTBI (local efficiency: $r=0.43$, $P<0.0001$; strength: $r=0.50$, $P<0.00001$) and in the chronic stage (local efficiency: $r=0.40$, $P<0.001$; strength: $r=0.45$, $P<0.0001$). Local betweenness centrality in the left postcentral cortex in acute/sub-acute stage was negatively correlated with the outcome ($r=-0.39$, $P<0.001$). Furthermore, in the chronic stage, higher local strengths in the left parahippocampal cortex ($r=0.38$, $P<0.001$) and the left entorhinal cortex ($r=0.39$, $P<0.001$) were associated with better outcome. Correlation between local network measures and the outcome are shown in Figure 22.

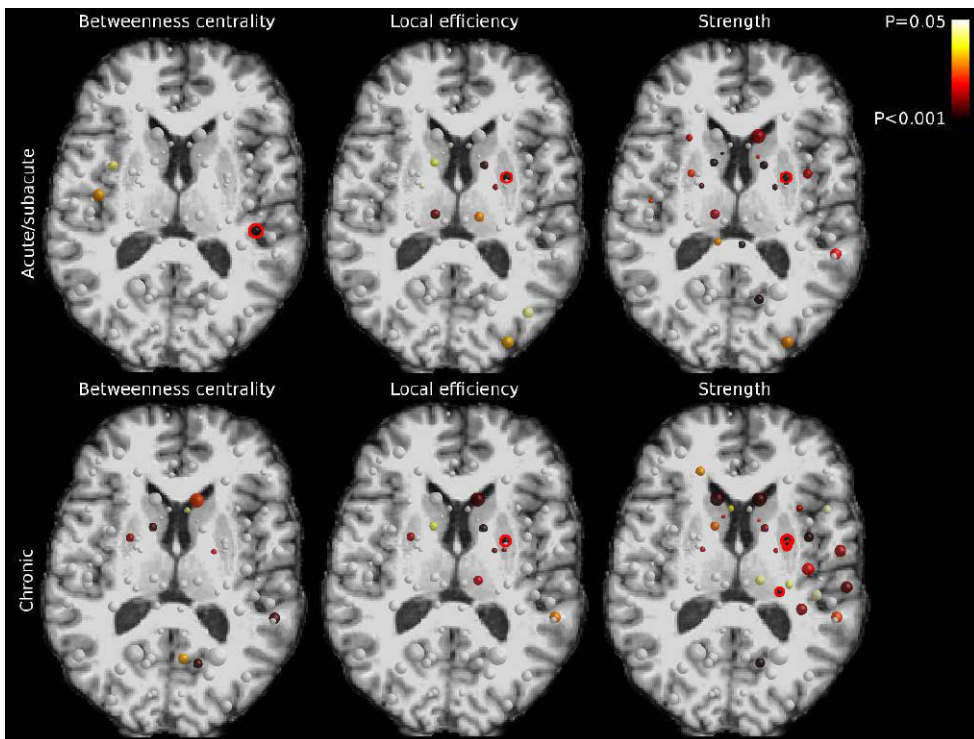


Figure 22. Correlations of the local graph theoretical properties with the neurological outcome in mild traumatic brain injury. The size of the nodes corresponds to the volume of the gray matter area and the color indicates the statistical significance (P-value) of the correlation with the neurological outcome measured with Extended Glasgow Outcome Scale (GOSE). Age and gender were used as covariates. Significant differences after Bonferroni correction for multiple comparisons are emphasized with red circles.

5.4.3 Correlation between microstructural properties, average fiber orientation and outcome (Publication III)

FA was positively correlated with GOSE in the left retrolenticular part of internal capsule (Spearman's $\rho = 0.34$, $p=0.002$) and the left cerebral peduncle (Spearman's $\rho = 0.2$, $p = 0.009$). MD and RD were negatively correlated with outcome in the left superior longitudinal fasciculus (Spearman's $\rho = -0.35$, $p = 0.001$) and (Spearman's $\rho = -0.4$, $p < 0.001$) respectively. RD was also negatively correlated with outcome in the right posterior limb of internal capsule (Spearman's $\rho = -0.4$, $p < 0.001$) and the left cingulum (cingulate gyrus) (Spearman's $\rho = -0.39$, $p < 0.001$).

Additionally, better outcome was associated with higher anisotropy and lower diffusivity in all clusters with similar average fiber orientations.

6 Discussion

Patients with mTBI had lower anisotropy and higher diffusivity measures compared to controls using a global approach in the acute/sub-acute stage in **Publication I**, and the local voxel-wise TBSS approach in **Publication III** in the chronic stage. The results of decreased anisotropy and increased diffusivity at the acute/sub-acute stage are in line with previous studies (Arfanakis et al., 2002; Messé et al., 2011; Narayana et al., 2014; Toth et al., 2013). Furthermore, decreased FA and increased MD, and RD in patients with mTBI at the chronic stage is in accordance with previous studies (Jorge et al., 2012; Kraus et al., 2007; Wada et al., 2012).

Increased diffusivity and reduced anisotropy could be indications of brain edema at the acute/sub-acute phase (Iffland et al., 2014) or axonal demyelination or degeneration (Song et al., 2003). Mac Donald et al., have shown that the degradation of axons is the primary pathology at the acute stage of TBI (Mac Donald et al., 2007). Decreased FA could be a reflection of demyelination or damaged axonal integrity (Beaulieu, 2002; Harsan et al., 2006; Song et al., 2003). Increased RD in the chronic stage could be because of the demyelination (Hutchinson et al., 2018). A combination of the primary and secondary injury at the chronic stage could be caused by Wallerian degeneration (Narayana, 2017).

6.1 Global approach (Publication I)

In **Publication I**, we showed that this difference between groups in microstructural properties is dependent on the analysis approach. Using CSD-based tractography, the analysis approach restricted to single-fiber voxels within the WM skeleton showed the highest sensitivity and reliability compared to complete WM skeleton or the tractogram. Furthermore, higher FA was associated with better outcome in all patients with mTBI and in patients with mTBI with a duration of PTA less than a day.

In the whole brain histogram analysis, we demonstrated that the differences between patients with mTBI and controls are visible, at both high and low FA values. Inglese et al., however, did not report such trends and they showed no differences in whole brain histograms between patients with mTBI and control subject in their

study (Inglese et al., 2005). Ilvesmäki and colleagues also reported that DTI is not capable of detecting WM changes associated with DAI in patients with mTBI at the acute stage (Ilvesmäki et al., 2014). It is noteworthy to mention that both of these studies were limited regarding the number of diffusion gradient directions. This would suggest that common DTI-based approaches such as TBSS may not be sensitive enough to the subtle changes in association with DAI after TBI at the acute/sub-acute stage due to the choice of acquisition parameters or post-processing techniques. Choosing proper acquisition parameters such as increasing the number of applied diffusion gradients could enhance the sensitivity, although the inherent limitations of DTI will not be resolved.

6.2 Structural brain connectivity (Publication II)

In *Publication II* we showed that brain connectivity is altered after mTBI but not at the global level, although global network metrics at both acute/sub-acute and chronic stages correlated with outcome. Finding no global difference in brain network metrics between patients with mTBI and OI controls could be because by looking at the brain as a network, patients with mTBI do not significantly differ from the controls. Therefore, it is expected that no difference in global brain structural network metrics is found in mild cases of TBI compared with OI controls.

Furthermore, local structural network was disrupted at both stages after mTBI, and similar to the global network metrics, local network measures were also associated with outcome. Local network disruption was prominent at the chronic stage and in the right pars opercularis region of the brain. The right pars opercularis is known to be part of the Broca's area (Broca, 1861) that is involved in speech production (Hickok, 2012; Indefrey and Levelt, 2004). Studies have shown that the disruption of right pars opercularis is found in major depressive disorder (Qiu et al., 2014), autism spectrum disorder (Rudie et al., 2012), and anxiety (Hölzel et al., 2013).

Investigation of structural brain connectivity after TBI mostly focused on patients with moderate to severe TBI. Only a few studies have assessed the structural brain network disruption after mTBI (Dall'Acqua et al., 2017, 2016; van der Horn et al., 2017). Our findings of no significant differences in global network metrics between patients with mTBI and controls are in accordance with these recent studies (Dall'Acqua et al., 2016; van der Horn et al., 2017). Despite showing no difference in global measures compared to controls, global network metrics at both acute/sub-acute and chronic stages were associated with the outcome. Furthermore, local network properties in several nodes were correlated with the outcome. Left putamen was the prominent region showing a significant correlation between local network measures (strength and efficiency) and the outcome. The disruption of structural

connectivity in putamen after TBI has not been reported in the literature before, but volumetric changes in putamen after TBI have been reported previously (Gooijers et al., 2016; Zagorchev et al., 2016), and the decreased putamen volume is shown to be associated with deficits in motor skills after TBI (Gooijers et al., 2016).

Our findings of correlation between local and global network metrics and the outcome could indicate that brain structural connectivity could be a predictor of the outcome after TBI. Although stronger correlations were found between network measures and outcome at the chronic stage, some of these network measures could provide clinically valuable information and could perhaps be used for outcome prediction already at the acute/sub-acute stage after TBI.

6.3 TBSS approach and the analysis of the principal fiber orientation (Publication III)

Whiter matter microstructural abnormalities were found in several brain regions showed. Patients with mTBI had lower anisotropy compared to OI controls. In addition, MD and RD values were higher in patients compared to controls. This could mean that diffusion properties are not affected along the axons, and diffusivity is altered most prominently perpendicular to axons and our findings suggest that the diffusion perpendicular to axons drives the results. Furthermore, microstructural properties were correlated with patients' outcome. Better outcome was associated with higher FA and lower MD and RD. Similar to average regional microstructural properties, mean FA, MD, and RD values from the clusters with similar average fiber orientations were associated with the outcome. High anisotropy and low diffusivity were associated with better outcome. In the post hoc analysis to see if the differences between patients with mTBI and controls are indeed due to the trauma, and to eliminate the effects of WM hyperintensities, we found no differences in anisotropy between patients and controls (with Fazekas score of 1). However, this could be because of the sample size as the results were similar to the results in subjects without WM hyperintensities when a more strict significant level ($p < 0.025$) was introduced to the results of the whole cohort. This indicated that sample size could in fact be the reason for the difference in the results.

Four distinct clusters of voxels with significant WM abnormalities were found that had similar average fiber orientations. As there is no such study in patients with mTBI to our knowledge, it is unclear that these findings are because of the prevalence of these fiber orientations in the FA skeleton or they could indeed indicate the orientation susceptibility of these WM abnormalities due to brain trauma.

6.4 Limitations

It is worth mentioning that our TBI cohort does not represent the general population of patients with mTBI and our findings may not translate to all patients with mTBI. Furthermore, regardless of having available data for both acute/sub-acute and chronic stages after mTBI, we only performed cross-sectional analyses hence lacking the longitudinal analysis to assess abnormalities and their trajectory over time. The reason was an agreement between us and our collaborators that only cross-sectional results would be included in this doctoral dissertation. In addition, we only included patients scanned at the acute or sub-acute stage in *Publication I*, which could have had an impact on our results. Nevertheless, we found no association between our findings and the time of scan after injury. Also, we could not assess the handedness of the patients and controls as structural brain network or even WM tracts might have been slightly different between right-handed and left-handed subjects.

Recently, Wilde et al. showed that using healthy controls in contrast to OI controls would yield results that are closer to reality and reliable (Wilde et al., 2018). Patients with extracranial orthopedic injuries were used as controls in this doctoral research and although careful considerations were considered when recruiting patients, the possibility of any indirect impact on the head cannot be completely ruled out.

Furthermore, while a b-value of 1000 s.mm^{-2} is not the optimal amount of diffusion weighting for CSD-based tractography (Tournier et al., 2013), 64 diffusion gradients with this rather low b-value were sufficient to detect crossing fibers with a $l_{\max} = 6$. Single-shell diffusion data was utilized in all of the studies included in this doctoral research while using multi-shell DW-MR data would have improved the characterization of WM tracts (Jeurissen et al., 2014).

CSD-based approach and DTI approaches are affected by partial volume effects (Alexander et al., 2000; Roine et al., 2014; T. Roine et al., 2015). By using skeletonized WM (in *Publications I, III*), however, we tried to minimize these effects. It is noteworthy that WM skeletonization suffers from inherent limitations (Bach et al., 2014), though it is still useful as it mitigates the partial volume effect problem.

7 Summary/Conclusions

We aimed to look for imaging markers for DAI in patients with mTBI for both diagnostic and prognostic purposes by investigating WM microstructural abnormalities associated with DAI in patients with mTBI at the acute/sub-acute and chronic stages. Consequently, we focused on using a commonly used DTI technique called TBSS as well as more advanced HARDI methods. Although each of these methods has its advantages and disadvantages, we showed that HARDI methods at the acute/sub-acute phase could be sensitive enough to detect WM abnormalities while commonly used DTI-based approaches (TBSS in this book) lack such sensitivity. Furthermore, we demonstrated that the structural brain network is altered locally (and not globally) following mTBI. We showed that these WM microstructure and structural network alterations following mTBI are associated with the outcome.

As the next step, combining blood biomarkers and imaging could help us better characterize axonal injury and would be one step forward to achieving a prognostic model for patients with mTBI.

Acknowledgements

In this chapter, I would like to thank a (rather large) group of excellent people each of whom have had an impact not only career-wise but also in all aspects of my life during these past years.

First and foremost, I want to express my sincerest gratitude to my outstanding supervisors, Prof. Olli Tenovuo, Adjunct Professor Timo Kurki, and Dr. Timo Roine.

Olli, you have been the best supervisor one can ever ask for. It is now years since we talked about my PhD topic in your office and I still have your constant support and supervision as I had in the beginning. Thank you for seeing the potential in me to be part of your vibrant research group. You have provided me great opportunities and you've given me the chance to grow. I'm truly grateful to you. We've been through challenges during these years and I have always appreciated how you stay calm even in the most challenging and stressful times. I am forever grateful to you for welcoming me to your research group and giving me opportunities to improve myself not only academically but also on a personal level. Your kindness, humility, and great leadership skills have taught me a lot during these years. Timo Kurki, thank you for your great supervision and all the time that you put during these years. Timo Roine, not only have you been a great supervisor but also a peer from the beginning of my doctoral journey till today. Timo, I appreciate all the help and advice that you provided during these years and I still remember those days that we used to meet in different places in Espoo and Helsinki. Our meetings were short but very fruitful and I'm glad that I had you as my supervisor. I'm grateful to you and frankly, without you, this project wouldn't have progressed the way it did. I would also like to thank Adjunct Professor Jussi Hirvonen for all his great advice and support. Jussi, you have been always very helpful, and kind-spirited. You have helped a great deal with many matters from going over MR images with me to giving your great insights about the statistical methods. Adjunct Professor Jussi Posti should be thanked greatly. Jussi, I didn't have the chance to know you at the beginning of my doctoral journey but after knowing you, you've been like a mentor and a friend to me. You have a great personality and you are very humble. I've always appreciated your hardworking and can-do attitude. You have not been my supervisor officially, yet you have always

been there and have supported me with your great advice and indirect supervision. I am very glad to work with you and this journey continues.

Special thanks to my colleagues and office mates especially our former research coordinator and research nurse Satu Honkala. Satu, you are one of a kind. You're one of the kindest persons I have ever met. I have always appreciated your serenity and genuineness and I will never forget the days that we talked about many things about work and life. You have for most of my doctoral journey been the one that I spent time with, in the office and I'm glad that I had you as a colleague and still as a friend.

My former colleague and friend Dr. Iftakher Hossain must be thanked. Ifti, what started as a collaboration between two team members of the research group turned into a friendship that is going beyond borders. Although you are no longer in Finland, we talk almost on a daily basis and you're one of my dearest friends and our friendship is for a lifetime. I will always cherish all the memories and moments that we had together. We spent (and will continue to spend) a lot of time talking about research, science, and different aspects of life. You're truly a great friend and I'm really glad that I was fortunate to come to know you.

Shkar and Anne, thank you for being great office mates and friends. Shkar, although you joined our group later in my journey, we have known each other for quite a long time and you have been a great friend and office mate. Anne, you joined our research group a couple of years back and it's been great to have you as a colleague and a friend.

Thank you Adjunct Professor Riikka Takala and Dr. Ari Katila. Dear Riikka and Ari, although our schedules did not overlap much during these years but knowing you have been a great pleasure. You both are super kind and caring and working with you has wonderful.

Thanks to my co-authors; Jussi Tallus, Henna-Riikka Maanpää, and Janek Frantzen for their cooperation and contribution during these years. Working with you has been a great pleasure.

I would like to express my sincere gratitude to Prof. Risto Roine and Leila Laakso-Kantonen for their support during my doctoral journey. Prof. Roine, I still remember the day I knocked on your office door although I forgot to book a time and you were so welcoming. You have always supported the administrative aspects during these years and I'm grateful to you. Leila, thank you so much! I know that I had nothing but bother for you all these years, but you have always been responding to my emails quite promptly and have taken care of all things efficiently.

I would like to express my sincere gratitude to Professor David Menon and Associate Professor Virginia Newcombe for the great collaboration during these years. It has been a great honor to have had the opportunity to work with you. Also, thank you for allowing me to visit Addenbrooke's hospital and the University of

Cambridge. It has been a great experience both academically and life-wise and I very much appreciate your hospitality during my visit. I look forward to collaborating with you in the future.

I have been fortunate to collaborate with Prof. Laura Airas, Professor Juha Rinne, Dr. Eero Rissanen, and Jouni. Working with you has been a pleasure. Jouni, working with you especially has been a great pleasure and I hope that we can collaborate again in the future (and finish the unfinished one!).

I would also like to thank both the former and current students Svetlana Bezukladova, Giorgia Marino, Juho Dahl, and Malla Mononen with whom I had the opportunity to work. Working with you has taught me a lot and I appreciate all your perseverance and hard work. I hope that I can have the joy of working with you again in the future.

I also would like to thank the Doctoral Program in Clinical Research and Turku Graduate School for supporting my research and my travels during these years. Also, I express my gratitude to the TYKS foundation, Turku University Foundation, International Society for Magnetic Resonance in Medicine, and FinCEAL+ for their financial supports at times during these years. Professors. Inga Koerte and Tim Dyrby are deeply acknowledged for accepting to be pre-examiners for this thesis. Your constructive comments and suggestions have undoubtedly improved my thesis. I thank Prof. Asta Håberg for accepting to be the opponent in the public defense of this dissertation.

Other than the academic aspect of this doctoral research, life aspects have directly and indirectly impacted me and my research. As an immigrant who has been living in Finland for quite some time, it has not been easy to cope with all the challenges coming my way while being alone and far from family. I was however very fortunate to have come to know many great caring souls who have in their own way helped me pull through difficult times and shared with me all moments of joy and grief. I cannot name all of you as it takes a long list to mention you all but to those whom I knew from the beginning of (or even before) this journey, those who joined during the journey, those who I had the opportunity to meet later along my journey, and those who are no longer part of it but have been a great part at times, I am truly and humbly grateful to you all. Not only have you been my friends but also you have been my family here in this part of the world. I have many friends in Finland and also from outside of borders who have supported me during this journey, and I am grateful to you. You have all shown me that friendship has indeed no borders and some of you have gone above and beyond, that I cannot even explain my gratitude to you in words. You all have been (and are) part of my heart. Among all these great souls, I would like to especially thank Ms. Sepideh Parvanian. Sepideh, from the moment you stepped into my life you have brought with you great positive energy. Thank you for being there with me through thick and thin and

bringing the joy and happiness. You have shown me the meaning of love and friendship on another level. You've made me want to be a better man. You've always been encouraging and supportive and pushed me right when I needed it. Thank you from the bottom of my heart.

Last but not least, I want to express my heartfelt gratitude to my parents, and my beautiful sister, whose love and support although from a far distance, have always been with me. When I came to Finland to pursue my dreams and continue my education, I left part of my heart at home, but you have always been with me at all times in my heart and mind. You have always been supportive and encouraging, I love you. My mother Farnoush, thank you for your unconditional love and devotion. You always lift me up and your smile always brightens my life. My father Mozaffar, you are my best friend in the whole world. You have shown me how to be disciplined, to never give up on dreams, and how hard work always pays off. You taught me how to live and be strong. You are my rock. You have always been my inspiration in this path from the very beginning. My lovely sister Mehrsa, since our childhood you have been more than a sibling for me, you've been my true friend all along. I have a deep appreciation for you, and I am thankful for your support and everything that you have done especially the things that became your burden after I left. You're always in my heart. I cannot truly express my gratitude in words properly as it takes more than a few words to even begin to explain my appreciation and love for you three. I am sorry for the times of being absent when I had to be there, but I wasn't, especially during the last two years. Your strength and resilience are what kept me moving forward and I hope that I can make you proud one day.

Turku - March 2021
Mehrbod Mohammadian

References

- Achard, S., Bullmore, E., 2007. Efficiency and Cost of Economical Brain Functional Networks. *PLoS Comput. Biol.* 3, e17. <https://doi.org/10.1371/journal.pcbi.0030017>
- Alexander, A.L., Hasan, K., Kindlmann, G., Parker, D.L., Tsuruda, J.S., 2000. A geometric analysis of diffusion tensor measurements of the human brain. *Magn. Reson. Med.* [https://doi.org/10.1002/1522-2594\(200008\)44:2<283::AID-MRM16>3.0.CO;2-V](https://doi.org/10.1002/1522-2594(200008)44:2<283::AID-MRM16>3.0.CO;2-V)
- Alexander, M.P., 1995. Mild traumatic brain injury: Pathophysiology, natural history, and clinical management. *Neurology.* <https://doi.org/10.1212/WNL.45.7.1253>
- American Congress of Rehabilitation Medicine Mild Traumatic Brain Injury Committee of the Head Injury Interdisciplinary Special Interest, 1993. Definition of mild traumatic brain injury. *J. Head Trauma Rehabil.*
- Andersson, Jesper L R, Jenkinson, M., Smith, S., 2007. Non-linear registration aka Spatial normalisation. FMRIB Technial Report. In Pract.
- Andersson, Jesper L.R., Jenkinson, M., Smith, S., 2007. Non-linear optimisation. FMRIB technical report TR07JA1 from www.fmrib.ox.ac.uk/analysis/techrep. Univ. Oxford FMRIB
- Arfanakis, K., Haughton, V.M., Carew, J.D., Rogers, B.P., Dempsey, R.J., Meyerand, M.E., 2002. Diffusion tensor MR imaging in diffuse axonal injury. *AJNR Am J Neuroradiol* 23, 794–802.
- Bach, M., Laun, F.B., Leemans, A., Tax, C.M.W., Biessels, G.J., Stieltjes, B., Maier-Hein, K.H., 2014. Methodological considerations on tract-based spatial statistics (TBSS). *Neuroimage* 100, 358–369. <https://doi.org/10.1016/j.neuroimage.2014.06.021>
- Baliyan, V., Das, C.J., Sharma, R., Gupta, A.K., 2016. Diffusion weighted imaging: Technique and applications. *World J. Radiol.* 8, 785–798. <https://doi.org/10.4329/wjr.v8.i9.785>
- Barbagallo, G., Caligiuri, M.E., Arabia, G., Cherubini, A., Lupo, A., Nisticò, R., Salsone, M., Novellino, F., Morelli, M., Cascini, G.L., Galea, D., Quattrone, A., 2017. Structural connectivity differences in motor network between tremor-dominant and nontremor Parkinson’s disease. *Hum. Brain Mapp.* 38, 4716–4729. <https://doi.org/10.1002/hbm.23697>
- Barnes, S.R.S., Haacke, E.M., 2009. Susceptibility-Weighted Imaging: Clinical Angiographic Applications. *Magn. Reson. Imaging Clin. N. Am.* 17, 47–61. <https://doi.org/10.1016/j.mric.2008.12.002>
- Basser, P.J., Mattiello, J., LeBihan, D., 1994a. MR diffusion tensor spectroscopy and imaging. *Biophys. J.* 66, 259–267. [https://doi.org/10.1016/S0006-3495\(94\)80775-1](https://doi.org/10.1016/S0006-3495(94)80775-1)
- Basser, P.J., Mattiello, J., LeBihan, D., 1994b. Estimation of the effective self-diffusion tensor from the NMR spin echo. *J. Magn. Reson. B* 103, 247–254. <https://doi.org/10.1006/jmrb.1994.1037>
- Basser, P.J., Pajevic, S., Pierpaoli, C., Duda, J., Aldroubi, A., 2000. In vivo fiber tractography using DT-MRI data. *Magn. Reson. Med.* 44, 625–632. [https://doi.org/10.1002/1522-2594\(200010\)44:4<625::AID-MRM17>3.0.CO;2-O](https://doi.org/10.1002/1522-2594(200010)44:4<625::AID-MRM17>3.0.CO;2-O)
- Basser, P.J., Pierpaoli, C., 1996. Microstructural and Physiological Features of Tissues Elucidated by Quantitative-Diffusion-Tensor MRI. *J. Magn. Reson. Ser. B* 111, 209–219. <https://doi.org/10.1006/JMRB.1996.0086>

- Bastiani, M., Shah, N.J., Goebel, R., Roebroeck, A., 2012. Human cortical connectome reconstruction from diffusion weighted MRI: The effect of tractography algorithm. *Neuroimage* 62, 1732–1749. <https://doi.org/10.1016/j.neuroimage.2012.06.002>
- Bazarian, J.J., McClung, J., Shah, M.N., Cheng, Y.T., Flesher, W., Kraus, J., 2005. Mild traumatic brain injury in the United States, 1998--2000. *Brain Inj.* 19, 85–91. <https://doi.org/10.1080/02699050410001720158>
- Beaulieu, C., 2002. The basis of anisotropic water diffusion in the nervous system - A technical review. *NMR Biomed.* <https://doi.org/10.1002/nbm.782>
- Behrens, T.E.J., Berg, H.J., Jbabdi, S., Rushworth, M.F.S., Woolrich, M.W., 2007. Probabilistic diffusion tractography with multiple fibre orientations: What can we gain? *Neuroimage* 34, 144–155. <https://doi.org/10.1016/j.neuroimage.2006.09.018>
- Behrens, T.E.J., Jbabdi, S., 2009. MR diffusion tractography, in: *Diffusion MRI*. Elsevier Inc., pp. 333–351. <https://doi.org/10.1016/B978-0-12-374709-9.00015-8>
- Bianchetti, M.G., Simonetti, G.D., Bettinelli, A., 2009. Body fluids and salt metabolism - Part I. *Ital. J. Pediatr.* 35, 36. <https://doi.org/10.1186/1824-7288-35-36>
- Bigler, E.D., 2011. Structural Imaging, in: *Textbook of Traumatic Brain Injury*. American Psychiatric Publishing. <https://doi.org/doi:10.1176/appi.books.9781585624201.js05>
- Bigler, E.D., 2005. Structural Imaging, in: Silver, J.M., McAllister, T.W., Yudofsky, S.C. (Eds.), *Textbook of Traumatic Brain Injury*. American Psychiatric Publishing.
- Bonilha, L., Gleichgerrcht, E., Fridriksson, J., Rorden, C., Breedlove, J.L., Nesland, T., Paulus, W., Helms, G., Focke, N.K., 2015. Reproducibility of the Structural Brain Connectome Derived from Diffusion Tensor Imaging. *PLoS One* 10, e0135247. <https://doi.org/10.1371/journal.pone.0135247>
- Borg, J., Holm, L., Peloso, P.M., Cassidy, J.D., Carroll, L.J., von Holst, H., Paniak, C., Yates, D., WHO Collaborating Centre Task Force on Mild Traumatic Brain Injury, 2004. Non-surgical intervention and cost for mild traumatic brain injury: results of the WHO Collaborating Centre Task Force on Mild Traumatic Brain Injury. *J. Rehabil. Med.* 76–83.
- Brandes, U., 2001. A faster algorithm for betweenness centrality*. *J. Math. Sociol.* 25, 163–177. <https://doi.org/10.1080/0022250X.2001.9990249>
- Broca, P., 1861. Remarques sur le siège de la faculté du langage articulé suivies d'une observation d'aphemie. *Bull Soc Anthr.*
- Browne, K.D., Chen, X.H., Meaney, D.F., Smith, D.H., 2011. Mild traumatic brain injury and diffuse axonal injury in swine. *J. Neurotrauma* 28, 1747–1755. <https://doi.org/10.1089/neu.2011.1913>
- Buchanan, C.R., Pernet, C.R., Gorgolewski, K.J., Storkey, A.J., Bastin, M.E., 2014. Test-retest reliability of structural brain networks from diffusion MRI. *Neuroimage* 86, 231–243. <https://doi.org/10.1016/j.neuroimage.2013.09.054>
- Budde, M.D., Janes, L., Gold, E., Turtzo, L.C., Frank, J.A., 2011. The contribution of gliosis to diffusion tensor anisotropy and tractography following traumatic brain injury: validation in the rat using Fourier analysis of stained tissue sections. *Brain* 134, 2248–2260. <https://doi.org/10.1093/brain/awr161>
- Bullmore, E., Sporns, O., 2009. Complex brain networks: graph theoretical analysis of structural and functional systems. *Nat. Rev. Neurosci.* 10, 186–198. <https://doi.org/10.1038/nrn2618>
- Bullmore, E.T., Bassett, D.S., 2011. Brain Graphs: Graphical Models of the Human Brain Connectome. *Annu. Rev. Clin. Psychol.* 7, 113–140. <https://doi.org/10.1146/annurev-clinpsy-040510-143934>
- Bullmore, E.T., Sporns, O., 2009. Complex brain networks: graph theoretical analysis of structural and functional systems. *Nat Rev Neurosci.* 10, 186–198. <https://doi.org/10.1038/nrn2575>
- Bushberg, J.T., Seibert, J.A., Leidholdt, E.M., Boone, J.M., 2012. *The essential physics of medical imaging*, 3rd ed. Wolters Kluwer / Lippincott Williams & Wilkins, Philadelphia, PA.
- Caeyenberghs, K., Leemans, A., Leunissen, I., Gooijers, J., Michiels, K., Sunaert, S., Swinnen, S.P., 2014. Altered structural networks and executive deficits in traumatic brain injury patients. *Brain Struct. Funct.* 219, 193–209. <https://doi.org/10.1007/s00429-012-0494-2>

- Cassidy, J.D., Carroll, L.J., Peloso, P.M., Borg, J., von Holst, H., Holm, L., Kraus, J., Coronado, V.G., WHO Collaborating Centre Task Force on Mild Traumatic Brain Injury, 2004. Incidence, risk factors and prevention of mild traumatic brain injury: results of the WHO Collaborating Centre Task Force on Mild Traumatic Brain Injury. *J. Rehabil. Med.* 28–60.
- Chung, A.W., Mannix, R., Feldman, H.A., Grant, P.E., Im, K., 2019. Longitudinal structural connectomic and rich-club analysis in adolescent mTBI reveals persistent, distributed brain alterations acutely through to one year post-injury. *Sci. Rep.* 9, 1–11. <https://doi.org/10.1038/s41598-019-54950-0>
- Conturo, T.E., Lori, N.F., Cull, T.S., Akbudak, E., Snyder, A.Z., Shimony, J.S., McKinstry, R.C., Burton, H., Raichle, M.E., 1999. Tracking neuronal fiber pathways in the living human brain. *Proc. Natl. Acad. Sci.* 96, 10422–10427. <https://doi.org/10.1073/pnas.96.18.10422>
- Dall'Acqua, P., Johannes, S., Mica, L., Simmen, H.-P., Glaab, R., Fandino, J., Schwendinger, M., Meier, C., Ulbrich, E.J., Müller, A., Baetschmann, H., Jäncke, L., Hänggi, J., 2017. Functional and Structural Network Recovery after Mild Traumatic Brain Injury: A 1-Year Longitudinal Study. *Front. Hum. Neurosci.* 11, 280. <https://doi.org/10.3389/fnhum.2017.00280>
- Dall'Acqua, P., Johannes, S., Mica, L., Simmen, H.-P., Glaab, R., Fandino, J., Schwendinger, M., Meier, C., Ulbrich, E.J., Müller, A., Jäncke, L., Hänggi, J., 2016. Connectomic and Surface-Based Morphometric Correlates of Acute Mild Traumatic Brain Injury. *Front. Hum. Neurosci.* 10, 127. <https://doi.org/10.3389/fnhum.2016.00127>
- Dell'Acqua, F., Tournier, J.-Donal., 2019. Modelling white matter with spherical deconvolution: How and why? *NMR Biomed.* 32, e3945. <https://doi.org/10.1002/nbm.3945>
- Desikan, R.S., Ségonne, F., Fischl, B., Quinn, B.T., Dickerson, B.C., Blacker, D., Buckner, R.L., Dale, A.M., Maguire, R.P., Hyman, B.T., Albert, M.S., Killiany, R.J., 2006. An automated labeling system for subdividing the human cerebral cortex on MRI scans into gyral based regions of interest. *Neuroimage* 31, 968–980. <https://doi.org/10.1016/j.neuroimage.2006.01.021>
- Diaz-Arrastia, R., Vos, P.E., 2014. The clinical problem of traumatic head injury. *Trauma. Brain Inj.*, Wiley Online Books. <https://doi.org/doi:10.1002/9781118656303.ch1>
- Dimond, D., Schuetze, M., Smith, R.E., Dhollander, T., Cho, I., Vinette, S., Ten Eycke, K., Lebel, C., McCrimmon, A., Dewey, D., Connelly, A., Bray, S., 2019. Reduced White Matter Fiber Density in Autism Spectrum Disorder. *Cereb. Cortex* 29, 1778–1788. <https://doi.org/10.1093/cercor/bhy348>
- Douek, P., Turner, R., Pekar, J., Patronas, N., Le Bihan, D., 1991. Mr color mapping of myelin fiber orientation. *J. Comput. Assist. Tomogr.* 15, 923–929. <https://doi.org/10.1097/00004728-199111000-00003>
- Douglas, D.B., Ro, T., Toffoli, T., Krawchuk, B., Muldermans, J., Gullo, J., Dulberger, A., Anderson, A.E., Douglas, P.K., Wintermark, M., 2019. Neuroimaging of Traumatic Brain Injury. *Med. Sci.* 7. <https://doi.org/10.3390/MEDSCI7010002>
- Douglas, D.B., Ro, T., Toffoli, T., Krawchuk, B., Muldermans, J., Gullo, J., Dulberger, A., Anderson, A.E., Douglas, P.K., Wintermark, M., 2018. Neuroimaging of Traumatic Brain Injury. *Med. Sci. (Basel, Switzerland)* 7. <https://doi.org/10.3390/medsci7010002>
- Eierud, C., Craddock, R.C., Fletcher, S., Aulakh, M., King-Casas, B., Kuehl, D., LaConte, S.M., 2014. Neuroimaging after mild traumatic brain injury: Review and meta-analysis. *NeuroImage Clin.* 4, 283–294. <https://doi.org/10.1016/j.nicl.2013.12.009>
- Einstein, A., 1905. Über die von der molekularkinetischen Theorie der Wärme geforderte Bewegung. *Ann. Phys.*
- Fagerholm, E.D., Hellyer, P.J., Scott, G., Leech, R., Sharp, D.J., 2015. Disconnection of network hubs and cognitive impairment after traumatic brain injury. *Brain* 138, 1696–1709. <https://doi.org/10.1093/brain/awv075>
- Fakhry, S.M., Trask, A.L., Waller, M.A., Watts, D.D., IRTC Neurotrauma Task Force, 2004. Management of brain-injured patients by an evidence-based medicine protocol improves outcomes and decreases hospital charges. *J. Trauma* 56, 492–9; discussion 499–500.

- Farquharson, S., Tournier, J.-D., Calamante, F., Fabbinyi, G., Schneider-Kolsky, M., Jackson, G.D., Connelly, A., 2013. White matter fiber tractography: why we need to move beyond DTI. *J. Neurosurg.* 118, 1367–77. <https://doi.org/10.3171/2013.2.JNS121294>
- Fazekas, F., Chawluk, J.B., Alavi, A., 1987. MR signal abnormalities at 1.5 T in Alzheimer's dementia and normal aging. *Am. J. Neuroradiol.* <https://doi.org/10.2214/ajr.149.2.351>
- Feng, F., Zhou, B., Wang, L., Yao, H.X., Guo, Y.E., An, N.Y., Wang, L.N., Zhang, X., 2019. [The correlation of functional connectivity and structural connectivity between hippocampus and thalamus in Alzheimer's disease and amnesic mild cognitive impairment]. *Zhonghua nei ke za zhi* 58, 662–667. <https://doi.org/10.3760/cma.j.issn.0578-1426.2019.09.006>
- Fischl, B., 2012. *FreeSurfer.* *Neuroimage* 62, 774–81. <https://doi.org/10.1016/j.neuroimage.2012.01.021>
- Fischl, B., Salat, D.H., Busa, E., Albert, M., Dieterich, M., Haselgrove, C., van der Kouwe, A., Killiany, R., Kennedy, D., Klaveness, S., Montillo, A., Makris, N., Rosen, B., Dale, A.M., 2002. Whole Brain Segmentation: Automated Labeling of Neuroanatomical Structures in the Human Brain. *Neuron* 33, 341–355. [https://doi.org/10.1016/S0896-6273\(02\)00569-X](https://doi.org/10.1016/S0896-6273(02)00569-X)
- Fischl, B., van der Kouwe, A., Destrieux, C., Halgren, E., Ségonne, F., Salat, D.H., Busa, E., Seidman, L.J., Goldstein, J., Kennedy, D., Caviness, V., Makris, N., Rosen, B., Dale, A.M., 2004. Automatically parcellating the human cerebral cortex. *Cereb. Cortex* 14, 11–22.
- Freeman, L.C., 1978. Centrality in social networks conceptual clarification. *Soc. Networks* 1, 215–239. [https://doi.org/10.1016/0378-8733\(78\)90021-7](https://doi.org/10.1016/0378-8733(78)90021-7)
- Galgano, M., Toshkezi, G., Qiu, X., Russell, T., Chin, L., Zhao, L.R., 2017. Traumatic brain injury: Current treatment strategies and future endeavors. *Cell Transplant.* <https://doi.org/10.1177/0963689717714102>
- Gennarelli, Graham, 1998. Neuropathology of the Head Injuries. *Semin. Clin. Neuropsychiatry* 3, 160–175.
- Gennarelli, T.A., 1983. Head injury in man and experimental animals: clinical aspects. *Acta Neurochir. Suppl. (Wien)*. 32, 1–13.
- Ghajari, M., Hellyer, P.J., Sharp, D.J., 2017. Computational modelling of traumatic brain injury predicts the location of chronic traumatic encephalopathy pathology. *Brain* 140, 333–343. <https://doi.org/10.1093/brain/aww317>
- Gigandet, X., Griffa, A., Kober, T., Daducci, A., Gilbert, G., Connelly, A., Hagmann, P., Meuli, R., Thiran, J.P., Krueger, G., 2013. A Connectome-Based Comparison of Diffusion MRI Schemes. *PLoS One* 8. <https://doi.org/10.1371/journal.pone.0075061>
- Glauser, J., 2004. Head injury: which patients need imaging? Which test is best? *Cleve. Clin. J. Med.* 71, 353–7.
- Gooijers, J., Chalavi, S., Beeckmans, K., Michiels, K., Lafosse, C., Sunaert, S., Swinnen, S.P., 2016. Subcortical Volume Loss in the Thalamus, Putamen, and Pallidum, Induced by Traumatic Brain Injury, Is Associated with Motor Performance Deficits. *Neurorehabil. Neural Repair.* <https://doi.org/10.1177/1545968315613448>
- Grover, V.P.B., Tognarelli, J.M., Crossey, M.M.E., Cox, I.J., Taylor-Robinson, S.D., McPhail, M.J.W., 2015. Magnetic Resonance Imaging: Principles and Techniques: Lessons for Clinicians. *J. Clin. Exp. Hepatol.* 5, 246–55. <https://doi.org/10.1016/j.jceh.2015.08.001>
- Hagmann, P., Cammoun, L., Gigandet, X., Meuli, R., Honey, C.J., Van Wedeen, J., Sporns, O., 2008. Mapping the structural core of human cerebral cortex. *PLoS Biol.* 6, 1479–1493. <https://doi.org/10.1371/journal.pbio.0060159>
- Hagmann, P., Kurant, M., Gigandet, X., Thiran, P., Wedeen, V.J., Meuli, R., Thiran, J.-P., 2007. Mapping human whole-brain structural networks with diffusion MRI. *PLoS One* 2, e597. <https://doi.org/10.1371/journal.pone.0000597>
- Harsan, L.A., Poulet, P., Guignard, B., Steibel, J., Parizel, N., de Sousa, P.L., Boehm, N., Grucker, D., Ghandour, M.S., 2006. Brain dysmyelination and recovery assessment by noninvasive in vivo

- diffusion tensor magnetic resonance imaging. *J. Neurosci. Res.* 83, 392–402. <https://doi.org/10.1002/jnr.20742>
- Hart, M.G., Ypma, R.J.F., Romero-Garcia, R., Price, S.J., Suckling, J., 2016. Graph theory analysis of complex brain networks: New concepts in brain mapping applied to neurosurgery. *J. Neurosurg.* 124, 1665–1678. <https://doi.org/10.3171/2015.4.JNS142683>
- Hashim, E., Caverzasi, E., Papinutto, N., Lewis, C.E., Jing, R., Charles, O., Zhang, S., Lin, A., Graham, S.J., Schweizer, T.A., Bharatha, A., Cusimano, M.D., 2017. Investigating Microstructural Abnormalities and Neurocognition in Sub-Acute and Chronic Traumatic Brain Injury Patients with Normal-Appearing White Matter: A Preliminary Diffusion Tensor Imaging Study. *Front. Neurol.* 8, 97. <https://doi.org/10.3389/fneur.2017.00097>
- Hawryluk, G.W.J., Manley, G.T., 2015. Classification of traumatic brain injury: past, present, and future. *Handb. Clin. Neurol.* 127, 15–21. <https://doi.org/10.1016/B978-0-444-52892-6.00002-7>
- Hayes, J.P., Bigler, E.D., Verfaellie, M., 2016. Traumatic Brain Injury as a Disorder of Brain Connectivity. *J. Int. Neuropsychol. Soc.* 22, 120–137. <https://doi.org/10.1017/S1355617715000740>
- Hickok, G., 2012. Computational neuroanatomy of speech production. *Nat. Rev. Neurosci.* <https://doi.org/10.1038/nrn3158>
- Hilgetag, C.C., Goulas, A., 2016. Is the brain really a small-world network? *Brain Struct. Funct.* 221, 2361–2366. <https://doi.org/10.1007/s00429-015-1035-6>
- Hill, L.L., 1990. Body Composition, Normal Electrolyte Concentrations, and the Maintenance of Normal Volume, Tonicity, and Acid-Base Metabolism. *Pediatr. Clin. North Am.* 37, 241–256. [https://doi.org/10.1016/S0031-3955\(16\)36865-1](https://doi.org/10.1016/S0031-3955(16)36865-1)
- Hirsiger, S., Koppelmans, V., Mérellat, S., Liem, F., Erdeniz, B., Seidler, R.D., Jäncke, L., 2016. Structural and functional connectivity in healthy aging: Associations for cognition and motor behavior. *Hum. Brain Mapp.* 37, 855–867. <https://doi.org/10.1002/hbm.23067>
- Hölzel, B.K., Hoge, E.A., Greve, D.N., Gard, T., Creswell, J.D., Brown, K.W., Barrett, L.F., Schwartz, C., Vaitl, D., Lazar, S.W., 2013. Neural mechanisms of symptom improvements in generalized anxiety disorder following mindfulness training. *NeuroImage Clin.* <https://doi.org/10.1016/j.nicl.2013.03.011>
- Horn, A., Reich, M., Vorwerk, J., Li, N., Wenzel, G., Fang, Q., Schmitz-Hübsch, T., Nickl, R., Kupsch, A., Volkmann, J., Kühn, A.A., Fox, M.D., 2017. Connectivity Predicts deep brain stimulation outcome in Parkinson disease. *Ann. Neurol.* 82, 67–78. <https://doi.org/10.1002/ana.24974>
- Huo, Y., Bao, S., Landman, B.A., Parvathaneni, P., 2018. Improved stability of whole brain surface parcellation with multi-atlas segmentation, in: *Proceedings of SPIE--the International Society for Optical Engineering*. SPIE-Intl Soc Optical Eng, p. 113. <https://doi.org/10.1117/12.2281509>
- Hutchinson, E.B., Schwerin, S.C., Avram, A. V., Juliano, S.L., Pierpaoli, C., 2018. Diffusion MRI and the detection of alterations following traumatic brain injury. *J. Neurosci. Res.* 96, 612–625. <https://doi.org/10.1002/jnr.24065>
- Hyder, A.A., Wunderlich, C.A., Puvanachandra, P., Gururaj, G., Kobusingye, O.C., 2007. The impact of traumatic brain injuries: a global perspective. *NeuroRehabilitation* 22, 341–353. <https://doi.org/http://iospress.metapress.com/content/103177/?sortorder=asc>
- Iffland, P.H., Grant, G.A., Janigro, D., 2014. Mechanisms of cerebral edema leading to early seizures after traumatic brain injury., in: Lo, E.H., Lok, J., Ning, M., Whalen, M.J. (Eds.), *Vascular Mechanisms in CNS Trauma*. New York, pp. 29–45.
- Ilvesmäki, T., Luoto, T.M., Hakulinen, U., Brander, A., Ryymin, P., Eskola, H., Iverson, G.L., Ohman, J., 2014. Acute mild traumatic brain injury is not associated with white matter change on diffusion tensor imaging. *Brain* 137, 1876–82. <https://doi.org/10.1093/brain/awu095>
- Imms, P., Clemente, A., Cook, M., D’Souza, W., Wilson, P.H., Jones, D.K., Caeyenberghs, K., 2019. The structural connectome in traumatic brain injury: A meta-analysis of graph metrics. *Neurosci. Biobehav. Rev.* <https://doi.org/10.1016/j.neubiorev.2019.01.002>

- Indefrey, P., Levelt, W.J.M., 2004. The spatial and temporal signatures of word production components. *Cognition* 92, 101–144. <https://doi.org/10.1016/j.cognition.2002.06.001>
- Inglese, M., Makani, S., Johnson, G., Cohen, B.A.B. a., Silver, J. a. J.A., Gonen, O., Grossman, R.I.R.I., 2005. Diffuse axonal injury in mild traumatic brain injury: a diffusion tensor imaging study. *J. Neurosurg.* 103, 298–303. <https://doi.org/10.3171/jns.2005.103.2.0298>
- Iturria-Medina, Y., Canales-Rodríguez, E.J., Melie-García, L., Valdés-Hernández, P.A., Martínez-Montes, E., Alemán-Gómez, Y., Sánchez-Bornot, J.M., 2007. Characterizing brain anatomical connections using diffusion weighted MRI and graph theory. *Neuroimage* 36, 645–660. <https://doi.org/10.1016/j.neuroimage.2007.02.012>
- Jenkinson, M., Beckmann, C.F., Behrens, T.E.J., Woolrich, M.W., Smith, S.M., 2012. FSL. *Neuroimage* 62, 782–790. <https://doi.org/10.1016/j.neuroimage.2011.09.015>
- Jenkinson, M., Smith, S., 2001. A global optimisation method for robust affine registration of brain images. *Med. Image Anal.* [https://doi.org/10.1016/S1361-8415\(01\)00036-6](https://doi.org/10.1016/S1361-8415(01)00036-6)
- Jeurissen, B., Leemans, A., Jones, D.K., Tournier, J.D., Sijbers, J., 2011. Probabilistic fiber tracking using the residual bootstrap with constrained spherical deconvolution. *Hum. Brain Mapp.* 32, 461–479. <https://doi.org/10.1002/hbm.21032>
- Jeurissen, B., Leemans, A., Tournier, J.D., Jones, D.K., Sijbers, J., 2013. Investigating the prevalence of complex fiber configurations in white matter tissue with diffusion magnetic resonance imaging. *Hum. Brain Mapp.* 34, 2747–2766. <https://doi.org/10.1002/hbm.22099>
- Jeurissen, B., Tournier, J.-D., Dhollander, T., Connelly, A., Sijbers, J., 2014. Multi-tissue constrained spherical deconvolution for improved analysis of multi-shell diffusion MRI data. *Neuroimage* 103, 411–426. <https://doi.org/10.1016/j.neuroimage.2014.07.061>
- Jolly, A.E., Scott, G.T., Sharp, D.J., Hampshire, A.H., 2020. Distinct patterns of structural damage underlie working memory and reasoning deficits after traumatic brain injury. *Brain* 143, 1158–1176. <https://doi.org/10.1093/brain/awaa067>
- Jones, D.K., 2004. Fundamentals of diffusion MR imaging, in: Gillard, J.H., Waldman, A.D., Barker, P.B. (Eds.), *Clinical MR Neuroimaging*. Cambridge University Press, Cambridge, pp. 54–85. <https://doi.org/10.1017/CBO9780511544958.006>
- Jones, N.R., Blumbers, P.C., Brown, C.J., McLean, A.J., Manavis, J., Perrett, L. V., Sandhu, A., Scott, G., Simpson, D.A., 1998. Correlation of postmortem MRI and CT appearances with neuropathology in brain trauma: a comparison of two methods. *J. Clin. Neurosci.* 5, 73–9.
- Jorge, R.E., Acion, L., White, T., Tordesillas-Gutierrez, D., Pierson, R., Crespo-Facorro, B., Magnotta, V.A., 2012. White matter abnormalities in veterans with mild traumatic brain injury. *Am. J. Psychiatry* 169, 1284–91. <https://doi.org/10.1176/appi.ajp.2012.12050600>
- Jung, B.A., Weigel, M., 2013. Spin echo magnetic resonance imaging. *J. Magn. Reson. Imaging* 37, 805–817. <https://doi.org/10.1002/jmri.24068>
- Katz, D.I., Cohen, S.I., Alexander, M.P., 2015. Mild traumatic brain injury, in: *Handbook of Clinical Neurology*. Elsevier B.V., pp. 131–156. <https://doi.org/10.1016/B978-0-444-52892-6.00009-X>
- Kelly, A.B., Zimmerman, R.D., Snow, R.B., Gandy, S.E., Heier, L.A., Deck, M.D., 1988. Head trauma: comparison of MR and CT--experience in 100 patients. *AJNR. Am. J. Neuroradiol.* 9, 699–708.
- Koerte, I.K., Hufschmidt, J., Muehlmann, M., Lin, A.P., Shenton, M.E., 2016. *Advanced Neuroimaging of Mild Traumatic Brain Injury, Translational Research in Traumatic Brain Injury*. CRC Press/Taylor and Francis Group.
- Kou, Z., Wu, Z., Tong, K.A., Holshouser, B., Benson, R.R., Hu, J., Haacke, M.E., 2010. The role of advanced MR imaging findings as biomarkers of traumatic brain injury. *J. Head Trauma Rehabil.* <https://doi.org/10.1097/HTR.0b013e3181e54793>
- Kraus, M.F., Susmaras, T., Caughlin, B.P., Walker, C.J., Sweeney, J.A., Little, D.M., 2007. White matter integrity and cognition in chronic traumatic brain injury: A diffusion tensor imaging study. *Brain* 130, 2508–2519. <https://doi.org/10.1093/brain/awm216>

- La Rocca, M., Amoroso, N., Monaco, A., Bellotti, R., Tangaro, S., 2018. A novel approach to brain connectivity reveals early structural changes in Alzheimer's disease. *Physiol. Meas.* 39, 074005. <https://doi.org/10.1088/1361-6579/aac11f>
- Laskowski, R.A., Creed, J.A., Raghupathi, R., 2015. Pathophysiology of Mild TBI: Implications for Altered Signaling Pathways, Brain Neurotrauma: Molecular, Neuropsychological, and Rehabilitation Aspects. CRC Press/Taylor & Francis.
- Latora, V., Marchiori, M., 2001. Efficient Behavior of Small-World Networks. *Phys. Rev. Lett.* 87, 198701-1-198701-4. <https://doi.org/10.1103/PhysRevLett.87.198701>
- Le Bihan, D., 2010. Magnetic Resonance Diffusion Imaging: Introduction and Concepts, in: *Diffusion MRI*. Oxford University Press, pp. 57–78. <https://doi.org/10.1093/med/9780195369779.003.0005>
- Le Bihan, D., 1991. Molecular diffusion nuclear magnetic resonance imaging. *Magn Reson Q* 7, 1–30.
- Le Bihan, D., Breton, E., 1985. Imagerie de diffusion in-vivo par résonance magnétique nucléaire. *Comptes-Rendus l'Académie des Sci.* 93, 27–34.
- Le, T.H., Gean, A.D., 2009. Neuroimaging of traumatic brain injury. *Mt. Sinai J. Med. A J. Transl. Pers. Med.* 76, 145–162. <https://doi.org/10.1002/msj.20102>
- Lee, B., Newberg, A., 2005. Neuroimaging in traumatic brain imaging. *NeuroRx* 2, 372–83. <https://doi.org/10.1602/neurorx.2.2.372>
- Lee, H., Wintermark, M., Gean, A.D., Ghajar, J., Manley, G.T., Mukherjee, P., 2008. Focal Lesions in Acute Mild Traumatic Brain Injury and Neurocognitive Outcome: CT versus 3T MRI. *J. Neurotrauma* 25, 1049–1056. <https://doi.org/10.1089/neu.2008.0566>
- Lee, J.H., Kyeong, S., Kang, H., Kim, D.H., 2019. Structural and functional connectivity correlates with motor impairment in chronic supratentorial stroke: A multimodal magnetic resonance imaging study. *Neuroreport* 30, 526–531. <https://doi.org/10.1097/WNR.0000000000001247>
- Leemans, A., Jeurissen, B., Sijbers, J., Jones, D., 2009. ExploreDTI: a graphical toolbox for processing, analyzing, and visualizing diffusion MR data, in: *Proceedings 17th Scientific Meeting, International Society for Magnetic Resonance in Medicine*. p. 3537.
- Levi, L., Guilburd, J.N., Lemberger, A., Soustiel, J.F., Feinsod, M., 1990. Diffuse axonal injury: analysis of 100 patients with radiological signs. *Neurosurgery* 27, 429–32.
- Li, L., Rilling, J.K., Preuss, T.M., Glasser, M.F., Hu, X., 2012. The effects of connection reconstruction method on the interregional connectivity of brain networks via diffusion tractography. *Hum. Brain Mapp.* 33, 1894–1913. <https://doi.org/10.1002/hbm.21332>
- Li, W., Andreasen, N.C., Nopoulos, P., Magnotta, V.A., 2013. Automated parcellation of the brain surface generated from magnetic resonance images. *Front. Neuroinform.* 7, 23. <https://doi.org/10.3389/fninf.2013.00023>
- Linke, J.O., Stavish, C., Adleman, N.E., Sarlls, J., Towbin, K.E., Leibenluft, E., Brotman, M.A., 2020. White matter microstructure in youth with and at risk for bipolar disorder. *Bipolar Disord.* 22, 163–173. <https://doi.org/10.1111/bdi.12885>
- Lipp, I., Parker, G.D., Tallantyre, E.C., Goodall, A., Grama, S., Patitucci, E., Heveron, P., Tomassini, V., Jones, D.K., 2020. Tractography in the presence of multiple sclerosis lesions. *Neuroimage* 209, 116471. <https://doi.org/10.1016/j.neuroimage.2019.116471>
- Liu, J., Li, M., Pan, Y., Lan, W., Zheng, R., Wu, F.-X., Wang, J., 2017. Complex Brain Network Analysis and Its Applications to Brain Disorders: A Survey. *Complexity* 2017, 8362741. <https://doi.org/10.1155/2017/8362741>
- Liu, Y., Spulber, G., Lehtimäki, K.K., Könönen, M., Hallikainen, I., Gröhn, H., Kivipelto, M., Hallikainen, M., Vanninen, R., Soininen, H., 2011. Diffusion tensor imaging and Tract-Based Spatial Statistics in Alzheimer's disease and mild cognitive impairment. *Neurobiol. Aging* 32, 1558–1571. <https://doi.org/10.1016/j.neurobiolaging.2009.10.006>
- Maas, A.I.R., Menon, D.K., Adelson, P.D., Andelic, N., Bell, M.J., Belli, A., Bragge, P., Brazinova, A., Büki, A., Chesnut, R.M., Citerio, G., Coburn, M., Cooper, D.J., Crowder, A.T., Czeiter, E., Czosnyka, M., Diaz-Arrastia, R., Dreier, J.P., Duhaime, A.-C., Ercole, A., van Essen, T.A., Feigin, V.L., Gao, G., Giacino, J., Gonzalez-Lara, L.E., Gruen, R.L., Gupta, D., Hartings, J.A., Hill, S.,

- Jiang, J.-Y., Ketharanathan, N., Kompanje, E.J.O., Lanyon, L., Laureys, S., Lecky, F., Levin, H., Lingsma, H.F., Maegele, M., Majdan, M., Manley, G., Marsteller, J., Mascia, L., McFadyen, C., Mondello, S., Newcombe, V., Palotie, A., Parizel, P.M., Peul, W., Piercy, J., Polinder, S., Puybasset, L., Rasmussen, T.E., Rossaint, R., Smielewski, P., Söderberg, J., Stanworth, S.J., Stein, M.B., von Steinbüchel, N., Stewart, W., Steyerberg, E.W., Stocchetti, N., Synnot, A., Te Ao, B., Tenovuo, O., Theadom, A., Tibboel, D., Videtta, W., Wang, K.K.W., Williams, W.H., Wilson, L., Yaffe, K., InTBIR Participants and Investigators, H., Agnoletti, V., Allanson, J., Amrein, K., Andaluz, N., Anke, A., Antoni, A., As, A.B. van, Audibert, G., Azaševac, A., Azouvi, P., Azzolini, M.L., Baciú, C., Badenes, R., Barlow, K.M., Bartels, R., Bauerfeind, U., Beauchamp, M., Beer, D., Beer, R., Belda, F.J., Bellander, B.-M., Bellier, R., Benali, H., Benard, T., Beqiri, V., Beretta, L., Bernard, F., Bertolini, G., Bilotta, F., Blaabjerg, M., Boogert, H. den, Boutis, K., Bouzat, P., Brooks, B., Brorsson, C., Bullinger, M., Burns, E., Calappi, E., Cameron, P., Carise, E., Castaño-León, A.M., Causin, F., Chevillard, G., Chieregato, A., Christie, B., Cnossen, M., Coles, J., Collett, J., Corte, F. Della, Craig, W., Csato, G., Csomos, A., Curry, N., Dahyot-Fizelier, C., Dawes, H., DeMatteo, C., Depreitere, B., Dewey, D., Dijck, J. van, Đilvesi, Đ., Dippel, D., Dizdarevic, K., Donoghue, E., Duek, O., Dulière, G.-L., Dzeko, A., Eapen, G., Emery, C.A., English, S., Esser, P., Ezer, E., Fabricius, M., Feng, J., Fergusson, D., Figaji, A., Fleming, J., Foks, K., Francony, G., Freedman, S., Freo, U., Frisvold, S.K., Gagnon, I., Galanaud, D., Gantner, D., Giraud, B., Glocker, B., Golubovic, J., López, P.A.G., Gordon, W.A., Gradisek, P., Gravel, J., Griesdale, D., Grossi, F., Haagsma, J.A., Håberg, A.K., Haitsma, I., Hecke, W. Van, Helbok, R., Helseth, E., Heugten, C. van, Hoedemaekers, C., Höfer, S., Horton, L., Hui, J., Huijben, J.A., Hutchison, P.J., Jacobs, B., Jagt, M. van der, Jankowski, S., Janssens, K., Jelaca, B., Jones, K.M., Kamnitsas, K., Kaps, R., Karan, M., Katila, A., Kaukonen, K.-M., Keyser, V. De, Kivisaari, R., Koliás, A.G., Kolumbán, B., Kolundžija, K., Kondziella, D., Koskinen, L.-O., Kovács, N., Kramer, A., Kutsogiannis, D., Kyprianou, T., Lagares, A., Lamontagne, F., Latini, R., Lauzier, F., Lazar, I., Ledig, C., Lefering, R., Legrand, V., Levi, L., Lightfoot, R., Lozano, A., MacDonald, S., Major, S., Manara, A., Manhes, P., Maréchal, H., Martino, C., Masala, A., Masson, S., Mattern, J., McFadyen, B., McMahan, C., Meade, M., Melegh, B., Menovsky, T., Moore, L., Correia, M.M., Morganti-Kossmann, M.C., Muchlan, H., Mukherjee, P., Murray, L., Naalt, J. van der, Negru, A., Nelson, D., Nieboer, D., Noirhomme, Q., Nyirádi, J., Oddo, M., Okonkwo, D.O., Oldenbeuving, A.W., Ortolano, F., Osmond, M., Payen, J.-F., Perlberg, V., Persona, P., Pichon, N., Piippo-Karjalainen, A., Pili-Floury, S., Pirinen, M., Ple, H., Poca, M.A., Posti, J., Praag, D. Van, Ptitto, A., Radoi, A., Ragauskas, A., Raj, R., Real, R.G.L., Reed, N., Rhodes, J., Robertson, C., Rocka, S., Røe, C., Røise, O., Roks, G., Rosand, J., Rosenfeld, J. V., Rosenlund, C., Rosenthal, G., Rossi, S., Rueckert, D., Ruiters, G.C.W. de, Sacchi, M., Sahakian, B.J., Sahuquillo, J., Sakowitz, O., Salvato, G., Sánchez-Porrás, R., Sándor, J., Sangha, G., Schäfer, N., Schmidt, S., Schneider, K.J., Schnyer, D., Schöhl, H., Schoonman, G.G., Schou, R.F., Sir, Ö., Skandsen, T., Smeets, D., Sorinola, A., Stamatakis, E., Stevanovic, A., Stevens, R.D., Sundström, N., Taccone, F.S., Takala, R., Tanskanen, P., Taylor, M.S., Telgmann, R., Temkin, N., Teodorani, G., Thomas, M., Toliaš, C.M., Trapani, T., Turgeon, A., Vajkoczy, P., Valadka, A.B., Valeinis, E., Vallance, S., Vámos, Z., Vargiolu, A., Vega, E., Verheyden, J., Vik, A., Vilcinis, R., Vleggeert-Lankamp, C., Vogt, L., Volovici, V., Voormolen, D.C., Vulekovic, P., Vyvere, T. Vande, Waesberghe, J. Van, Wessels, L., Wildschut, E., Williams, G., Winkler, M.K.L., Wolf, S., Wood, G., Xirouchaki, N., Younsi, A., Zaaroor, M., Zelinkova, V., Zemek, R., Zumbo, F., 2017. Traumatic brain injury: integrated approaches to improve prevention, clinical care, and research. *Lancet. Neurol.* 16, 987–1048. [https://doi.org/10.1016/S1474-4422\(17\)30371-X](https://doi.org/10.1016/S1474-4422(17)30371-X)
- Mac Donald, C.L., Dikranian, K., Bayly, P., Holtzman, D., Brody, D., 2007. Diffusion tensor imaging reliably detects experimental traumatic axonal injury and indicates approximate time of injury. *J. Neurosci.* 27, 11869–76. <https://doi.org/10.1523/JNEUROSCI.3647-07.2007>

- Matthews, P.M., Filippini, N., Douaud, G., 2013. Brain structural and functional connectivity and the progression of neuropathology in Alzheimer's disease. *J. Alzheimer's Dis.* <https://doi.org/10.3233/JAD-2012-129012>
- McColgan, P., Seunarine, K.K., Gregory, S., Razi, A., Papoutsis, M., Long, J.D., Mills, J.A., Johnson, E., Durr, A., Roos, R.A., Leavitt, B.R., Stout, J.C., Scahill, R.I., Clark, C.A., Rees, G., Tabrizi, S.J., Investigators, T.T.O.H., 2017. Topological length of white matter connections predicts their rate of atrophy in premanifest Huntington's disease. *JCI insight* 2. <https://doi.org/10.1172/jci.insight.92641>
- McCrea, M.A., Nelson, L.D., Guskiewicz, K., 2017. Diagnosis and Management of Acute Concussion. *Phys. Med. Rehabil. Clin. N. Am.* <https://doi.org/10.1016/j.pmr.2016.12.005>
- McGinn, M.J., Povlishock, J.T., 2016. Pathophysiology of Traumatic Brain Injury. *Neurosurg. Clin. N. Am.* <https://doi.org/10.1016/j.nec.2016.06.002>
- Mears, D., Pollard, H.B., 2016. Network science and the human brain: Using graph theory to understand the brain and one of its hubs, the amygdala, in health and disease. *J. Neurosci. Res.* 94, 590–605. <https://doi.org/10.1002/jnr.23705>
- Mechtler, L.L., Shastri, K.K., Crutchfield, K.E., 2014. Advanced neuroimaging of mild traumatic brain injury. *Neurol. Clin.* <https://doi.org/10.1016/j.ncl.2013.08.002>
- Menon, D.K., Schwab, K., Wright, D.W., Maas, A.I., Demographics and Clinical Assessment Working Group of the International and Interagency Initiative toward Common Data Elements for Research on Traumatic Brain Injury and Psychological Health, 2010. Position Statement: Definition of Traumatic Brain Injury. *Arch. Phys. Med. Rehabil.* 91, 1637–1640.
- Messé, A., Caplain, S., Parodot, G., Garrigue, D., Mineo, J.-F., Soto Ares, G., Ducreux, D., Vignaud, F., Rozec, G., Desal, H., Péligrini-Issac, M., Montreuil, M., Benali, H., Lehericy, S., 2011. Diffusion tensor imaging and white matter lesions at the subacute stage in mild traumatic brain injury with persistent neurobehavioral impairment. *Hum. Brain Mapp.* 32, 999–1011. <https://doi.org/10.1002/hbm.21092>
- Mishra, V.R., Sreenivasan, K.R., Yang, Z., Zhuang, X., Cordes, D., Mari, Z., Litvan, I., Fernandez, H.H., Eidelberg, D., Ritter, A., Cummings, J.L., Walsh, R.R., 2020. Unique white matter structural connectivity in early-stage drug-naïve Parkinson disease. *Neurology* 94, e774–e784. <https://doi.org/10.1212/WNL.0000000000008867>
- Mito, R., Raffelt, D., Dhollander, T., Vaughan, D.N., Tournier, J.-D., Salvado, O., Brodtmann, A., Rowe, C.C., Villemagne, V.L., Connelly, A., 2018. Fibre-specific white matter reductions in Alzheimer's disease and mild cognitive impairment. *Brain* 141, 888–902. <https://doi.org/10.1093/brain/awx355>
- Mittl, R.L., Grossman, R.I., Hiehle, J.F., Hurst, R.W., Kauder, D.R., Gennarelli, T.A., Alburger, G.W., 1994. Prevalence of MR evidence of diffuse axonal injury in patients with mild head injury and normal head CT findings. *AJNR. Am. J. Neuroradiol.* 15, 1583–9.
- Mori, S., Crain, B.J., Chacko, V.P., van Zijl, P.C., 1999. Three-dimensional tracking of axonal projections in the brain by magnetic resonance imaging. *Ann. Neurol.* 45, 265–9.
- Mori, S., Oishi, K., Jiang, H., Jiang, L., Li, X., Akhter, K., Hua, K., Faria, A. V., Mahmood, A., Woods, R., Toga, A.W., Pike, G.B., Neto, P.R., Evans, A., Zhang, J., Huang, H., Miller, M.I., van Zijl, P., Mazziotta, J., 2008. Stereotaxic white matter atlas based on diffusion tensor imaging in an ICBM template. *Neuroimage* 40, 570–582. <https://doi.org/10.1016/j.neuroimage.2007.12.035>
- Mori, S., van Zijl, P.C.M., 2002. Fiber tracking: principles and strategies - a technical review. *NMR Biomed.* 15, 468–480. <https://doi.org/10.1002/nbm.781>
- Mosley, P.E., Paliwal, S., Robinson, K., Coyne, T., Silburn, P., Tittgemeyer, M., Stephan, K.E., Breakspear, M., Perry, A., 2019. The structural connectivity of discrete networks underlies impulsivity and gambling in Parkinson's disease. *Brain* 142, 3917–3935. <https://doi.org/10.1093/brain/awz327>

- Nagy, K.K., Joseph, K.T., Krosner, S.M., Roberts, R.R., Leslie, C.L., Dufty, K., Smith, R.F., Barrett, J., 1999. The utility of head computed tomography after minimal head injury. *J. Trauma* 46, 268–70.
- Narayana, P.A., 2017. White matter changes in patients with mild traumatic brain injury: MRI perspective. *Concussion* 2, CNC35. <https://doi.org/10.2217/cnc-2016-0028>
- Narayana, P.A., Yu, X., Hasan, K.M., Wilde, E.A., Levin, H.S., Hunter, J. V., Miller, E.R., Patel, V.K.S., Robertson, C.S., McCarthy, J.J., 2014. Multi-modal MRI of mild traumatic brain injury. *NeuroImage Clin.* <https://doi.org/10.1016/j.nicl.2014.07.010>
- Ng, S.Y., Lee, A.Y.W., 2019. Traumatic Brain Injuries: Pathophysiology and Potential Therapeutic Targets. *Front. Cell. Neurosci.* <https://doi.org/10.3389/fncel.2019.00528>
- Niogi, S.N., Mukherjee, P., 2010. Diffusion Tensor Imaging of Mild Traumatic Brain Injury. *J. Head Trauma Rehabil.* 25, 241–255. <https://doi.org/10.1097/HTR.0b013e3181e52e2a>
- Nolin, P., Heroux, L., 2006. Relations among sociodemographic, neurologic, clinical, and neuropsychologic variables, and vocational status following mild traumatic brain injury: A follow-up study. *J. Head Trauma Rehabil.* 21, 514–526. <https://doi.org/10.1097/00001199-200611000-00006>
- O’Muircheartaigh, J., Jbabdi, S., 2018. Concurrent white matter bundles and grey matter networks using independent component analysis. *Neuroimage.* <https://doi.org/10.1016/j.neuroimage.2017.05.012>
- Onnela, J.-P., Saramäki, J., Kertész, J., Kaski, K., 2005. Intensity and coherence of motifs in weighted complex networks. *Phys. Rev. E* 71, 065103. <https://doi.org/10.1103/PhysRevE.71.065103>
- Owen, J.P., Ziv, E., Bukshpun, P., Pojman, N., Wakahiro, M., Berman, J.I., Roberts, T.P.L., Friedman, E.J., Sherr, E.H., Mukherjee, P., 2013. Test–Retest Reliability of Computational Network Measurements Derived from the Structural Connectome of the Human Brain. *Brain Connect.* 3, 160–176. <https://doi.org/10.1089/brain.2012.0121>
- Patrick, A.M., Hartley, S.L., Wu, M., Dean, D.C., Zammit, M.D., Johnson, S.C., Tudorascu, D.L., Cohen, A., Cody, K.A., Laymon, C.M., Klunk, W.E., Zaman, S., Handen, B.L., Alexander, A.L., Christian, B.T., 2020. White matter microstructure and episodic memory in adults with down syndrome: A Tract-Based Spatial Statistics (TBSS) Study. *Alzheimer’s Dement.* 16. <https://doi.org/10.1002/alz.044673>
- Peeters, W., van den Brande, R., Polinder, S., Brazinova, A., Steyerberg, E.W., Lingsma, H.F., Maas, A.I.R., 2015. Epidemiology of traumatic brain injury in Europe. *Acta Neurochir. (Wien).* 157, 1683–1696. <https://doi.org/10.1007/s00701-015-2512-7>
- Perry, D.C., Sturm, V.E., Peterson, M.J., Pieper, C.F., Bullock, T., Boeve, B.F., Miller, B.L., Guskiewicz, K.M., Berger, M.S., Kramer, J.H., Welsh-Bohmer, K.A., 2016. Association of traumatic brain injury with subsequent neurological and psychiatric disease: A meta-analysis. *J. Neurosurg.* <https://doi.org/10.3171/2015.2.JNS14503>
- Petersen, M. V., Lund, T.E., Sunde, N., Frandsen, J., Rosendal, F., Juul, N., Østergaard, K., 2017. Probabilistic versus deterministic tractography for delineation of the cortico-subthalamic hyperdirect pathway in patients with Parkinson disease selected for deep brain stimulation. *J. Neurosurg.* 126, 1657–1668. <https://doi.org/10.3171/2016.4.JNS1624>
- Povlishock, J.T., Katz, D.I., 2005. Update of neuropathology and neurological recovery after traumatic brain injury. *J. Head Trauma Rehabil.* 20, 76–94.
- Prince, C., Bruhns, M.E., 2017. Evaluation and treatment of mild traumatic brain injury: The role of neuropsychology. *Brain Sci.* <https://doi.org/10.3390/brainsci7080105>
- Provenzale, J.M., 2010. Imaging of Traumatic Brain Injury: A Review of the Recent Medical Literature. *Am. J. Roentgenol.* 194, 16–19. <https://doi.org/10.2214/AJR.09.3687>
- Qiu, L., Lui, S., Kuang, W., Huang, X., Li, J., Li, J., Zhang, J., Chen, H., Sweeney, J.A., Gong, Q., 2014. Regional increases of cortical thickness in untreated, first-episode major depressive disorder. *Transl. Psychiatry* 4, e378. <https://doi.org/10.1038/tp.2014.18>

- Reijmer, Y.D., Leemans, A., Heringa, S.M., Wielaard, I., Jeurissen, B., Koek, H.L., Biessels, G.J., 2012. Improved Sensitivity to Cerebral White Matter Abnormalities in Alzheimer's Disease with Spherical Deconvolution Based Tractography. *PLoS One* 7. <https://doi.org/10.1371/journal.pone.0044074>
- Roine, T., Jeurissen, B., Perrone, D., Aelterman, J., Leemans, A., Philips, W., Sijbers, J., 2014. Isotropic non-white matter partial volume effects in constrained spherical deconvolution. *Front. Neuroinform.* 8, 28. <https://doi.org/10.3389/fninf.2014.00028>
- Roine, T., Jeurissen, B., Perrone, D., Aelterman, J., Philips, W., Leemans, A., Sijbers, J., 2015. Informed constrained spherical deconvolution (iCSD). *Med. Image Anal.* 24, 269–81. <https://doi.org/10.1016/j.media.2015.01.001>
- Roine, T., Jeurissen, B., Perrone, D., Aelterman, J., Philips, W., Sijbers, J., Leemans, A., 2019. Reproducibility and intercorrelation of graph theoretical measures in structural brain connectivity networks. *Med. Image Anal.* 52, 56–67. <https://doi.org/10.1016/j.media.2018.10.009>
- Roine, U., Salmi, J., Roine, T., Wendt, T.N., Leppamäki, S., Rintahaka, P., Tani, P., Leemans, A., Sams, M., 2015. Constrained spherical deconvolution-based tractography and tract-based spatial statistics show abnormal microstructural organization in Asperger syndrome. *Mol Autism* 6, 4. <https://doi.org/10.1186/2040-2392-6-4>
- Rousseeuw, P.J., 1987. Silhouettes: A graphical aid to the interpretation and validation of cluster analysis. *J. Comput. Appl. Math.* 20, 53–65. [https://doi.org/10.1016/0377-0427\(87\)90125-7](https://doi.org/10.1016/0377-0427(87)90125-7)
- Rubinov, M., Sporns, O., 2010. Complex network measures of brain connectivity: Uses and interpretations. *Neuroimage* 52, 1059–1069. <https://doi.org/10.1016/j.neuroimage.2009.10.003>
- Rudie, J.D., Shehzad, Z., Hernandez, L.M., Colich, N.L., Bookheimer, S.Y., Iacoboni, M., Dapretto, M., 2012. Reduced functional integration and segregation of distributed neural systems underlying social and emotional information processing in Autism spectrum disorders. *Cereb. Cortex.* <https://doi.org/10.1093/cercor/bhr171>
- Ruff, R., 2005. Two decades of advances in understanding of mild traumatic brain injury. *J. Head Trauma Rehabil.* <https://doi.org/10.1097/00001199-200501000-00003>
- Saatman, K.E., Duhaime, A.-C., Bullock, R., Maas, A.I.R., Valadka, A., Manley, G.T., Workshop Scientific Team and Advisory Panel Members, 2008. Classification of traumatic brain injury for targeted therapies. *J. Neurotrauma* 25, 719–38. <https://doi.org/10.1089/neu.2008.0586>
- Shenton, M.E., Hamoda, H.M., Schneiderman, J.S., Bouix, S., Pasternak, O., Rathj, Y., Vu, M.A., Purohit, M.P., Helmer, K., Koerte, I., Lin, A.P., Westin, C.F., Kikinis, R., Kubicki, M., Stern, R.A., Zafonte, R., 2012. A review of magnetic resonance imaging and diffusion tensor imaging findings in mild traumatic brain injury. *Brain Imaging Behav.* 6, 137–192. <https://doi.org/10.1007/s11682-012-9156-5>
- Shigemoto, Y., Sone, D., Maikusa, N., Okamura, N., Furumoto, S., Kudo, Y., Ogawa, M., Takano, H., Yokoi, Y., Sakata, M., Tsukamoto, T., Kato, K., Sato, N., Matsuda, H., 2018. Association of deposition of tau and amyloid- β proteins with structural connectivity changes in cognitively normal older adults and Alzheimer's disease spectrum patients. *Brain Behav.* 8. <https://doi.org/10.1002/brb3.1145>
- Shrout, P.E., 1998. Measurement reliability and agreement in psychiatry. *Stat. Methods Med. Res.* 7, 301–317. <https://doi.org/10.1191/096228098672090967>
- Shrout, P.E., Fleiss, J.L., 1979. Intraclass correlations: Uses in assessing rater reliability. *Psychol. Bull.* <https://doi.org/10.1037/0033-2909.86.2.420>
- Smith, S., Nichols, T., 2009. Threshold-free cluster enhancement: Addressing problems of smoothing, threshold dependence and localisation in cluster inference. *Neuroimage* 44, 83–98. <https://doi.org/10.1016/j.neuroimage.2008.03.061>
- Smith, S.M., Jenkinson, M., Woolrich, M.W., Beckmann, C.F., Behrens, T.E.J., Johansen-Berg, H., Bannister, P.R., De Luca, M., Drobnjak, I., Flitney, D.E., Niazy, R.K., Saunders, J., Vickers, J., Zhang, Y., De Stefano, N., Brady, J.M., Matthews, P.M., 2004. Advances in functional and

- structural MR image analysis and implementation as FSL. *Neuroimage* 23 Suppl 1, S208-19. <https://doi.org/10.1016/j.neuroimage.2004.07.051>
- Snow, N.J., Peters, S., Borich, M.R., Shirzad, N., Auriat, A.M., Hayward, K.S., Boyd, L.A., 2016. A reliability assessment of constrained spherical deconvolution-based diffusion-weighted magnetic resonance imaging in individuals with chronic stroke. *J. Neurosci. Methods* 257, 109–120. <https://doi.org/10.1016/j.jneumeth.2015.09.025>
- Soares, J.M., Marques, P., Alves, V., Sousa, N., 2013. A hitchhiker’s guide to diffusion tensor imaging. *Front. Neurosci.* 7. <https://doi.org/10.3389/fnins.2013.00031>
- Song, S.-K., Sun, S.-W., Ju, W.-K., Lin, S.-J., Cross, A.H., Neufeld, A.H., 2003. Diffusion tensor imaging detects and differentiates axon and myelin degeneration in mouse optic nerve after retinal ischemia. *Neuroimage* 20, 1714–22.
- Sotelo, M.R., Kalinosky, B.T., Goodfriend, K., Hyngstrom, A.S., Schmit, B.D., 2020. Indirect Structural Connectivity Identifies Changes in Brain Networks after Stroke. *Brain Connect.* 10, 399–410. <https://doi.org/10.1089/brain.2019.0725>
- Spielberg, J.M., McGlinchey, R.E., Milberg, W.P., Salat, D.H., 2015. Brain network disturbance related to posttraumatic stress and traumatic brain injury in veterans. *Biol. Psychiatry* 78, 210–216. <https://doi.org/10.1016/j.biopsych.2015.02.013>
- Sporns, O., 2012. From simple graphs to the connectome: Networks in neuroimaging. *Neuroimage.* <https://doi.org/10.1016/j.neuroimage.2011.08.085>
- Sporns, O., Tononi, G., Kötter, R., 2005. The Human Connectome: A Structural Description of the Human Brain. *PLoS Comput. Biol.* 1, e42. <https://doi.org/10.1371/journal.pcbi.0010042>
- Sporns, O., Zwi, J.D., 2004. The small world of the cerebral cortex. *Neuroinformatics.* <https://doi.org/10.1385/NI:2:2:145>
- Stejskal, E.O., Tanner, J.E., 1965. Spin diffusion measurements: Spin echoes in the presence of a time-dependent field gradient. *J. Chem. Phys.* 42, 288–292. <https://doi.org/10.1063/1.1695690>
- Su, E., Bell, M., 2016. Diffuse Axonal Injury, Translational Research in Traumatic Brain Injury. CRC Press/Taylor and Francis Group.
- Takala, R.S., Posti, J.P., Runtti, H., Newcombe, V.F., Outtrim, J., Katila, A.J., Frantzen, J., Ala-Seppälä, H., Kyllönen, A., Maanpää, H.-R., Tallus, J., Hossain, M.I., Coles, J.P., Hutchinson, P., van Gils, M., Menon, D.K., Tenovuo, O., 2015. GFAP and UCH-L1 as outcome predictors in traumatic brain injury. *World Neurosurg.* <https://doi.org/10.1016/j.wneu.2015.10.066>
- Tax, C.M.W., Jeurissen, B., Vos, S.B., Viergever, M.A., Leemans, A., 2014. Recursive calibration of the fiber response function for spherical deconvolution of diffusion MRI data. *Neuroimage* 86, 67–80. <https://doi.org/10.1016/j.neuroimage.2013.07.067>
- Te Ao, B., Brown, P., Tobias, M., Ameratunga, S., Barker-Collo, S., Theadom, A., McPherson, K., Starkey, N., Dowell, A., Jones, K., Feigin, V.L., BIONIC Study Group, 2014. Cost of traumatic brain injury in New Zealand: Evidence from a population-based study. *Neurology* 83, 1645–1652. <https://doi.org/10.1212/WNL.0000000000000933>
- Teasdale, G., Knill-Jones, R., van der Sande, J., 1978. Observer variability in assessing impaired consciousness and coma. *J. Neurol. Neurosurg. Psychiatry* 41, 603–610. <https://doi.org/10.1136/jnnp.41.7.603>
- Tessitore, A., Giordano, A., Russo, A., Tedeschi, G., 2016. Structural connectivity in Parkinson’s disease. *Park. Relat. Disord.* 22, S56–S59. <https://doi.org/10.1016/j.parkreldis.2015.09.018>
- Toth, A., Kovacs, N., Perlaki, G., Orsi, G., Aradi, M., Komaromy, H., Ezer, E., Bukovics, P., Farkas, O., Janszky, J., Doczi, T., Buki, A., Schwarcz, A., 2013. Multi-modal magnetic resonance imaging in the acute and sub-acute phase of mild traumatic brain injury: can we see the difference? *J. Neurotrauma* 30, 2–10. <https://doi.org/10.1089/neu.2012.2486>
- Tournier, J.-D., Calamante, F., Gadian, D.G., Connelly, A., 2004. Direct estimation of the fiber orientation density function from diffusion-weighted MRI data using spherical deconvolution. *Neuroimage* 23, 1176–1185. <https://doi.org/10.1016/j.neuroimage.2004.07.037>

- Tournier, J.D., 2019. Diffusion MRI in the brain – Theory and concepts. *Prog. Nucl. Magn. Reson. Spectrosc.* <https://doi.org/10.1016/j.pnmrs.2019.03.001>
- Tournier, J.D., Calamante, F., Connelly, A., 2013. Determination of the appropriate b value and number of gradient directions for high-angular-resolution diffusion-weighted imaging. *NMR Biomed.* 26, 1775–1786. <https://doi.org/10.1002/nbm.3017>
- Tournier, J.D., Calamante, F., Connelly, A., 2012. MRtrix: Diffusion tractography in crossing fiber regions. *Int. J. Imaging Syst. Technol.* 22, 53–66. <https://doi.org/10.1002/ima.22005>
- Tournier, J.D., Calamante, F., Connelly, A., 2007. Robust determination of the fibre orientation distribution in diffusion MRI: Non-negativity constrained super-resolved spherical deconvolution. *Neuroimage* 35, 1459–1472. <https://doi.org/10.1016/j.neuroimage.2007.02.016>
- Tuch, D.S., 2004. Q-ball imaging. *Magn. Reson. Med.* 52, 1358–1372. <https://doi.org/10.1002/mrm.20279>
- Tuch, D.S., Reese, T.G., Wiegell, M.R., Makris, N., Belliveau, J.W., Wedeen, V.J., 2002. High angular resolution diffusion imaging reveals intravoxel white matter fiber heterogeneity. *Magn. Reson. Med.* 48, 577–582. <https://doi.org/10.1002/mrm.10268>
- Tucholka, A., Grau-Rivera, O., Falcon, C., Rami, L., Sánchez-Valle, R., Lladó, A., Gispert, J.D., Molinuevo, J.L., 2018. Structural connectivity alterations along the Alzheimer’s disease continuum: Reproducibility across two independent samples and correlation with cerebrospinal fluid amyloid- β and tau. *J. Alzheimer’s Dis.* 61, 1575–1587. <https://doi.org/10.3233/JAD-170553>
- Tzourio-Mazoyer, N., Landeau, B., Papathanassiou, D., Crivello, F., Etard, O., Delcroix, N., Mazoyer, B., Joliot, M., 2002. Automated anatomical labeling of activations in SPM using a macroscopic anatomical parcellation of the MNI MRI single-subject brain. *Neuroimage* 15, 273–289. <https://doi.org/10.1006/nimg.2001.0978>
- van der Horn, H.J., Kok, J.G., de Koning, M.E., Scheenen, M.E., Leemans, A., Spikman, J.M., van der Naalt, J., 2017. Altered Wiring of the Human Structural Connectome in Adults with Mild Traumatic Brain Injury. *J. Neurotrauma* 34, 1035–1044. <https://doi.org/10.1089/neu.2016.4659>
- van der Horn, H.J., Kok, J.G., de Koning, M.E., Scheenen, M.E., Leemans, A., Spikman, J.M., van der Naalt, J., 2016. Altered wiring of the human structural connectome in adults with mild traumatic brain injury. *J. Neurotrauma* neu.2016.4659. <https://doi.org/10.1089/neu.2016.4659>
- Vanderploeg, R.D., Curtiss, G., Belanger, H.G., 2005. Long-term neuropsychological outcomes following mild traumatic brain injury. *J. Int. Neuropsychol. Soc.* 11, 228–236. <https://doi.org/10.1017/S1355617705050289>
- Wada, T., Asano, Y., Shinoda, J., 2012. Decreased Fractional Anisotropy Evaluated Using Tract-Based Spatial Statistics and Correlated with Cognitive Dysfunction in Patients with Mild Traumatic Brain Injury in the Chronic Stage. *Am. J. Neuroradiol.* 33, 2117–2122. <https://doi.org/10.3174/ajnr.A3141>
- Wang, Z., Zhang, M., Sun, C., Wang, S., Cao, J., Wang, K.K.W., Gan, S., Huang, W., Niu, X., Zhu, Y., Sun, Y., Bai, L., 2019. Single mild traumatic brain injury deteriorates progressive inter-hemispheric functional and structural connectivity. *J. Neurotrauma*. <https://doi.org/10.1089/neu.2018.6196>
- Watts, D.J., Strogatz, S.H., 1998. Collective dynamics of ‘small-world’ networks. *Nature* 393, 440–442. <https://doi.org/10.1038/30918>
- Wedeen, V.J., Hagmann, P., Tseng, W.-Y.I., Reese, T.G., Weisskoff, R.M., 2005. Mapping complex tissue architecture with diffusion spectrum magnetic resonance imaging. *Magn. Reson. Med.* 54, 1377–1386. <https://doi.org/10.1002/mrm.20642>
- Wedeen, V.J., Wang, R.P., Schmahmann, J.D., Benner, T., Tseng, W.Y.I., Dai, G., Pandya, D.N., Hagmann, P., D’Arceuil, H., de Crespigny, A.J., 2008. Diffusion spectrum magnetic resonance imaging (DSI) tractography of crossing fibers. *Neuroimage* 41, 1267–1277. <https://doi.org/10.1016/j.neuroimage.2008.03.036>

- WESBEY, G.E., Moseley, M.E., EHMAN, R.L., 1984. Translational molecular self-diffusion in magnetic resonance imaging. II. Measurement of the self-diffusion coefficient. *Invest. Radiol.* 19, 491–8. <https://doi.org/10.1097/00004424-198411000-00005>
- Westin, C.-F., Maier, S.E., Mamata, H., Nabavi, A., Jolesz, F.A., Kikinis, R., 2002. Processing and visualization for diffusion tensor MRI. *Med. Image Anal.* 6, 93–108.
- Wilde, E.A., Ware, A.L., Li, X., Wu, T.C., McCauley, S.R., Barnes, A., Newsome, M.R., Biekman, B.D., Hunter, J. V., Chu, Z.D., Levin, H.S., 2018. Orthopedic Injured versus Uninjured Comparison Groups for Neuroimaging Research in Mild Traumatic Brain Injury. *J. Neurotrauma.* <https://doi.org/10.1089/neu.2017.5513>
- Wilson, J.T., Pettigrew, L.E., Teasdale, G.M., 1998. Structured interviews for the Glasgow Outcome Scale and the extended Glasgow Outcome Scale: guidelines for their use. *J. Neurotrauma* 15, 573–585. <https://doi.org/10.1089/neu.1998.15.573>
- Wright, R.M., Ramesh, K.T., 2012. An axonal strain injury criterion for traumatic brain injury. *Biomech. Model. Mechanobiol.* 11, 245–260. <https://doi.org/10.1007/s10237-011-0307-1>
- Wu, Y.C., Mustafi, S.M., Harezlak, J., Kodiweera, C., Flashman, L.A., McAllister, T.W., 2018. Hybrid Diffusion Imaging in Mild Traumatic Brain Injury. *J. Neurotrauma* 35, 2377–2390. <https://doi.org/10.1089/neu.2017.5566>
- Xiao, H., Yang, Y., Xi, J., Chen, Z., 2015. Structural and functional connectivity in traumatic brain injury. *Neural Regen. Res.* 10, 2062. <https://doi.org/10.4103/1673-5374.172328>
- Yamagata, B., Ueda, R., Tasato, K., Aoki, Y., Hotta, S., Hirano, J., Takamiya, A., Nakaaki, S., Tabuchi, H., Mimura, M., 2020. Widespread White Matter Aberrations Are Associated with Phonemic Verbal Fluency Impairment in Chronic Traumatic Brain Injury. *J. Neurotrauma* 37, 975–981. <https://doi.org/10.1089/neu.2019.6751>
- Yang, Y., Chen, Y., Chen, K., Wei, D., Li, P., Zeng, W., Pei, J., Mao, H., Jia, J., Zhang, Z., 2019. Increased intrinsic connectivity for structural atrophy and functional maintenance after acute ischaemic stroke. *Eur. J. Neurol.* 26, 935–942. <https://doi.org/10.1111/ene.13913>
- Yealy, D.M., Hogan, D.E., 1991. Imaging after head trauma. Who needs what? *Emerg. Med. Clin. North Am.* 9, 707–17.
- Yeo, R.A., Ryman, S.G., Van Den Heuvel, M.P., De Reus, M.A., Jung, R.E., Pommy, J., Mayer, A.R., Ehrlich, S., Schulz, S.C., Morrow, E.M., Manoach, D., Ho, B.C., Sponheim, S.R., Calhoun, V.D., 2016. Graph metrics of structural brain networks in individuals with schizophrenia and healthy controls: Group differences, relationships with intelligence, and genetics. *J. Int. Neuropsychol. Soc.* 22, 240–249. <https://doi.org/10.1017/S1355617715000867>
- Zagorchev, L., Meyer, C., Stehle, T., Wenzel, F., Young, S., Peters, J., Weese, J., Paulsen, K., Garlinghouse, M., Ford, J., Roth, R., Flashman, L., McAllister, T., 2016. Differences in regional brain volumes two months and one year after mild traumatic brain injury. *J. Neurotrauma.* <https://doi.org/10.1089/neu.2014.3831>
- Zakharova, N., Kornienko, V., Potapov, A., Pronin, I., 2014. *Neuroimaging of Traumatic Brain Injury.* Springer International Publishing, Cham. <https://doi.org/10.1007/978-3-319-04355-5>
- Zalesky, A., Fornito, A., Harding, I.H., Cocchi, L., Yücel, M., Pantelis, C., Bullmore, E.T., 2010. Whole-brain anatomical networks: Does the choice of nodes matter? *Neuroimage* 50, 970–983. <https://doi.org/10.1016/j.neuroimage.2009.12.027>
- Zhang, J., Zhang, Y., Wang, L., Sang, L., Yang, J., Yan, R., Li, P., Wang, J., Qiu, M., 2017. Disrupted structural and functional connectivity networks in ischemic stroke patients. *Neuroscience* 364, 212–225. <https://doi.org/10.1016/j.neuroscience.2017.09.009>
- Zheng, W.B., Liu, G.R., Kong, K.M., Wu, R.H., 2006. Coma Duration Prediction in Diffuse Axonal Injury: Analyses of Apparent Diffusion Coefficient and Clinical Prognostic Factors, in: 2006 International Conference of the IEEE Engineering in Medicine and Biology Society. IEEE, pp. 1052–1055. <https://doi.org/10.1109/IEMBS.2006.259627>
- Zhou, C., Gao, T., Guo, T., Wu, Jingjing, Guan, X., Zhou, W., Huang, P., Xuan, M., Gu, Q., Xu, X., Xia, S., Kong, D., Wu, Jian, Zhang, M., 2020. Structural Covariance Network Disruption and

- Functional Compensation in Parkinson's Disease. *Front. Aging Neurosci.* 12. <https://doi.org/10.3389/fnagi.2020.00199>
- Zhou, Y., 2017. Abnormal structural and functional hypothalamic connectivity in mild traumatic brain injury. *J. Magn. Reson. Imaging* 45, 1105–1112. <https://doi.org/10.1002/jmri.25413>
- Zuo, L.J., Li, Z.X., Zhu, R.Y., Chen, Y.J., Dong, Y., Wang, Y.L., Zhao, X.Q., Zhang, Z.J., Sachdev, P., Zhang, W., Wang, Y.J., 2018. The Relationship between Cerebral White Matter Integrity and Cognitive Function in Mild Stroke with Basal Ganglia Region Infarcts. *Sci. Rep.* <https://doi.org/10.1038/s41598-018-26316-5>



**TURUN
YLIOPISTO**
UNIVERSITY
OF TURKU

ISBN 978-951-29-8459-6 (PRINT)
ISBN 978-951-29-8460-2 (PDF)
ISSN 0355-9483 (Print)
ISSN 2343-3213 (Online)